

# Focus stacking: Comparing commercial top-end set-ups with a semi-automatic low budget approach. A possible solution for mass digitization of type specimens

Jonathan Brecko<sup>1,2</sup>, Aurore Mathys<sup>1,2</sup>, Wouter Dekoninck<sup>1</sup>,  
Maurice Leponce<sup>1</sup>, Didier VandenSpiegel<sup>2</sup>, Patrick Semal<sup>1</sup>

**1** Royal Belgian Institute of Natural Sciences, Vautierstraat 29, B-1000 Brussels, Belgium **2** Royal Museum for Central Africa, Tervurensesteenweg, Tervuren, Belgium

Corresponding author: *Jonathan Brecko* ([jonathan.brecko@naturalsciences.be](mailto:jonathan.brecko@naturalsciences.be))

---

Academic editor: *P. Stoev* | Received 18 September 2014 | Accepted 20 November 2014 | Published 16 December 2014

---

<http://zoobank.org/AB1A8252-6354-4E0A-BCF1-90836792FC19>

---

**Citation:** Brecko J, Mathys A, Dekoninck W, Leponce M, VandenSpiegel D, Semal P (2014) Focus stacking: Comparing commercial top-end set-ups with a semi-automatic low budget approach. A possible solution for mass digitization of type specimens. ZooKeys 464: 1–23. doi: 10.3897/zookeys.464.8615

---

## Abstract

In this manuscript we present a focus stacking system, composed of commercial photographic equipment. The system is inexpensive compared to high-end commercial focus stacking solutions. We tested this system and compared the results with several different software packages (CombineZP, Auto-Montage, Helicon Focus and Zerene Stacker). We tested our final stacked picture with a picture obtained from two high-end focus stacking solutions: a Leica MZ16A with DFC500 and a Leica Z6APO with DFC290. Zerene Stacker and Helicon Focus both provided satisfactory results. However, Zerene Stacker gives the user more possibilities in terms of control of the software, batch processing and retouching. The outcome of the test on high-end solutions demonstrates that our approach performs better in several ways. The resolution of the tested extended focus pictures is much higher than those from the Leica systems. The flash lighting inside the Ikea closet creates an evenly illuminated picture, without struggling with filters, diffusers, etc. The largest benefit is the price of the set-up which is approximately € 3,000, which is 8 and 10 times less than the LeicaZ6APO and LeicaMZ16A set-up respectively. Overall, this enables institutions to purchase multiple solutions or to start digitising the type collection on a large scale even with a small budget.

## Keywords

Focus Stacking, Cognisys, StackShot, Leica, Zerene Stacker, Helicon Focus, mass digitization

## Introduction

Since the first photographic equipment was developed, people have tried to record natural history specimens with their equipment. This has always worked for regularly sized objects; however, the micro-world remained unrecorded for a long time. When suitable lenses made it possible to capture small creatures on film it was clear that other problems arose. The low depth of field made it almost impossible to get the complete object in focus, unless the aperture was stepped down (Tindall and Kalms 2012). However this resulted in other aberrations as the optical resolution reduces due to the diffraction effect (Davies 2010, Gallo et al. 2014, Goldsmith 2000). As computers have become widely available, numerous software have been developed by microscope companies and researchers, making it possible to combine pictures with different depths of field to create a focus stack in which the entire object is in focus (Adelson et al. 1984, CombineZP ([www.hadleyweb.pwp.blueyonder.co.uk](http://www.hadleyweb.pwp.blueyonder.co.uk)), Helicon Focus ([www.heliconsoft.com/heliconsoft-products/helicon-focus](http://www.heliconsoft.com/heliconsoft-products/helicon-focus)), Auto-Montage ([www.syncroscopy.com/Auto-Montage](http://www.syncroscopy.com/Auto-Montage)), Zerene Stacker ([zerenesystems.com/cms/home](http://zerenesystems.com/cms/home))). In the beginning this technique was only available for laboratories or research groups with a large budget to spend on a state of the art stacking column or microscope, with special lenses, lighting, stage control, camera and software. Although results were better than a single image, the system itself was sometimes difficult to operate without a training period. These systems could be relatively fast, but often, post-processing was time consuming and most importantly, as techniques change rapidly, an update on the hardware of these systems is quite expensive.

The way to determine if a picture of a specimen is according to the right parameters and can be considered to be a ‘good’ and ‘useful’ picture is when the following settings have been met: i) the image needs to have an in-focus specimen; ii) there shouldn’t be any parts that are over-exposed or under-exposed; iii) all parts that are necessary to identify/study a specimen in a specific view have to be visible and distinguishable. As we live in a time where everything is digitally accessible, these last parameters might only be met when viewing the image at its full size at the highest resolution and not in the printed version within an article or a book. Secondly and equally important to the other previously defined parameters, these pictures need to be taken as fast as possible and the post-processing time needed to get a publishable, usable picture has to be as low as possible. If these different parameters are met, the system can be used to provide pictures for an occasional publication, and also for the mass digitization of type material. This is very important in collection management because in some cases digitization could replace the need to ship or send very fragile specimens for study in all kinds of disciplines.

The high resolution multimedia recording of small specimens is a real challenge for Natural History museums who are working on mass digitization programs. The quality of the resulting image, the cost of the equipment, the human work and the learning curve are important parameters in order to define a general digitization strategy.

We present here a low budget-high quality approach consisting of commercial products. We will compare different software packages using the pictures produced

from this set-up. In addition to this comparison we will have a closer look at several available high-end solutions regarding focus stacking and compare them to our set-up.

As it is important to compare the cost of purchasing the different techniques we will give a relative quotation (due to the confidentiality of price quotations) based on past purchase prices and recent received quotations. This will give an indication about the price range of the different stacking solutions.

## **Material and methods**

### **Choice of the tested specimens**

We chose two different specimens for the tests in this paper. The first is an ant from the genus *Meranoplus*, whilst the second is a beetle of the genus *Trachys*. Both specimens represent a challenge to obtain a decent picture. The main challenge for the ant specimen is that it has lots of hairs, it is reflective and has fine long body parts. The beetle does not have a lot of details, but the curvature and the brilliance of the elytra makes it very difficult to get an evenly exposed specimen, as they tend to reflect a lot of light. Only the ant will be used to compare the different stacking software, whilst both of the specimens will be used to check the different solutions for creating a focus stack. The reason we did not chose both specimens for each comparison is that for the creation of the stacked image the ant will be the most difficult as small intersecting details like hairs tend to create halos during the stacking process. However the beetle will not create such a problem, therefore, it is not necessary to use this specimen in the visual software comparison. Both specimens are interesting to consider in the solution section because this enables the comparison of lighting, stability of the system, etc.

### **Canon-Cognisys set-up**

We got the main idea for this set-up from the set-up developed by Dr. Anthony G. Gutierrez and Graham Snodgrass, which is described by Alexander and Droege (Sine Dato) from the USGS Bee Inventory and Monitoring Laboratory (BIML 2010). In this set-up we use a Canon EOS 600D camera with a resolution of 18 MP in 'large' picture mode. The camera is equipped with a Canon MP-E 65 mm 1:2.8 1–5× Macro Photo Lens (Figure 1). This lens starts where other macro lenses end, at 1:1, and is able to magnify the object 5×. We used two low budget flash lights (Yongnuo Flash YN560-II). One flash is controlled by a remote (Phottix PT-04 II), while the other works in the auto-slave mode to flash in synchrony. Both the specimen and the flash lights are positioned inside an Ikea kitchen closet (Metod, 40 × 60 cm, Håggeby White) with a removable background. This background was neutral grey for this test, but can be any colour desired. The flash lights are positioned away from the specimen. To automate control when taking the different images, we used a Cognisys StackShot which drives



**Figure 1.** The Canon-Cognisys set-up at the RBINS. The Canon 600D Camera, equipped with a Canon MP-E 65 mm 1:2.8 1–5× Macro Photo Lens, is mounted on the vertically positioned StackShot (Cognisys inc.). In the Ikea closet, at the bottom, you see the two Yongnuo YN560-II speedlights positioned frontally and above is the plexiglas plate covered with paper to position the specimen.

the camera from the set beginning to end positions, taking pictures every programmed number of microns. The StackShot is positioned vertically on top of the Ikea closet in which a hole is cut out to fit the camera and StackShot. The StackShot holds the camera and is attached to a metal reinforced corner.

We used the auto distance function (Auto-Dist) of the StackShot controller for the tests and did so for most of the stacking used in this set-up. In this way a certain step size in  $\mu\text{m}$  was chosen according to the size of the object and the magnification used. The f-stop is chosen depending on the magnification. Up to a magnification of  $2\times$ – $3\times$  we use an f-stop of 5.6 or 5.0, while a magnification of  $3\times$  to  $5\times$  was followed with an f-stop of 5.0 or 4.5 and sometimes 4.0, depending on the specimen photographed. The flash lights were set at a light intensity of 1/64th to 1/4th of the flash power for the smallest specimens. The StackShot controller triggers the camera through a shutter speed cable. Choosing the beginning and the end positions of the stack is done by means of the Live View function in the Canon Eos Utility software package for remote shooting. An additional LED light is positioned in the closet to light the specimen during the setting of the beginning and end positions. The Led light is switched on/off by a USB controlled power plug (USB Net Power 8800 by Aviosys, [www.aviosys.com/8800.html](http://www.aviosys.com/8800.html)). The StackShot itself can be controlled in Zerene Stacker, the stacking software, as well, but we preferred to do this directly on the StackShot.

### **Comparison of the software packages**

To compare a few of the software packages available we chose one set of pictures produced by the Canon-Cognisys setup described above. We recorded the time to process the stack of pictures and looked in detail at the quality of the stacked image. When addressing the details available in the pictures it is best to download the full resolution images as most of the details discussed were not visible on the downscaled pictures – <http://mars.naturalsciences.be/publications/zookeys>. All the tests below were performed using the default settings of the software packages.

### **Auto-Montage**

Auto-Montage is a stacking software program by Syncroscopy. This was one of the first software packages commercially available to perform focus stacking. It offers different ways to stack a set of images (fixed, blended, weighted, exponentially weighted and compound weighted). As well as this choice, the software has the possibility to align a stack of images before the stacking procedure starts. We used an evaluating version for this test. This made it rather difficult to look at fine details as the picture is imprinted

with watermarks. However, it was possible to get a time indication and allowed an overall view of the stacked image. The maximum number of pictures that are possible to load into one stack is 255 pictures. However, it is advised to make sub-stacks of such a large focus stack in other programs as well (cf. Zerene Stacker).

### **CombineZP**

CombineZP is widely used and one of the pioneer software packages to create an extended focus image. Therefore we tested this software package which is freely available. CombineZP has multiple options to stack a set of pictures (Do Stack, Do Soft Stack, Do Weighted Stack, Pyramid Weighted, Pyramid Do Stack, Pyramid Maximum Contrast). There are also two ways to align a stack of pictures. One is the quick alignment, while the other one is the thorough alignment. CombineZP offers a batch process program also, so if it is more suitable to use slower stacking methods, these can be used as a batch overnight. The only downside is the poor memory allocation of the software so a more powerful workstation is needed for larger and more extensive sets of images.

### **Helicon Focus**

Helicon Focus is another commercially available stacking software program, produced by Helicon Soft. It has a straightforward interface and enables the user to retouch the pictures after stacking in the Pro version. Helicon Focus offers three possibilities to stack a set of pictures. These are called method A, B and C, which are an average, depth and pyramid stacking method respectively. The maximum number of pictures that are possible to load into one stack is 255 pictures.

### **Zerene Stacker**

Zerene Stacker (Build T201404082055) is a commercially available image stacking software package, created by Zerene Systems, which enables the user to retouch stacks within the program when necessary. In Zerene Stacker there are two possibilities to stack a set of images, PMax and DMap. The main difference between the two stacking techniques is that PMax handles a large number of images per stack really well. But PMax can alter colour and contrast from what appears in the original unstacked source images. This behavior is common to all the comparable pyramid methods. The shifts are mostly a slight loss of saturation and increase of contrast. In addition, different specimens often have slightly different colors and those colors may have faded in storage. The DMap option will create better-looking pictures but creates halo effects when too many pictures are stacked using this option. If the morphology of the specimen pictured is more important than the colour then it is better to choose the PMax method. This is generally

the case for dried specimens, which have lost colour partially over time due to storage. When dealing with fresh material and colour is equally important, then DMap might be a better stacking option; however, calibration of the lighting setup is necessary in every step of the process. Therefore the best option is to combine both techniques and create substacks using PMax and stack the resulting substacks by employing DMap. But these settings are necessary only when it comes to a large (>100) number of pictures. This can all be done by using the automatic sub-stacking program written by Chris Slaybaugh (<https://dl.dropbox.com/u/51805918/SlabberJockey--V1.0.zip>). In this test we provide the results only for both stacking methods made without sub-stacks. Specimens with many fine structures, such as hairs, benefit from the sub-stacking technique to achieve sharpness without halos.

### **Comparison of the high-end focus stacking solutions**

We used two high-end approaches that were already available in-house, a Leica MZ16A set-up and a Leica Z6APO. These solutions will be compared to the Canon-Cognisys set-up we describe above.

#### **Leica MZ 16 A with DFC500**

The Leica MZ16A microsystem was equipped with a DFC500 camera. This camera is able to make pictures with a total size of 12 MP (4080 × 3072). The objective used is a 0.63× Leica Planapo. The lights used are two lights controlled by a Leica KL 1500 LCD. The software controlling the Z-stage is LAS Core by Leica. The aperture was set to its maximal opening. The exposure time was set according to the object and distance of the lights. Because two direct lights were used, the light needed to be diffused. This was done by using chalk paper and/or opaque plastic (Leica, S.D.).

#### **Leica Z6APO with DFC290**

The Leica Z6APO microscope tested is equipped with a DFC290 camera, which is able to take pictures of 3 MP. The objective used was the Leica Planapo 2.0×. The lighting used in this set-up were two Manfrotto ring systems consisting of 24 LEDs each. They are opposed to each other and a diffuser is set within the ring. This entire set-up was set over the specimen. The aperture was set to its maximal opening. The exposure time was positioned according to the colour and reflectivity of the specimen. Setting the start and end positions and well as the other settings for the camera is done with the LAS Core software (<http://projects.biodiversity.be/ants>).

For the comparison of the different techniques it was necessary to do the stacking with the same software package.

## Results

### Comparison of the focus stacking packages

To compare the times to calculate the extended focus image, there are two processes which need to be taken into account. First is the alignment of the images. This is an important process as images can be shifted in relation to one another, by movement of the camera or due to vibrations of the environment. During this alignment there is also a correction for the parallax effect. The second process is the actual combination of the several in-focus areas of the images into one in-focus image.

The pictures for both specimens were taken at a step-size of 40  $\mu\text{m}$ , resulting in 74 and 41 pictures for *Meranoplus* sp. and *Trachys* sp. respectively. The resolution of the images on 'Large' is 5184  $\times$  3456 pix. We used an aperture of f/4.5 and f/5.6 for the *Meranoplus* sp. and *Trachys* sp. respectively. For both specimens, the shutter speed was 1/100 s and ISO-100. The magnification of the 65 mm MP-E lens was 5 $\times$ .

When looking at the results from the Google and Google Scholar search it is apparent that more people are mentioning Helicon Focus and CombineZP than the

**Table 1.** Comparison of the stacking time in the different software packages in default settings. \* Auto-Montage is only able to stack 67 pictures on a workstation with the following parameters: Quad core 3.10 Intel i5 2400, 16 GB of RAM memory.

		<i>Meranoplus</i> sp.	<i>Trachys</i> sp.	Price	
Auto-Montage*	Alignment	1'11"	0'41"	€ 2,500–3,000	
	Fixed	0'56"	0'40"		
	Blended	0'58"	0'34"		
	Weighted	2'02"	0'37"		
	Exponentially Weighted	2'06"	1'27"		
	Compound Weighted	2'03"	1'25"		
CombineZP	Quick Alignment	1'40"	0'35"		Free
	Thorough Alignment	\	\		
	Do Stack	2'00"	1'13"		
	Do Soft Stack	2'03"	1'22"		
	Do Weighted Stack	5'30"	3'11"		
	Pyramid Weighted	2'49"	1'35"		
	Pyramid Do Stack	2'30"	1'31"		
	Pyramid Maximum Contrast	1'42"	1'00"		
Helicon Focus	Method A (Average)	1'45"	0'47"	€ 108–225 (Premium)	
	Method B (Depth Map)	2'10"	1'09"		
	Method C (Pyramid)	1'43"	0'57"		
Zerene Stacker	DMap (incl. alignment)	4'07"	3'15"	€ 89–283 (Pro: 3+: € 250 each)	
	PMax (incl. alignment)	4'40"	3'00"		

other two programs (Table 2). However, when performing a search on Flickr it becomes clear that the hobby and professional photographers prefer Zerene Stacker over the other software packages. Out of the four software packages tested, Auto-Montage is the least mentioned on the web and has no groups on Flickr. This is probably due to the difficulty of finding a trial version of the software. Moreover, the software is actually meant to be used by professional microscopy scientists.

### Auto-Montage

Alignment of the images took 1 min 11 s and 41 s for the ant and the beetle respectively. For the *Meranoplus* sp., stacking functions 'Fixed' and 'Blended' are the fastest, by accomplishing the job in just under one minute, while the other stacking methods take more than twice that time (Table 1). For the *Trachys* beetle the same is found for the first and the last two stacking options. However the third option, the 'Weighted' method, is equally fast as the first two, delivering a result after approximately 35 s to 40 s. Although the alignment of the stack and stacking of these images is quite fast, none of the above available stacking methods provides a satisfying result. The main problems are the production of a substantial number of halos and the creation of a lighter area around the edges of the specimen. The most disturbing problem is found in the several weighted methods, in which the final picture appears as if it were shot through a translucent window (Figure 2).

### CombineZP

CombineZP has two options to align a stack, 'quick alignment' and 'thorough alignment'. Unfortunately, we were only able to test the 'quick alignment' as the other option crashed the program every time. The alignment procedure took 1 min 40 s and 35 s for the *Meranoplus* and the *Trachys* specimen respectively (Table 1). Of the stacking procedures only the 'Do weighted stack' option is considerably longer than the other possible options, which are all well under three minutes for the *Meranoplus* sp. and max out at 1 min 35 s for the *Trachys* sp.

At first sight the results look satisfactory. But when the different images are viewed at actual size, the results of the stacking itself is somewhat disappointing. The 'Do stack' (Figures 3A, B) and 'Do Soft Stack' (Figures 3C, D) only creates a few artefacts around the hairs on the head, although some halos do still occur around the hairs on the abdomen and on the thorax of the *Meranoplus* specimen. The pyramid weighted stack (Figures 3G, H) gives somewhat similar results, but the halos are more apparent. The only two methods that do not create halos are the 'Do weighted stack' (Figures 3E, F) and the 'Pyramid Maximum Contrast' (Figures 3K, L). However, of these last two methods, the first creates a terrible light edge around the legs and other parts of the body, while the latter delivers a pixelated image when viewed at 100%.

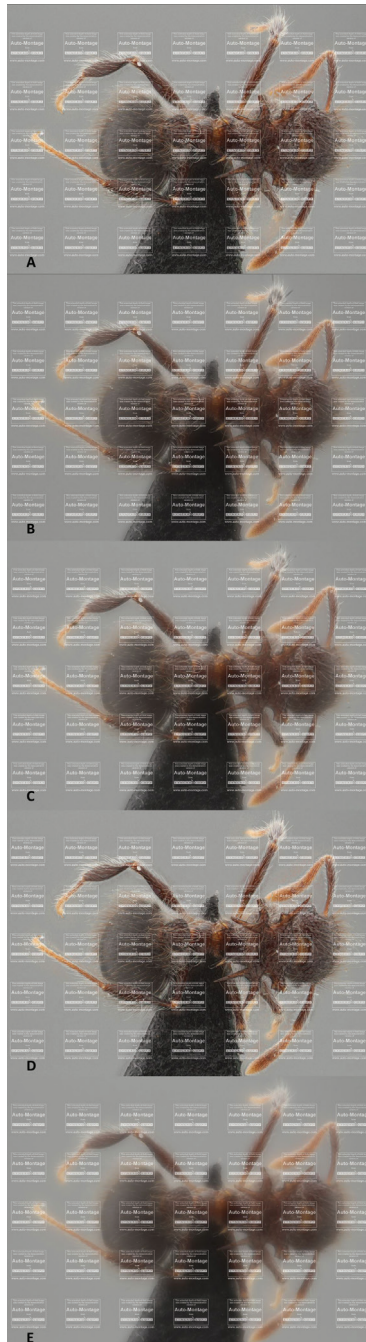


**Figure 2.** The results of the different stacking methods in Auto-Montage: each stacking option is provided with a single picture which is reduced in size by the Auto-Montage software itself and imprinted with watermarks. **A** represents the Blended Stacking option **B** picture composed by the Compound Weighted method **C** picture stacked by the Exponentially Weighted option **D** picture composed by the Fixed method and **E** picture stacked by the Weighted method.



**Figure 3.** The results of the different stacking methods in CombineZP: each stacking option is provided with a detail of a hairy leg and a part of the head with hairs. **A, B** details of the stack pictures by the Do Stack method **C, D** details of the stacked picture with the Do Soft Stack **E, F** details of the Do Weighted Stack method **G, H** details of the combined pictured with the Pyramid Weighted method **I, J** details of the stacked image with the Pyramid Do stack method **K, L** Details of the Stacked image with the Pyramid Maximum Contrast method.

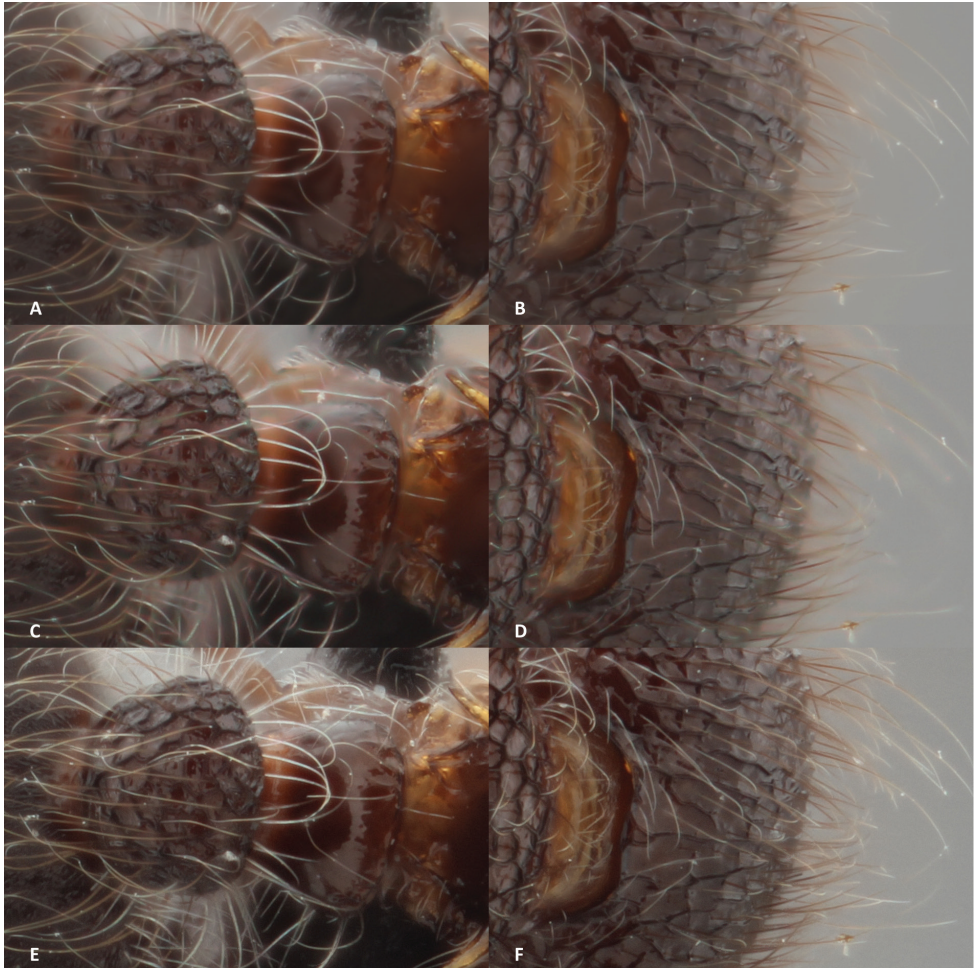


**Figure 4.** The results of the different stacking methods in Helicon Focus: each stacking option is provided with a detail of a hairy leg and a part of the head with hairs. **A, B** result of Method A (average) **C, D** result of Method B (depth) **E, F** result of Method C (pyramid).

### Helicon Focus

In Helicon Focus there are three options one can choose from to combine a stack of images. They all stack and align the pictures of the *Meranoplus* specimen in approximately 2 minutes, whilst the smaller stack of the *Trachys* specimen is produced in approximately one minute (Table 1). In the two first methods (the 'Average and Depth' methods) there is the possibility to change the parameters, whilst this is not possible for the 'Pyramid' method.

Of the three methods available, the 'Pyramid' method (Method C, Figures 4E, F), as suggested by the guidelines of Helicon Focus, proved the most satisfactory. There are almost no halos present on the image and it has a clean look, but the brightness and the contrast is changed by the software. The 'Average' method (Method A, Figures 4A,



**Figure 5.** The results of the different stacking methods in Zerene Stacker, each with a detail of a hairy leg and a part of the head with hairs. **A, B** details of the stack pictures by the PMax method **C, D** details of the stacked picture with the DMap method.

B) produces a composed picture with a few halos around the abdominal hairs, but this method creates a lighter edge around the entire specimen. On another background this may work, but here it further distorts the image rather than accentuating it. The 'Depth' method (Method B, Figures 4C, D) is not suited for these types of specimens as the hairs produce halos all over the specimen. However, this can be controlled by adjusting the radius when choosing the depth method. We didn't manage to find a set of parameters that gave a better result on this particular specimen. However, a specimen with less fine details, such as the beetle, would be fine with this method.

### Zerene Stacker

In Zerene stacker there are only two options to choose from, 'PMax', which is a pyramid stacking and 'DMap', a depth method. Both methods stack and align in a similar amount of time. The *Meranoplus* specimen is aligned and stacked in approximately 4 to 5 minutes, whilst the smaller stack of the *Trachys* specimen takes approximately 3 minutes to complete. In this software package it is also possible to change the parameters of the depth method.

Comparing the results (Figure 5) of the composed pictures, it is clear that the 'PMax' method works best. The image is well-composed, there are no halos, and details

are clearly visible. Although only visible when viewing at full size, 'DMap' creates halos around the hairs on the back of the abdomen and around those on the head, and are most apparent around the hairs with another body part behind it, like a leg for example.

Taking into account all tests, we chose to process the pictures made by the stacking solutions with Zerene Stacker.

## Comparison of the high-end focus stacking solutions

### Leica MZ 16 A with DFC500

The pictures are the result of 70 images taken of the *Meranoplus* sp. and 41 images of the *Trachys* sp. respectively. These images are the result of a step-size of 36  $\mu\text{m}$  and 39  $\mu\text{m}$  respectively. Considering they are both approximately the same size, the step-size can be considered to be the same. Although the camera was able to take pictures with a resolution of  $4080 \times 3072$  pix, the workstation connected to the set-up was not able to work at this resolution. The first resolution which successfully worked without affecting the quality of the pictures was  $2040 \times 1536$  pix (Table 3).

The composed picture of the *Meranoplus* sp. could have benefited from a larger magnification (Figure 6). In this way more detail of the ant would be visible. However, judging the overall look of the picture, it is clear that there are parts which are over- and underexposed. The tips of hairs all appear shiny and reflect a lot of light. The overall coloration of the ant is dark brown-red.

The focus stacked image of the *Trachys* specimen is bright and clear, although it took a little bit more time to position the lights and the light diffusers. There is a small dark part on the elytra which is the result of the reflection of the black hole in the lens. This effect can only be solved with a sophisticated lighting setup involving axial lighting with beamsplitters. Without such a setup, this effect is unavoidable (Littlefield, pers. comm.). As the beetle doesn't have a lot of fine details the picture looks better than the one of the ant. But again fine details are not visible because of the small picture dimensions. Purchasing this set-up will cost you approximately 10 Canon-Cognisys systems.

### Leica Z6 APO with DFC290

As we set more or less the same step-size for the *Meranoplus* sp. and the *Trachys* sp. while making the separate images (39.68  $\mu\text{m}$  and 39.19  $\mu\text{m}$  respectively) this resulted in 77 and 44 images for these two specimens. The camera provides HD pictures with a resolution of  $2048 \times 1536$  pix (Table 3).

The resulting picture (Figure 7) shows a well-illuminated and detailed specimen. There are no areas which are over- or underexposed. The ant itself has an overall dark blackish coloration with light highlighted hairs. The only downside is that the resolution doesn't offer more detail than is visible on a regular (21 inch) computer screen.



**Figure 6.** Focus stacking in Zerene Stacker. The small image in the upper corner provides a detailed close-up of  $518 \times 345$  pix of the image at 100%. **A** Stack of 70 pictures, aligned and combined with PMax **B** Stack of 41 pictures, aligned and combined with PMax. The individual pictures of both stacks are made with the Leica MZ16A with DFC500 camera and Leica KL 1500 LCD lights.



**Figure 7.** Focus stacking in Zerene Stacker. The small image in the upper corner provides a detailed close-up of  $518 \times 345$  pix of the image at 100%. **A** Stack of 77 pictures, aligned and combined with PMax **B** Stack of 44 pictures, aligned and combined with PMax The individual pictures of both stacks are made with the Leica Z6 APO with DFC290 and Manfrotto led light system.



**Figure 8.** Focus stacking in Zerene Stacker. The small image in the upper corner provides a detailed close-up of  $518 \times 345$  pix of the image at 100%. **A** Stack of 74 pictures, aligned and combined with PMax **B** Stack of 41 pictures, aligned and combined with PMax. The individual pictures of both stacks are made with the Canon-Cognisys set-up and double flash lights.

The *Trachys* specimen is quite dark on the elytra making it difficult to see details in that area. Aside from the illumination issue, the picture is sharp and there are no parts that are overexposed. Again it is unfortunate that the image dimensions aren't larger, because this would aid in viewing details on legs and antennae. The set-up we tested here can be purchased for approximately eight Canon-Cognisys set-ups.

### Canon-Cognisys set-up

Using the double flash lights inside a light chamber creates a smooth light resulting in even illumination without any over- or underexposed parts as can be seen in both the *Meranoplus* and the *Trachys* specimens (Figure 8). Apart from the easy illumination, the large benefit is the large image dimensions provided by the Canon 600D. Fine details such as the hairs on the ants' legs, head and abdomen can be clearly seen. The set-up we presented here costs approximately € 3,000 (Table 3).

**Table 2.** Comparison of the number of finds of analysed software: results obtained via Google and Google Scholar search engines and in the group search of Flickr.

	Google	Google Scholar	Flickr Groups
Auto-Montage	4K	2K	0
CombineZ	946K	1.7K	9
Helicon Focus	235K	1K	16
Zerene Stacker	114K	131	45

**Table 3.** Comparison of the settings.

	Resolution of images	Time to position specimen	Time for setting of stage	Time to set light conditions	Time to take pictures	Relative Price of the System
Leica MZ16A + DFC500	4080 × 3072	1–3 min	< 1 min	+/-5 min	1 image per 15 s	10–11
Leica Z6APO + DFC290	2048 × 1536	1–3 min	< 1 min	< 1 min	1 image per s	7–8
Canon-Cognisys	5184 × 3456	1–3 min	< 1 min	< 1 min	1 image per 2 s	1

**Table 4.** Sensor size versus magnification of the systems tested.

	Leica MZ16A + DFC500	Leica Z6APO + DFC290	Canon 600D + MP-E 65 mm
Magnification	16:01	06:01	05:01
Objective used	0.63	2	\
Resulting magnification	10	12	5
Sensor width (mm)	8.8	6.6	22.3
Pixels (width)	4080	2048	5184
# pixels/mm	4674	3318	1162
# pixels/μm	4.67	3.32	1.16
# μm/pixel	0.21	0.3	0.86
Sensor filling (mm)	0.87	0.62	4.46

## Discussion

### Comparison of the software packages

All the different software packages tested compose (aligning and stacking) a new picture in three to four minutes, except for Helicon Focus, which does the job in half the time. Lowering the values of the alignment parameters or even unchecking this option in Zerene Stacker, will reduce the stacking time as well. To speed up the stacking process there are many parameters available in the professional version of Zerene Stacker, which can lower the process time by a factor of three when altered (Littlefield 2014). However, in CombineZP, there are some settings which make the process last slightly longer as with the 'Do Weighted Stack' method. The two stacking methods of Zerene Stacker and those of CombineZP are slower than the ones from Helicon Focus and Auto-Montage. But time isn't the most important factor as the computing can be done after working hours. In the end the quality of the focus stacked picture is what really matters: in these tests both Helicon Focus and Zerene Stacker provided the best results and both have more or less the same price. Helicon Focus has the possibility to make a 3D model made out of the information available in the image stack. This might be an interesting feature, however it has little scientific value as it only delivers a decent model with objects that are smooth and does not demonstrate fine structures such as insect legs. In fact as Zerene Stacker is also able to compute depth maps, but it is also possible to make similar models using third party software. Besides depth maps, Zerene Stacker can make stereo and 'rocking' pictures (gifs) which give the impression of 3D when viewed cross-eyed for the stereo option. A huge benefit of both Helicon Focus and Zerene Stacker is that they can control a StackShot through their own interface. This might be useful when the stacking is done immediately after taking the pictures. However, many more images will be stacked during a working day when processed as a batch file. Helicon Remote, bundled within the premium edition of Helicon Focus, also enables the direct control of an auto-focus lens, when the attached DSLR is a fairly recent one (for the exact list see the Helicon Focus web page). Other third-party software also exists for Zerene Stacker or other focus stacking software (ControlmyNikon ([www.Controlmynikon.com](http://www.Controlmynikon.com)); Magic Lantern ([www.magiclantern.fm](http://www.magiclantern.fm))). Both of these packages have easy tools to retouch the final image when necessary, but Zerene Stacker's tools are more extensive. We did not use this option as we wanted to see the results before the actual retouching; better raw results need less time retouching afterwards. The only disadvantage of the software packages, might be that Helicon Focus is only able to deal with a stack of less than 255 pictures. But as mentioned before, unless the object is quite straightforward, without any fine details, it is better to make substacks when dealing with such a large amount of pictures. This will take more time to process a stack, although it is also possible to do this during the night as a batch file. Overall the two software packages deliver the same results, although we have seen that Helicon Focus sometimes creates a few more halos than Zerene Stacker in certain cases. Given the more or less similar end result one might benefit from purchasing both software packages as Zerene Stacker has more retouching abilities and Helicon Focus can stack images faster. This is more or less visible

in the internet search results as well; researchers are going for the fast processing of Helicon Focus, while professional/hobby photographers chose Zerene Stacker because of the ability to manipulate each step during and even after the focus stacking.

### **Comparing the high-end focus stacking solutions**

There is a large difference in sensor size between the three systems (Table 4). The sensor size of the Canon CMOS sensor on the D600 makes it possible to fill the sensor with an object of 22 mm to 4.4 mm size depending on the magnification of the MP-E lens (1× to 5× respectively). The two Leica systems are able to fill the sensors of their cameras with an object measuring 0.9 mm and 0.6 mm for the MZ16A and Z6APO, respectively.

However, when an object is pictured that is sensor-filling on the Canon CMOS sensor, the Canon-Cognisys set-up is able to deliver a picture more than twice the size of the other two techniques. The Leica MZ16A would perform better with a adequate processing power and memory. In that case the difference in resolution wouldn't be as apparent, but would still be noticeable ( $5184 \times 3456$  to  $4080 \times 3072$ ). When the final stacked picture is sharp, even with less resolution, it will still be suitable for a publication. However, it will not be possible to see more detail by enlarging the picture although this is possible with higher resolution pictures.

The time needed to make the set of pictures on the Leica MZ16A was substantially longer than with the other two techniques. This might of course be due to the difference in computing power and perhaps the older camera in this set-up.

Another difference between the different approaches is the lack of a good lighting set-up with the MZ16A. Using two microscope lights is far from perfect to obtain a smooth illumination. However this can be solved by using a similar light as used in the Z6APO set-up or perhaps even a standard Leica solution as the 5000 LED dome. But again as this set-up is already the most expensive of the three tested, one might chose a more budget-friendly approach or go for another high-end solution. The light used with the Z6APO and the Canon-Cognisys deliver more or less the same results, although they are two complete different approaches as one is continuous lightning and the other is flash light. Looking at the colour of the specimens on the different images, there appears to be a problem: none of them actually has the same colour composition, while all of them were calibrated with a grey card.

One might argue why should you bother with taking focus stacked pictures as photogrammetry enables the creation of 3D models of insects (Nguyen et al. 2014). We tried this approach as well, although we used a different software package, Agisoft Photoscan ([www.agisoft.com](http://www.agisoft.com)). Previously the software had had difficulties in aligning images with a low depth of field. Recent software updates made the software package stronger and making insect 3D models is no longer an issue (Figure 9). However, looking at the details provided by these models, both with and without texture, they are far from detailed, even with the better resolution provided by the Agisoft Photoscan software compared to the BOB Capture models in Nguyen et al. 2014

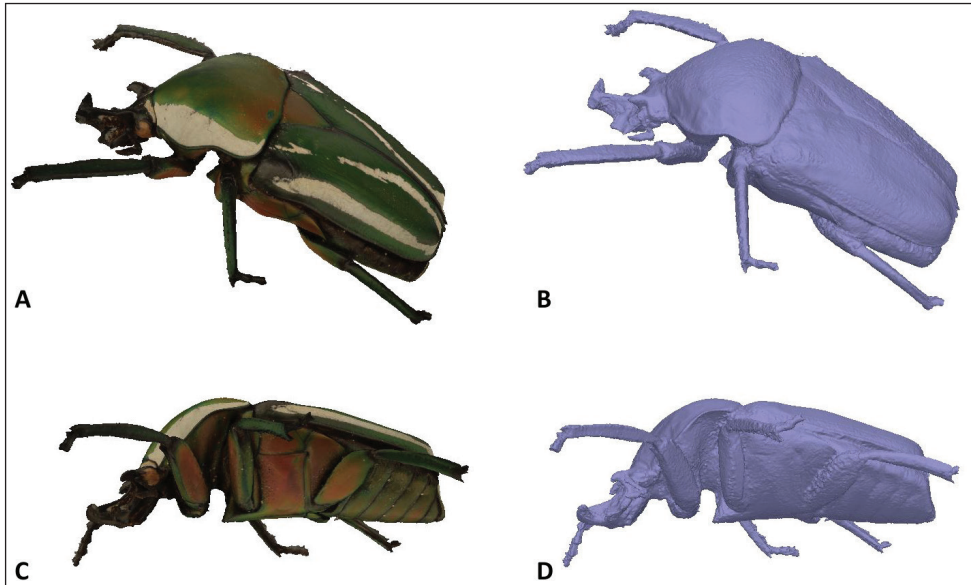


**Figure 9.** A 3D model of a *Dicranorrhina* sp. beetle. The left pictures (**A**, **C**) represent the 3D model with its texture, while the right pictures (**B**, **D**) are from the model with the mesh only and show the level of detail of the 3D model made in Agisoft Photoscan.

(Model of a longhorn beetle similarly-sized to our *Dicranorrhina* beetle: <http://dx.doi.org/10.4225/08/531E573D7F06C>) (3DSOM is now incorporated in BOB Capture, [www.bigobjectbase.com/bob-capture](http://www.bigobjectbase.com/bob-capture)). Areas with hairs or transparent parts lack any detail. In fact the only way to get a decent 3D model of an insect is by  $\mu$ CT scanning. Photogrammetry works very well in other fields of research (Mathys et al. 2013a, 2013b) but for species recognition and determination it is not precise enough, although they could be great educational models to show on websites or in museum exhibitions. Therefore we think that focus stacking is still an appropriate way to digitize entomological specimens, as it delivers detail which scientists need for their research.

## General conclusion

Based on the results presented we can conclude that the Canon-Cognisys set-up as we currently use it delivers results that are equal, or even better, than high-end approaches. This merely is due to the simple lighting set-up, the high resolution, and the low noise delivered by the Canon DSLR. All this combined makes it possible even for untrained people to take good quality pictures. The fact that everything is easy to replace when better cameras or lenses become available is a huge advantage of this set-up. By changing lenses (60 mm Macro or 100 mm Macro) it is also possible to photograph specimens of 10 cm to 20 cm (e.g. butterflies, spiders, scorpions, even minerals), which show large depths and benefit from focus stacking. Preliminary tests show that even specimens in liquids (alcohol, glycol-

erine, etc.) can be photographed without the need to change the set-up. Moreover, the low cost for the entire set-up enables the use of it for mass digitization as multiple packages can be purchased and operated simultaneously, which will considerably speed up the amount of specimens digitized. After a few months of testing in a mass digitization context, we are able to easily generate focus stacked images of 50 specimens a day, when only one view is needed or 16 specimens when three views per specimen is necessary (picture of the labels and processing of focus stacked picture included). Within a full-time contract one person can process 10 000 specimens in 50 weeks with a cost of approximately € 4.30 per specimen or per view (picture of the labels included). We expect that the cost per specimen will decrease and the amount of specimens photographed a day will increase once the workflow becomes more fluid.

The huge challenge for the future will be managing the load of data produced by the stacking process, keeping track of all the metadata created, and providing it in an automated way online.

When needing to decide upon the software packages one might be attracted to the freely available software package CombineZP. The results are satisfactory when the picture itself has a low number of pixels (for instance those produced by the Leica DFC290) and the use is for a printed publication where the resulting picture is smaller than its actual size. In this case the software could be a temporary solution. However, as these days full-size high pixel images are easy to download, one has to choose the best results especially when Helicon Focus and Zerene Stacker deliver considerably better results and only cost approximately € 250 for the full packages with permanent licenses.

## **Acknowledgements**

We would like to thank Arnaud Henrard and Yves Laurent for taking the pictures, using the Leica MZ16A and Z6APO set-ups. We would also like to thank Tara Chapman for proof reading and the reviewers for their comments, which improved the manuscript.

This research has been conducted in the context of the Agora 3D Project (AG/LL/164), and the DIGIT03 program, funded by the federal Belgian Science Policy (BELSPO) and the European FP7 SYNTHESYS 3 program.

## **References**

- Adelson EH, Anderson CH, Bergen JR, Burt PJ, Ogden JM (1984) Pyramid methods in image processing. *RCA Engineer* 29(6): 33–41. <https://alliance.seas.upenn.edu/~cis581/wiki/Lectures/Pyramid.pdf>
- Alexander B, Droegge S (Sine Dato) Detailed Macrophotography of insect specimens: A laboratory set-up. <ftp://ftpext.usgs.gov/pub/er/md/laurel/Droegge/How%20to%20Take%20MacroPhotographs%20of%20Insects%20BIML%20Lab2.pdf>

- BIML (2010) USGS Bee Inventory and Monitoring Lab. <https://www.flickr.com/photos/usgs-biml/> and <http://www.pwrc.usgs.gov/nativebees/>
- Davies A (2010) *Close-up and macro photography*. Focal Press, Elsevier, Oxford, 172 pp.
- Gallo A, Muzzupappa M, Bruno F (2014) 3D reconstruction of small sized objects from a sequence of multi-focused images. *Journal of Cultural Heritage* 15(2): 173–182. doi: 10.1016/j.culher.2013.04.009
- Goldsmith NT (2000) Deep focus; a digital image processing technique to produce improved focal depth in light microscopy. *Image Analysis & Stereology* 19: 163–167. doi: 10.5566/ias.v19.p163-167
- Leica, S.D., *Leica Stereo Microscopes & Macroscopes*. <http://www.leica-microsystems.com/products/stereo-microscopes-macroscopes/>
- Littlefield R (2014) *Photomacrography.net*. <http://www.photomacrography.net/forum/view-topic.php?p=142943#142943>
- Mathys A, Lemaitre S, Brecko J, Semal P (2013b) Agora 3D: evaluating 3D imaging technology for the research, conservation and display of museum collections. *Antiquity Project Gallery* 087(336). <http://antiquity.ac.uk/projgall/mathys336/>
- Mathys A, Brecko J, Semal P (2013a) Comparing 3D digitizing technologies: what are the differences? In: Addison AC, De Luca L, Guidi G, Pescarin S (Eds) *Proceedings of the Digital Heritage International Congress*. Volume 1, CNRS, Marseille.
- Nguyen CV, Lovell DR, Adcock M, La Salle J (2014) Capturing natural-colour 3D models of insects for species discovery and diagnostics. *PLoS ONE* 9(4): 1–11. doi: 10.1371/journal.pone.0094346
- Tindall A, Kalms B (2012) *Guidance: Photographing specimens in natural history collections*. Atlas of Living Australia. [http://www.ala.org.au/wp-content/uploads/2011/10/BK-Guidance-on-Photographing-specimens\\_FINAL.pdf](http://www.ala.org.au/wp-content/uploads/2011/10/BK-Guidance-on-Photographing-specimens_FINAL.pdf)



# Three species of *Hitobia* Kamura, 1992 (Araneae, Gnaphosidae) from south-west China

Cheng Wang<sup>1</sup>, Xian-Jin Peng<sup>1</sup>

<sup>1</sup> College of Life Sciences, Hunan Normal University, Changsha, Hunan 410081, China

Corresponding author: Xian-Jin Peng ([xjpeng@126.com](mailto:xjpeng@126.com))

---

Academic editor: Shuqiang Li | Received 8 August 2014 | Accepted 12 November 2014 | Published 16 December 2014

<http://zoobank.org/A0CD9D06-38D9-4560-8079-FCDD90138325>

---

**Citation:** Wang C, Peng X-J (2014) Three species of *Hitobia* Kamura, 1992 (Araneae, Gnaphosidae) from south-west China. ZooKeys 464: 25–34. doi: 10.3897/zookeys.464.8403

---

## Abstract

Two new species and one new record of the *Hitobia* are described from Gaoligong Mountains, Yunnan Province, China: *Hitobia tengchong* sp. n. (male), *Hitobia hirtella* sp. n. (male) and *Hitobia makotoi* Kamura, 2011. Distributional data and illustrations of body and copulatory organs are provided. The differences between the new species and their related species are discussed.

## Keywords

Ground spider, south-east Asia

## Introduction

The genus *Hitobia* was established by Kamura 1992 with the type species *Micaria unifascigera* Bösenberg & Strand, 1906. A total of 14 species have been reported from south-east Asia only (Platnick 2014). Subsequent papers about this genus were published by scholars from both Chinese and overseas such as Yin et al. (1996), Deeleman-Reinhold (2001), Zhang et al. (2009), Kamura (2011) and so on. Song et al. (2004) and Yin et al. (2012) made detailed studies on Chinese species of *Hitobia* and described 5 new species. Kamura (1992) transferred *unifascigera* from *Poecilochroa* and *asiatica* from *Berlandina* to this genus from Japan. Deeleman-Reinhold (2011) transferred *tenuicincta* from *Ladissa* to this genus from Vietnam. To date, all species of this genus (Platnick 2014) are known in China except for *H. makotoi* Kamura, 2011

occurring in Japan, *H. tenuicincta* (Simon, 1909) from Vietnam and *H. yaginumai* Deeleman-Reinhold, 2001 from Thailand. *Hitobia* is similar to *Litopyllus* Chamberlin, 1922 in the condition of female median spinnerets and male palpal structure, but can be separated from the latter by the slightly recurved posterior eye row, instead of being procurved in *Litopyllus* (Kamura, 1992).

While examining the specimens collected from the Gaoligong Mountains (Yunnan province, south-west China) by the Sino-American Expeditions (1998–2008), one female specimen was identified to be *H. makotoi*, two male specimens were identified to be the members of *Hitobia*, but differ from any other males of the genus. Because of the habits of ground spider and their similar appearance, it is not easy to match male to female in each species, and many species were recorded only with single male or female in a same genus of Gnaphosidae (e. g. *Micaria logunovi* Zhang, Song & Zhu, 2001 based on only one male specimen and *Micaria marusiki* Zhang, Song & Zhu, 2001 based on 2 female specimens). So, we described the two male specimens as two new species. Goal of this paper is to provide the distributional data, illustrations of body and copulatory organs, and the differences between the new species and their related species.

## Material and methods

All specimens were kept in 75% ethanol, examined, measured and drawn with an Olympus SZX16 stereomicroscope and an Olympus BX53 compound microscope. Photos were taken with a digital camera Canon PowerShot G12 mounted on an Olympus SZX16 and compound focus images were generated using Helicon Focus software (3.10 Free).

All measurements were given in millimeters. Leg measurements are giving as: total length (femur, patella + tibia, metatarsus, tarsus). The abbreviations used in text including: **AER** anterior eye row; **ALE** anterior lateral eyes; **AME** anterior median eyes; **MOA** median ocular area; **PER** posterior eye row; **PLE** posterior lateral eyes; **PME** posterior median eyes. Specimens are deposited in College of Life Sciences, Hunan Normal University.

## Taxonomy

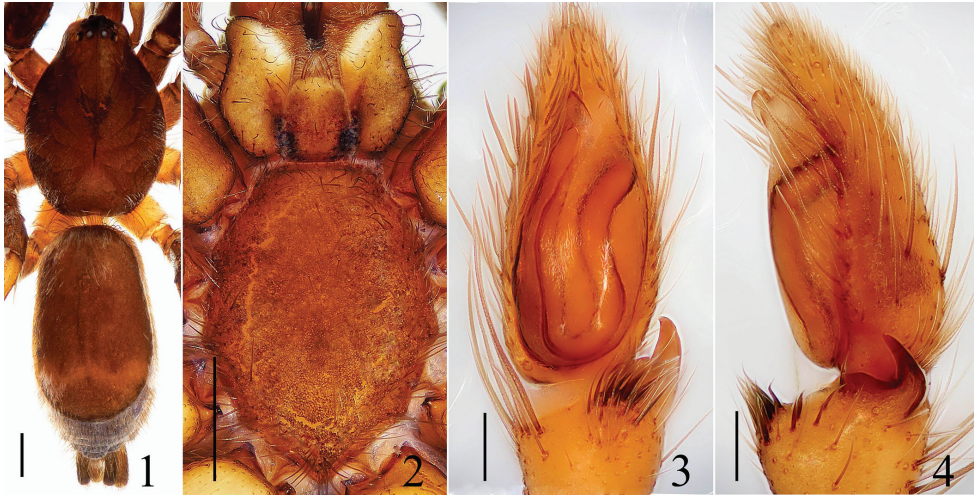
### *Hitobia* Kamura, 1992

#### *Hitobia tengchong* sp. n.

<http://zoobank.org/A2EE881F-D6ED-4EA4-8C53-5512D8BC3B00>

Figs 1–8

**Type material. Holotype:** ♂, **China, Yunnan:** Tengchong County, Jietou Township, 8# boundary post of Yakou (25°80.894'N, 98°62.080'E, 2890 m), 23 May 2006, Xingping Wang, Xianjin Peng leg.

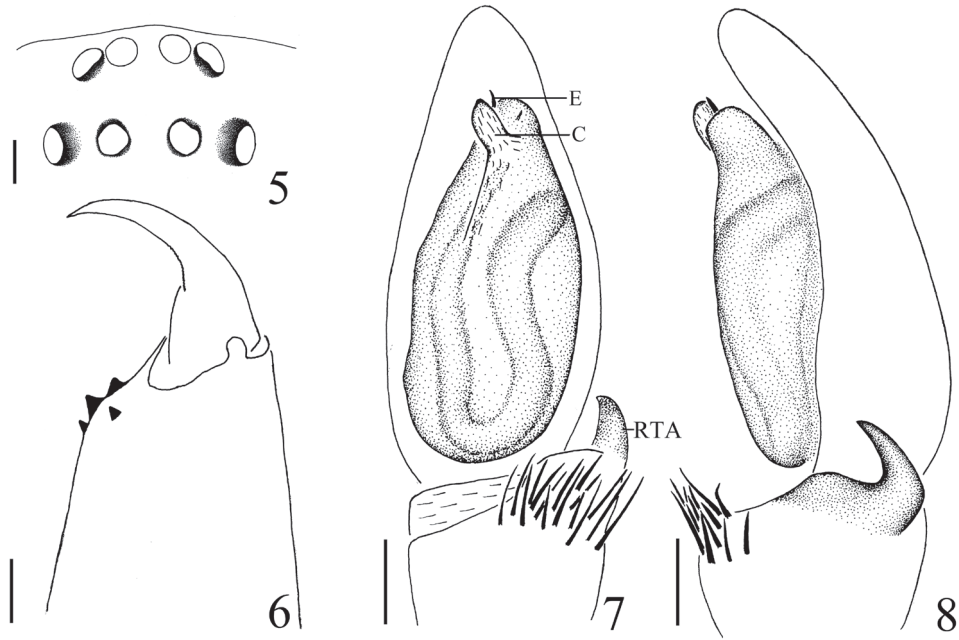


**Figures 1–4.** *Hitobia tengchong* sp. n. **1** male body, dorsal view **2** prosoma, ventral view **3** male palp, ventral view **4** male palp, retrolateral view. Scale bars: 0.5 mm (**1–2**); 0.1 mm (**3–4**).

**Etymology.** The specific name refers to the type locality; adjective.

**Diagnosis.** This new species is somewhat similar to *H. yaginumai* Deeleman-Reinhold, 2001 (see Deeleman-Reinhold 2001: figs 868–874), especially in opisthosoma having a large dorsal scutum, retrolateral tibial apophysis bearing a tuft of long setae on the base, male palp with a obvious conductor, but can be distinguished from the latter by: 1) embolus erect, the tip reached to the position of 11:00 o'clock approximately (Figs 3, 7) versus encircling along the top of bulb prolaterally, the tip reached to the position of 2:00 o'clock in *H. yaginumai*; 2) conductor lamellate in retrolateral view (Figs 4, 8) versus almost semicircular in *H. yaginumai*; 3) retrolateral tibial apophysis hornlike and its apex only extending to the quarter of cymbium in retrolateral view (Figs 4, 8) versus hook-like and its apex extending about to the middle part of cymbium in *H. yaginumai*; 4) abdominal dorsum only with one transverse white stripe (Fig. 1) versus with two additional short longitudinal white stripes on each side except for one transverse white stripe in *H. yaginumai*; 5) chelicerae with 3 promarginal teeth (Fig. 6) versus 2 in *H. yaginumai*.

**Description. Male:** Total length 5.15. Prosoma 2.29 long, 1.67 wide. Opisthosoma 2.72 long, 1.52 wide. Clypeus 0.05 high. Carapace dark brown, long oval, widest at coxae II and III, covered with some white hair. Cervical grooves, fovea and radial grooves dark brown. AER and PER both slightly recurved, wider posteriorly (Fig. 5). Eyes sizes and interdistances: AME 0.08, ALE 0.08, PME 0.07, PLE 0.09, AME–AME 0.04, AME–ALE 0.01, PME–PME 0.09, PME–PLE 0.09, ALE–PLE 0.14. MOA anterior width 0.18, posterior width 0.22, length 0.25. Chelicerae brown, with 3 promarginal teeth and 1 retromarginal (Fig. 6). Endites yellowish brown, almost parallel (Fig. 2). Labium yellowish brown, longer than wide, ligulate (Fig. 2). Sternum colored as labium, covered with some dark bristles, anterior straight and posterior



**Figures 5–8.** *Hitobia tengchong* sp. n. **5** eye area, dorsal view **6** left chelicera, posterior view **7** male palp, ventral view **8** male palp, retrolateral view. Scale bars: 0.1 mm (**5–8**). C conductor E embolus RTA retrolateral tibial apophysis.

subacute (Fig. 2). Legs femur, coxae I and II dark brown, others yellowish brown. Trochanters I and II without ventral notch, trochanters III and IV with a shallow ventral notch. Legs spination: femur: I, II, III d1-1-0, r0-0-1; IV d0-0-1; patella: I, II, III p0-1-0; IV p0-1-0; tibia: I v1-1-1; II v1-1-1; III d1-0-0, p1-0-0, v1-0-0, r1-1-1; IV d1-0-0, v1-0-1, r0-1-0; metatarsi: I v1-0-0; II v1-0-0, p1-0-0; III d1-0-0, p0-1-0, v1-0-0; IV d1-1-0, p0-1-0, r0-1-0, v1-1-0. Legs length: I 4.65 (1.31, 1.72, 1.02, 0.60), II 4.61 (1.29, 1.70, 1.02, 0.60), III 4.28 (1.02, 1.45, 1.21, 0.60), IV 5.84 (1.71, 2.00, 1.53, 0.60). Dorsum of opisthosoma (Fig. 1) dark brown, long oval, with a large scutum about four-fifths of the whole abdominal length and one transverse white stripe posteriorly, covered with white thin hair. Venter brown.

Male palp (Figs 3–4, 7–8): tibia short, with several long prolateral macrosetae, the retrolateral apophysis hornlike and bearing a tuft of long and curved macrosetae on the base. Bulb elongated, widest at middle part. Embolus thin and short, originating from the prolateral top of bulb, erect, the tip reached to the position of 11:00 o'clock approximately in ventral view. Conductor large relatively, membranous, situated retrolaterally at embolus, lamellate in retrolateral view.

**Female:** Unknown.

**Distribution.** China (Yunnan).



**Figures 9–12.** *Hitobia subhirsuta* sp. n. **9** male body, dorsal view **10** prosoma, ventral view **11** male palp, ventral view **12** male palp, retrolateral view. Scale bars: 0.5 mm (9–10); 0.1 mm (11–12).

***Hitobia hirtella* sp. n.**

<http://zoobank.org/67B532D8-9C8E-477A-8339-EFDDE055615C>

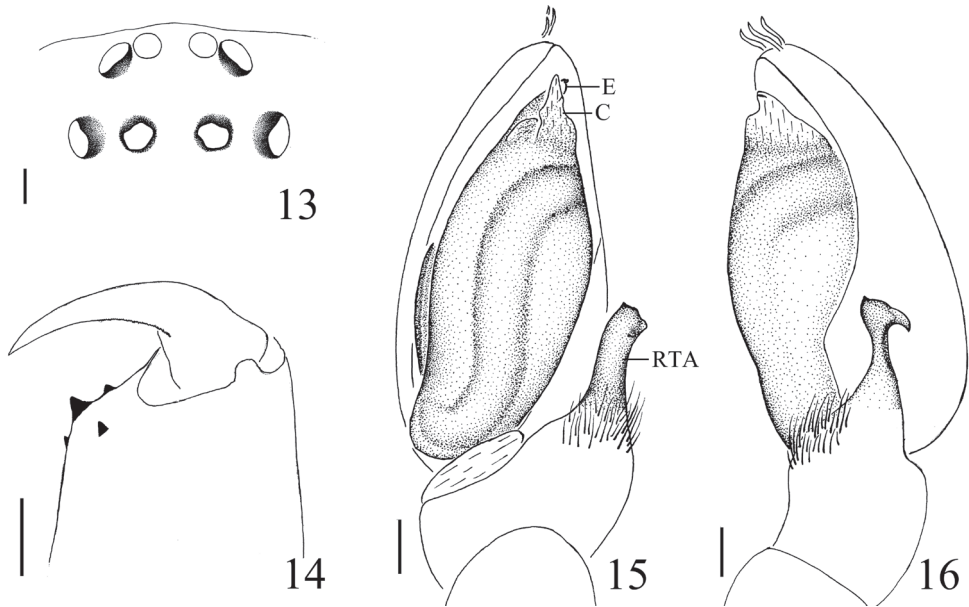
Figs 9–16

**Type material. Holotype** ♂, **China, Yunnan:** Nujiang Prefecture, Gongshan County, Pengdang Township, Longpo Village, 12.5 air km of Gongshan (27°85.608'N, 98°68.448'E, 1550 m), 4–7 July 2000, Hengmei Yan leg.

**Etymology.** The specific name comes from the Latin *hirtella* (with macrosetae), referring to the three thick setae on the cymbial tip.

**Diagnosis.** This new species resembles *H. shaohai* Yin & Bao, 2012 (see Yin et al. 2012: figs 631a–h) in having a similar size of dorsal scutum, retrolateral tibial apophysis bearing a cluster of bristles on the base, but can be separated by: 1) conductor visible in ventral view (Figs 11, 15) versus invisible in *H. shaohai*; 2) retrolateral tibial apophysis longer, stronger, the distal end not bifurcated (Figs 11–12, 15–16) versus with two rami in *H. shaohai*; 3) opisthosoma dorsum without obvious markings (Fig. 9) versus with one median pale transverse white stripe in *H. shaohai*; 4) chelicerae with 3 promarginal teeth (Fig. 14) versus with 2 in *H. shaohai*.

**Description. Male:** Total length 5.30. Prosoma 2.33 long, 1.75 wide. Opisthosoma 2.85 long, 1.63 wide. Clypeus 0.06 high. Carapace brown, long oval, widest at coxae II and III, covered with some white hair. Fovea, cervical grooves and radial grooves dark brown. AER and PER both slightly recurved, wider posteriorly (Fig. 13). Eyes sizes and interdistances: AME 0.08, ALE 0.10, PME 0.09, PLE 0.09, AME–AME 0.05, ALE–AME 0.01, PME–PME 0.10, PME–PLE 0.10, ALE–PLE 0.14. MOA



**Figures 13–16.** *Hitobia subhirsuta* sp. n. **13** eye area, dorsal view **14** left chelicera, posterior view **15** male palp, ventral view **16** male palp, retrolateral view. Scale bars: 0.1 mm (**13–16**). C conductor E embolus RTA retrolateral tibial apophysis.

anterior width 0.21, posterior width 0.25, length 0.29. Chelicerae dark brown, with 3 promarginal teeth and 1 retromarginal tooth (Fig. 14). Endites yellowish brown, almost parallel (Fig. 10). Labium brown, longer than wide, ligulate (Fig. 10). Sternum brown, with some dark bristles, anterior straight and posterior subacute (Fig. 10). Legs femur, coxae I and II dark brown, others yellow. Trochanters I and II without ventral notch, trochanters III and IV with a shallow ventral notch. Leg spination: femur: I, II, III d1-1-1; IV d1-0-0; tibia: I v2-2-1; II v2-2-1; III d1-0-0, p0-1-0, v0-2-0; IV v1-2-1, r1-1-0; metatarsi: Iv0-1-0; II v1-0-0; III d0-1-0, p1-0-1, v2-0-0, r1-0-0; IV d1-0-0, p1-0-1, r0-1-0. Legs length: I 4.85 (1.50, 1.79, 0.91, 0.65), II 4.82 (1.50, 1.76, 0.91, 0.65), III 4.7 (1.32, 1.51, 1.22, 0.65), IV 6.11 (1.75, 2.00, 1.71, 0.65). Dorsum of opisthosoma (Fig. 18) brown, long oval, with three pairs of muscle impressions and a scutum about three-fifths of whole abdominal length, without obvious markings. Venter pale brown.

Male palp (Figs 11–12, 15–16): tibia short and strong, with several long prolateral macrosetae, the retrolateral apophysis long and bearing a tuft of long bristles on the swollen base. Cymbial tip with three thick setae. Embolus thin, twisted in middle part and the distal part covered by large conductor is, membranous, almost triangular in ventral view.

**Female:** Unknown.

**Distribution.** China (Yunnan).



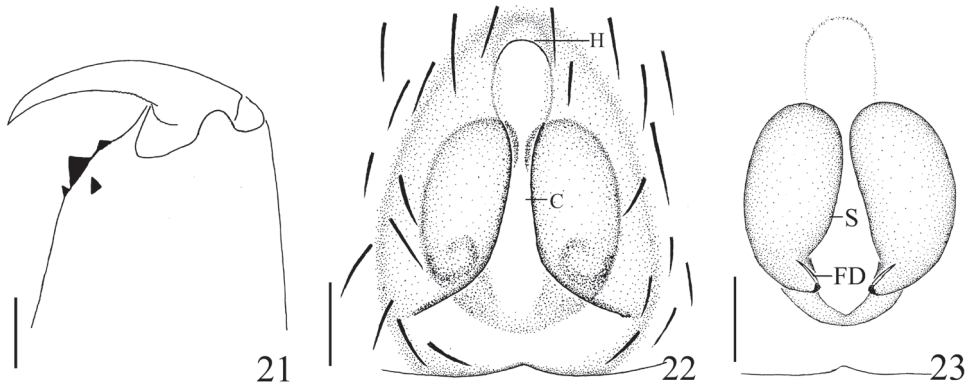
**Figures 17–20.** *Hitobia makotoi* Kamura, 2011 **17** female body, dorsal view **18** prosoma, ventral view **19** epigyne, ventral view **20** vulva, dorsal view. Scale bars: 0.5 mm (**17–18**); 0.1 mm (**19–20**).

***Hitobia makotoi* Kamura, 2011**

Figs 17–23

*Hitobia makotoi* Kamura, 2011: 104, f. 3–7 (Df).

**Material examined.** 1♀, **China, Yunnan:** Tengchong County, Qingshui Township, Rehai area, Liangyong Village (24°94.919'N, 98°44.921'E, 1450 m), 1 June 2006, D. H. Kavanaugh, R. L. Brett, Dazhi Dong leg.



**Figures 21–23.** *Hitobia makotoi* Kamura, 2011, **21** left chelicera, posterior view **22** epigynum, ventral view **23** vulva, dorsal view. Scale bars: 0.1 mm (**21–23**). C concavity FD fertilization ducts H hood S spermathecae.

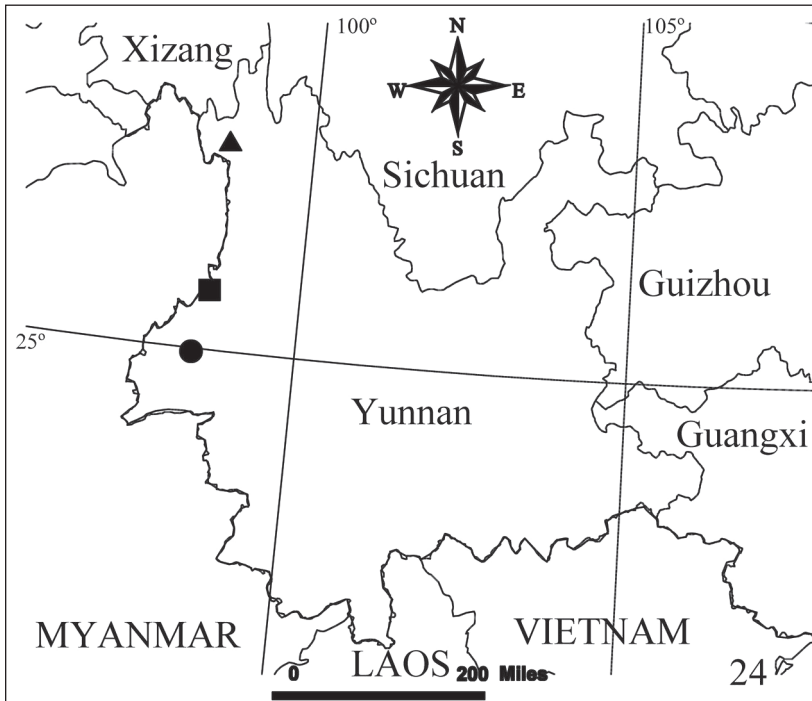


**Figure 24.** Distribution records of the three species of genus *Hitobia* from south-west China. ▲ *H. hirtella*; ■ *H. tengchong*; ● *H. makotoi*.

**Description. Female:** Total length 5.08. Prosoma 2.28 long, 1.45 wide. Opisthosoma 2.63 long, 1.47 wide. Clypeus 0.06 high. Carapace blackish brown, long oval, widest at coxae II and III, covered with some white hair. Fovea, cervical grooves indistinct. AER and PER both slightly recurved, wider posteriorly. Eyes sizes and interdistances: AME

0.09, ALE 0.09, PME 0.07, PLE 0.08, AME–AME 0.03, AME–ALE 0.01, PME–PME 0.08, PME–PLE 0.09, ALE–PLE 0.13. MOA anterior width 0.18, posterior width 0.21, length 0.23. Chelicerae dark brown, with 3 promarginal teeth and 1 retromarginal (Fig. 21). Endites narrowed medianly and slightly convergent apically, almost parallel (Fig. 18). Labium yellowish brown, longer than wide, ligulate (Fig. 18). Sternum colored as labium, with some dark bristles, anterior straight and posterior subacute (Fig. 18). Legs femur, trochanters I and II, coxae I and II brown, others light yellow. Trochanters I and II without ventral notch, trochanters III and IV with a shallow ventral notch. Legs spination: femur: I, II v1-1-1; III d1-1-1, p0-0-1; IV d1-1-1, r0-0-1; patella: I, II, III, IV; tibia: I v1-1-1; II v1-0-0; III d1-1-0, p1-0-0, v1-2-1, r1-1-1; IV v1-0-2, r0-1-1; metatarsi: I d0-1-0; II v1-0-0; III d0-1-1, p0-1-1, v1-0-2, r1-0-1; IV d1-1-0, p0-1-0, v0-2-1, r0-0-1. Measurements of legs: I 4.36 (1.35, 1.65, 0.75, 0.61), II 4.28 (1.30, 1.62, 0.75, 0.61), III 4.21 (1.15, 1.31, 1.00, 0.75), IV 5.30 (1.75, 1.85, 1.00, 0.70). Dorsum of opisthosoma (Fig. 17) grayish brown, long oval, with three pairs of muscle impressions at central part and one narrow transverse white stripe posteriorly, covered with recumbent hair. Venter pale brown. Spinneret cylindrical, median spinneret long, with spigots on distal part, blackish brow.

Epigyne (Figs 19–20, 22–23) longer than wide, with a distinct anterior hood, and shallow longitudinal concavity in median part. Spermathecae big, elongated and the distal parts close to each other.

**Male:** Unknown.

**Distribution.** China (Yunnan), Japan (Amami-ōshima Is.).

**Comments.** Although the spermathecae of the specimen are smaller, the distal parts close to each other (almost parallel to each other in the original description of Kamura (2011)), the following characters of the specimen are almost as same as those described in the original description: the position and form of stripes on the dorsum of opisthosoma; epigyne with a distinct anterior hood, a shallow longitudinal concavity in median part, copulatory opening indistinct; hence the specimen was identified as *Hitobia makotoi* Kamura, 2011.

## Acknowledgements

We are grateful to Dr. Peter Fritsch (California Academy of Sciences) and Prof. Heng Li (Kunming Institute of Botany, Chinese Academy of Science Kunming Institute of Botany, Chinese Academy of Science) for supporting the joint biodiversity survey of the Gaoligong Mountains. We thank Prof. D. H. Kavanaugh, R. L. Brett, Hengmei Yan, Xingping Wang and Mr. Dazhi Dong for collecting the specimens. Special thanks also should be given to Prof. T. Kamura for his kind help on specimens identification. This research was sponsored by the National Science Foundation of the USA through the grant “Biotic survey of the Gaoligongshan, a biodiversity hotspot in western Yunnan, China” (No. DEB-0103795). It is also partly supported by the National Natural Sciences Foundation of China (NSFC-30970327, 31272271, 31272272),

Hunan Provincial Natural Science Foundation of China (No.11JJ1004/12JJ3028), Program for New Century Excellent Talents in University (NCET-12-0717), China Postdoctoral Science Foundation (No. 20100471221/201104506), the program of Hunan Provincial Science and Technology Plans (No. 2010RS4006) and by the Hunan Provincial Program for Development of Key Disciplines in Ecology.

## References

- Deeleman-Reinhold CL (2001) Forest spiders of South East Asia: with a revision of the sac and ground spiders (Araneae: Clubionidae, Corinnidae, Liocranidae, Gnaphosidae, Prodidomidae and Trochanteriidae [sic]). Brill, Leiden, 591 pp.
- Kamura T (1992) Two new genera of the family Gnaphosidae (Araneae) from Japan. *Acta arachnol* 41: 119–132.
- Kamura T (2009) Trochanteriidae, Gnaphosidae, Prodidomidae, Corinnidae. In: Ono H (Ed.) *The Spiders of Japan with keys to the families and genera and illustrations of the species*. Tokai University Press, Kanagawa, 482–500, 551–557.
- Kamura T (2011) Two new species of the genera *Drassyllus* and *Hitobia* (Araneae: Gnaphosidae) from Amami-ōshima Island, southwest Japan [J]. *Acta Arachnologica* 60 (2): 103–106. doi: 10.2476/asjaa.60.103
- Platnick NI (2013) The world spider catalog, version 14.5. American Museum of Natural History. <http://research.amnh.org/entomology/spiders/catalog/> [accessed 31 December 2013]
- Song DX, Zhu MS, Chen J (1999) *The Spiders of China*. Hebei Science and Technology Publishing House, Shijiazhuang, 640.
- Song DX, Zhu MS, Zhang F (2004) *Fauna Sinica: Arachnida: Araneae: Gnaphosidae*. Science Press, Beijing, 362 pp.
- Wang JL, Peng XJ (2013) Description of *Leucauge tengchongensis* sp. nov. and the female of *Okileucauge elongatus* from Yunnan, China (Araneae: Tetragnathidae). *Acta Arachnol. Sin.* 22: 16–23.
- Yin CM, Peng XJ, Gong LS, Kim JP (1996) Description of three new species of the genus *Hitobia* (Araneae: Gnaphosidae) from China. *Korean Arachnology* 12(2): 47–54.
- Yin CM, Peng XJ, Yan HM, Bao YH, Xu X, Tang G, Zhou SQ, Liu P (2012) *Fauna Hunan: Araneae in Hunan, China*. Hunan Science and Technology Press, Changsha, 1590 pp.
- Zhang F, Zhu MS, Tso IM (2009) Three new species and two new records of Gnaphosidae (Arachnida: Araneae) from Taiwan. *Journal of Hebei Normal University* 29: 528–532.

# A new species of tiger beetle from southeastern Arizona and Mexico (Coleoptera, Carabidae, Cicindelini)

Daniel P. Duran<sup>1</sup>, Stephen J. Roman<sup>2</sup>

<sup>1</sup> Department of Biodiversity, Earth and Environmental Sciences, Drexel University, 3245 Chestnut St., Philadelphia, PA 19104, USA <sup>2</sup> 5335 Oxbow Place, Champlin, MN 55316, USA

Corresponding author: Daniel P. Duran ([dpd56@drexel.edu](mailto:dpd56@drexel.edu))

---

Academic editor: Terry Erwin\* | Received 12 August 2014 | Accepted 4 December 2014 | Published 16 December 2014

<http://zoobank.org/50F680BE-37C4-43FD-A099-8D9D25062783>

---

**Citation:** Duran DP, Roman SJ (2014) A new species of tiger beetle from southeastern Arizona and Mexico (Coleoptera, Carabidae, Cicindelini). ZooKeys 464: 35–47. doi: 10.3897/zookeys.464.8424

---

## Abstract

A new tiger beetle species, *Cicindelidia melissa* Duran & Roman, **sp. n.**, of the tribe Cicindelini, is described from high elevation montane forests of southeastern Arizona and Mexico. It appears to be most closely related to *C. nebuligera* (Bates) but is distinguished on the basis of multiple morphological characters and geographic range. The new species is also superficially similar to the widespread *C. sedecimpunctata* (Klug), but distinguished on the basis of multiple morphological characters and habitat. Habitus, male and female reproductive structures, and known distribution map are presented.

## Keywords

Coleoptera, Cicindelini, *Cicindelidia*, new species, Arizona, Chiracahua Mountains, Mexico

---

\* Subject Editor's Note: This single new species description was accepted due to a need in the forthcoming book by Pearson et al. "A field guide to the Tiger Beetles of the United States and Canada" (Second Edition). Oxford University Press.

## Introduction

The New World tiger beetle genus *Cicindelidia* Rivalier (1954) includes approximately 60 described species (Wiesner 1992) and is distributed from Canada south to Chile, reaching its highest diversity in Mexico and the southern United States. Members of the genus are diurnally active insect predators and are typically found in open or sparsely vegetated muddy, rocky, or sandy habitats. The majority of species inhabit areas that range from sea level to mid elevations, with only a few species known to occur at elevations above 2000 m. Herein we describe *C. melissa* sp. n., an inhabitant of high elevation Ponderosa pine forests and discuss its hypothesized systematic placement within the genus.

## Methods

Specimens of a previously undescribed *Cicindelidia* had been collected over the past several decades by David Brzoska (Naples, FL), Ron Huber (Bloomington, MN), Walter Johnson (Minneapolis, MN) and John Stamatov (Armonk, NY) from a site in the Chiracahua Mountains of southeastern Arizona and from 29 localities in the Mexican states of Sonora, Chihuahua and Durango. Additional Chiracahua specimens were collected in 2009 by Eric Sangregorio and donated to the first author. In total the authors examined 153 specimens of the new species. Type material is deposited in the following institutional and private collections (acronyms used in the text are in parentheses): National Museum of Natural History, Smithsonian Institution, Washington, DC, USA (NMNH), Arizona State University Frank Hasbrouck Entomology Collection, Tempe, AZ (ASUHIC), Collection of David W. Brzoska, Naples, FL (DWBC), Ronald L. Huber Collection, Bloomington, MN (RLHC), Collection of Walter N. Johnson, MN (WNJC), Collection of Daniel P. Duran, Philadelphia, PA (DPDC), Collection of John Stamatov, Armonk, NY (JSC). Specimens were compared to material of all putative close relatives, including *C. sedecimpunctata* and its subordinate taxa *mellyi* and *sallei*, *C. flobri*, and *C. nebuligera*.

Images of the dorsal, lateral, and frontal habitus and elytral apex were captured using a Canon EOS 7D attached to a Visionary Digital Imaging System (Visionary Digital, Palmyra, VA). Images were then montaged and edited using Adobe Photoshop. Genitalia were extracted, manually cleaned with minuten pins and 10% KOH solution, and placed on glycerin slide mounts for observation and imaging. Scale bars were calibrated with an ocular micrometer using SPOT Advanced software on the images of the genitalia, which were taken with a digital camera attached to a Nikon SMZ1500 dissecting microscope. The final digital images were processed using Adobe Photoshop CS6. The distribution map was created with Quantum GIS Version 1.4.0.

Body measurements are defined as in Duran and Moravek (2013) and are as follows. The total body length excludes the labrum and is measured as the distance from the anterior margin of the clypeus to the elytral apex, including the sutural spine. The width of the pronotum is measured to include the lateral margins of the proepisterna. The width of the head is measured as the distance between the outer margins of the eyes.

## Systematics

### *Cicindelidia melissa* Duran & Roman, sp. n.

<http://zoobank.org/E474385B-6B10-474A-A705-1F340C0B8FD5>

Figs 2–10

**Type material.** HOLOTYPE: ♂, “USA, Arizona / Cochise Co / Barfoot Park (31.910, -109.273) D. Brzoska Aug 4, 2012” (USNM). ALLOTYPE: ♀, “USA, Arizona / Cochise Co / Barfoot Park (31.910, -109.273) D. Brzoska, Aug 4, 2012” (USNM).

PARATYPES: 1 ♂, USA, Portal Ariz / Barfoot Park / 08-VIII-1957 8000ft. / leg J.R.Beer. 13 ♂♂, 9 ♀♀, same label data as Holotype. 1 ♂, 3 ♀♀, USA, Arizona / Cochise Co / Barfoot Park (31.910, -109.273) E. Sangregorio, Aug 4, 2009. 1 ♂, 1 ♀, MEXICO, Chihuahua / Hwy.25 km157, .5 S. Cusarare (27.332, -107.005) D. Brzoska, July 29, 2005. 1 ♂, 1 ♀, MEXICO, Chihuahua / Road to Z.A. Conjunio Anasezi / 1.6mi. S., .09mi. W-Madera (29.172, -108.173) D. Brzoska, July 11, 1997. 1 ♂, 1 ♀, MEXICO, Chihuahua / Creel, Divisadero Rd, 0.5m S Divisadero (29.528, -107.830) D. Brzoska, July 21, 2005. 1 ♂, 1 ♀, MEXICO, Chihuahua / Hwy. 26, (Road to Topia), km 38 (25.063, -105.655) D. Brzoska, July 24, 1997. 2 ♂♂, 2 ♀♀, MEXICO, Chihuahua / Chi Hwy. 25, E. of/ Guachochi-km104 / 26-VII-2005 R.L. Huber. 1 ♂, MEXICO; Chihuahua / Chi Hy 25 KM 157/ 20-VII-2005 R.L. Huber. 2 ♂♂, MEXICO, Chihuahua / KM 25 Road to Batopilas / Quirare Village / 26-VII-2005 R.L. Huber. 3 ♂♂, MEXICO, Chihuahua / km 18, N of Batopilas / Road to Creel / 21-VII-2005 R.L. Huber. 4 ♂♂, 9 ♀♀, MEXICO, Chihuahua / Chi Hwy 25 KM 157 / S of Cusarare / 26-VII-2005 R.L. Huber. 3 ♂♂, 4 ♀♀, MEXICO, Chihuahua / Ej.Guadalupe Victoria / 9.8mi W. San Jose Babicora / on Hwy 180, near km 14 / 10-VII-1992 R.L. Huber. 1 ♀, MEXICO, Chihuahua / Hwy 180 9.1 mi W / San Jose Bibicora / 13-VIII-1989 R.L. Huber. 1 ♀, MX / Chihuahua; Madera / June 1966 leg B. Rotger. 1 ♂, MX Chihuahua / 20mi S la Junta / 29-VI-1989 D.B. Thomas and J.C. Burne.

5 ♂♂, 2 ♀♀, MEX, Chihuahua / Road to Divisadero / (27°38.72N, 107°46.27W) / July 2, 1997 R.L. Huber. 5 ♂♂, 6 ♀♀, MEX, Chihuahua / .5mi S Divisadero / (27°31.69N, 107°49.80W) / July 12, 1997, R.L. Huber. 2 ♂♂, 2 ♀♀, MEX, Chihuahua / S. of Creel / (27°41.64N, 107°35.14W) / July 12, 1997 R.L. Huber. 1 ♂, 2 ♀♀, MEX, Chihuahua / Ejido Guadalupe / (29°12.86N, 107°52.81W) / July 11, 1997 R.L. Huber. 1 ♂, 2 ♀♀, MEX, Chihuahua / 2mi SW Madera / Rd to Sirupa / (29°10.21N, 108°09.64W) / July 11, 1997 R.L. Huber. 2 ♂♂, 1 ♀, MEX, Chihuahua / 2.5mi W Madera / Rd to Huapaca Archaeo site / (29°10.29N, 108°10.40W) / July 11, 1997, R.L. Huber. 1 ♂, 1 ♀ MEX, Chihuahua / N of Madera / HWY 11, KM13.5 / (29°18.8N, 108°08.4W) / July 25, 2008 R.L. Huber.

1 ♀, MEX, Chihuahua / Ejido Guadalupe Victoria / HWY 10, km 13.5 / (29°12.9N, 107°52.3W), 2300m / Aug 06, 2008 R.L. Huber. 1 ♂, MEX, Chihuahua / Creel N. HWY 25 KM72 / (27°51.7N, 107°34.7W), 2362m / Aug 05, 2008 R.L. Huber. 1 ♂, MEX, Chihuahua / San Juanito, NNW / on Chi HWY110 KM5.5 /



**Figure 1.** Habitat of *Cicindelidia melissa*, Durango, Mexico. Photo by Walter Johnson.

(27°58.9N, 107°31.9W), 2440m / Aug 05.2008 R.L. Huber. 1 ♀, MEX, Chihuahua / 5KM S Madera, Rd to Sirupa / (29°09.0N, 108°10.6W), 2230m / July 25, 2008 R L Huber. 1 ♂, MX Chihuahua / Hwy 180 9.1 mi W / San Jose Bibicora / 13-VIII -1989 R.L. Huber. 2 ♂♂, 3 ♀♀, Durango Mexico / Lagoya de Golondrines / July 23, 1997 / Walter N Johnson. 2 ♂♂, 1 ♀, Durango Mexico / Rancho Chapultepec / July 23, 1997 / Walter N Johnson. 3 ♂♂, 1 ♀ Durango Mexico / Los Altares, HWY 26 / July 24, 1997 / Walter N Johnson. 3 ♂♂, 1 ♀, Durango Mexico / Los Ranos / July 23, 1997 / Walter N Johnson. 1 ♀, Durango Mexico / Los Ranos / July 24, 1997 / Walter N Johnson. 2 ♂♂, Durango Mexico / 2.5mi E. Los Ranos / July 23, 1997 / Walter N Johnson. 9 ♂♂, 5 ♀♀, MEXICO Chihuahua / Ejodo Guadalupe Victoria / 9.8 mi W S.J. Bibicora / 10-VII-1992 J.Stamatov. 4 ♂♂, 6 ♀♀, MEXICO Chihuahua / Hy 25, km157.5 2172m / S of Cusarare (27°19.9 107°30.3) / July-26-2005 Coll: J. Stamatov. 1 ♂, 3 ♀♀, MEXICO Durango / 13.5 mi E of Canelas / 15-VII-1997 / Coll: J. Stamatov.

All type specimens labelled: HOLOTYPE, ALLOTYPE or PARATYPE, respectively.

**Diagnosis.** This species can be distinguished from all other similar *Cicindelidia* by its dark green-violet abdominal venter with the two apical segments dull orange or orange-brown, a brassy-cupreous head and pronotum with metallic blue reflections in sulci, small shallow subsutural foveae present in most individuals, and microserrate elytral apices. It inhabits rocky upland soils in ponderosa pine forests above 2000 m (Fig. 1). *C. sedecimpunctata* (Klug, 1834) has an entirely orange-red to orange-brown

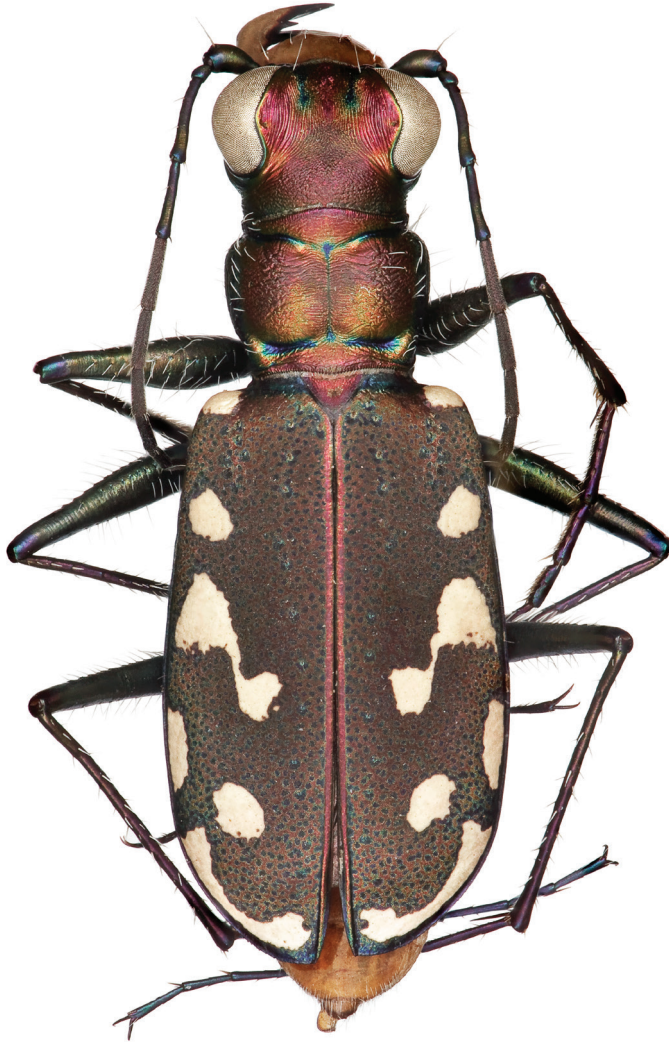


**Figure 2.** Dorsal habitus of male (holotype).

abdominal venter, a more uniform dull brown dorsal coloration, and lacks apparent subsutural foveae. It also differs from the new species by inhabiting muddy ground at nearly any elevation. *C. nebuligera* (Bates, 1890) has dark elytral infuscations that surround the middle band, and lacks elytral apical microserrations. It may be found in similar habitats, but is apparently allopatric with the new species and does not appear to be restricted to elevations above 2000 m.

**Description.** Small to medium sized *Cicindelidia*. Body (Figs 2–5) length 7.90–10.50 mm, mean ♀ 9.7 mm, mean ♂ 9.0 mm. Head (Figs 6–7) slightly wider than pronotum, width 2.3–2.7 mm, brassy-cupreous red with metallic blue and cupreous reflections present in sulci, all head portions glabrous except for 2 supraorbital setae

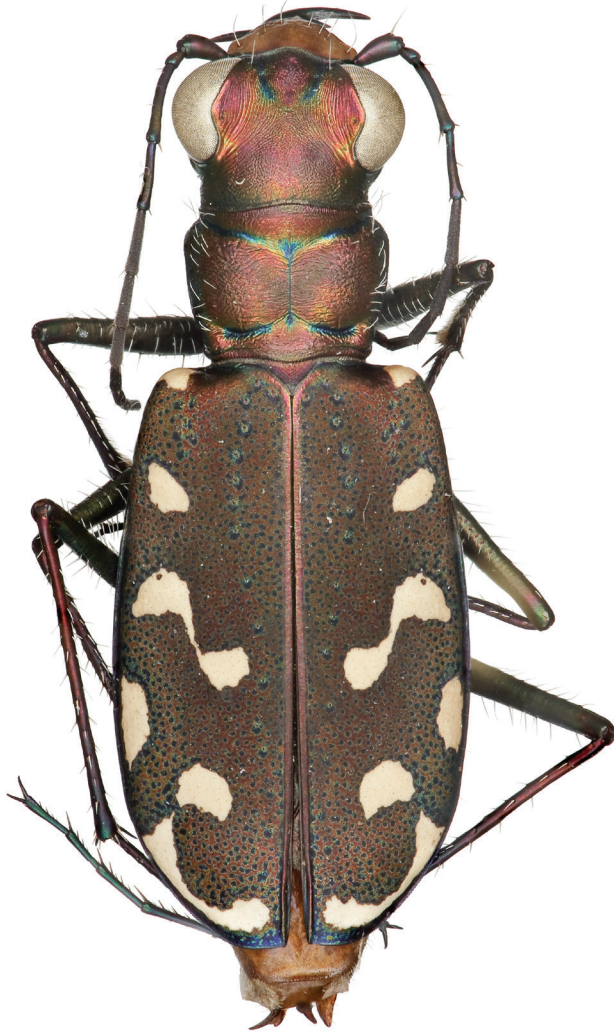


**Figure 3.** Dorsal habitus of female (allotype).



**Figure 4.** Lateral habitus of male (holotype).



**Figure 5.** Lateral habitus of female (allotype).

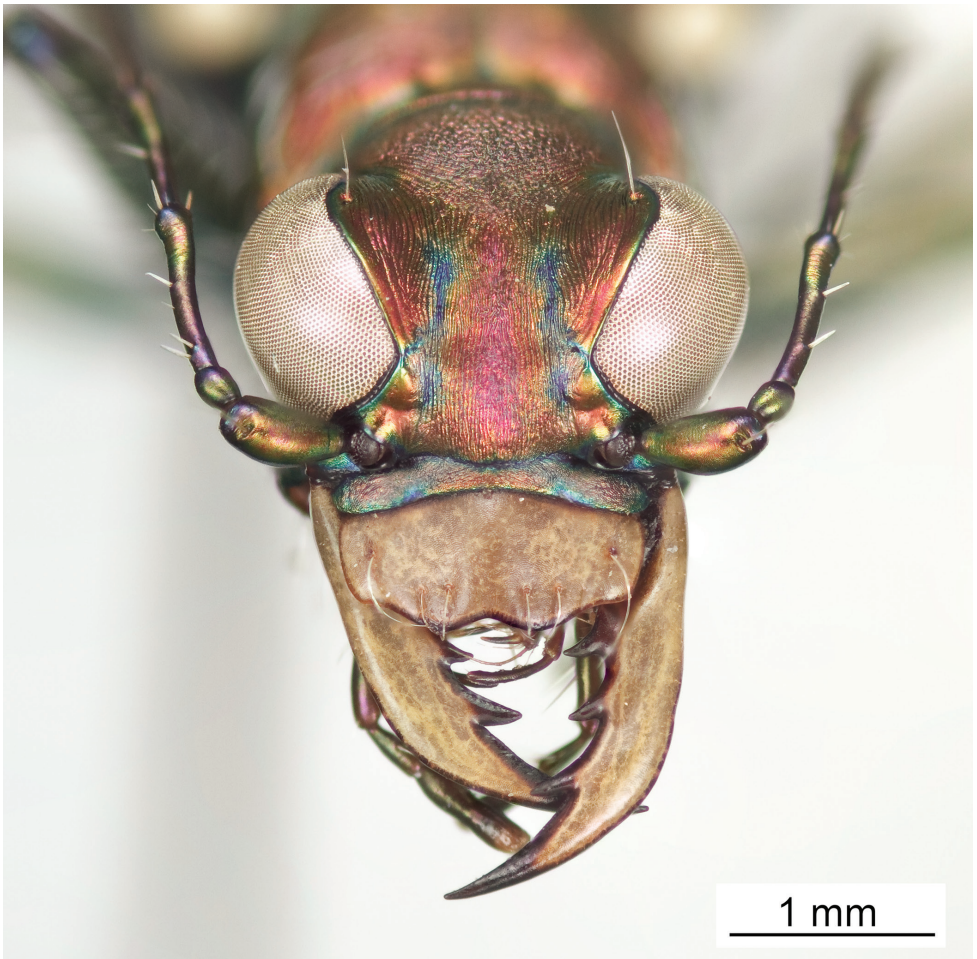


**Figure 6.** Frontal habitus of male (holotype).

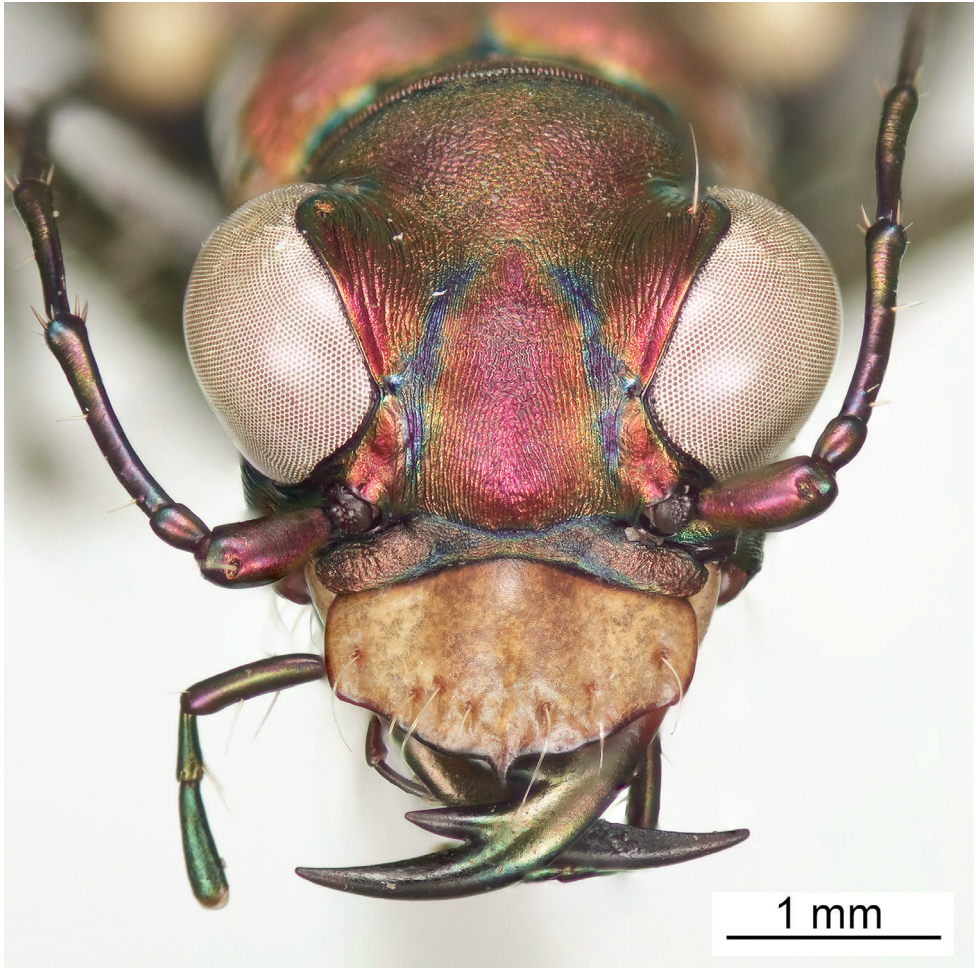


**Figure 7.** Frontal habitus of female (allotype).

next to each eye. Frons concave in median area especially in male, bulging towards slightly convex near anterior margin, clearly delimited from clypeus, gradually blending into vertex. Frons surface with distinct longitudinal striae especially in lateral areas bordering eyes, vermiculate-striate in median area. Vertex dark brassy colored, slightly convex, with surface indistinctly finely vermiculate, posterior areas with cupreous-olive lustre. Genae bright polished copper with deep longitudinal striae abruptly ending at border of vertex. Clypeus cupreous blending to blue along borders, irregularly wrinkled to finely vermiculate. Labrum with 6 setae, ochre-testaceous with a thin dark brown to black border; female labrum rather long, length 0.60–0.90 mm, width 1.3–1.6 mm, with single median tooth; male labrum short to medium, length 0.45–0.80 mm, width 1.2–1.7 mm, shape varies from nearly straight across anterior edge with only slightly protruding median tooth to an unusual slightly notched median edge (see holotype).

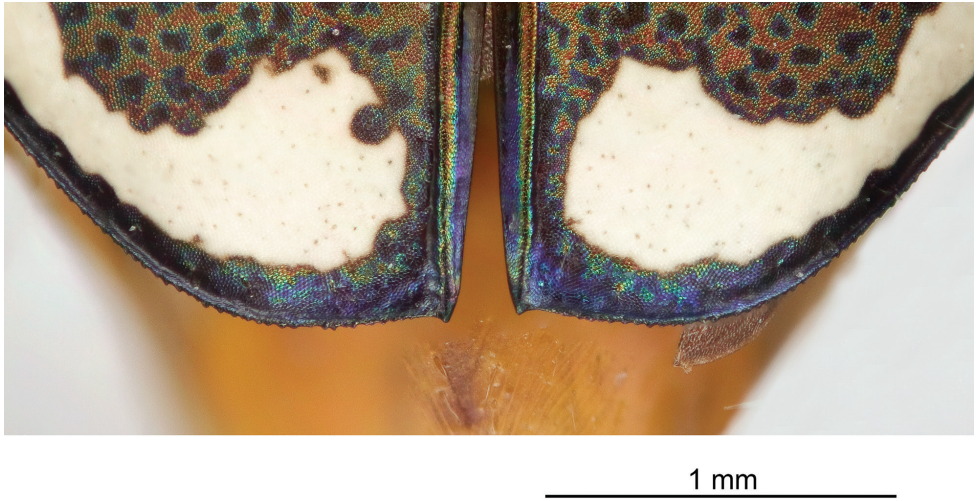


**Figure 8.** Elytral apex, showing microsculpture and apical spine.



**Figure 9.** Cleared aedeagus in ventral and lateral (left side) views.



**Figure 10.** Ovipositor in ventral view.

Mandibles medium-sized, ochraceous in male, dark ochraceous with metallic gold, green and black reflections in female, teeth of both sexes dark testaceous along edges. Maxillary palpi dark testaceous with metallic reflections; apical segment usually darker than sub-apical segment. Labial palpi in male ivory to pale yellow-ochre in male with dark metallic green to violet apical segment, in female entirely dark testaceous with metallic reflections throughout. Antennae normal length, reaching humerus to basal third of elytron, slightly longer in male than female; scape dark testaceous to black with metallic reflections of cupreous, gold, and violet, with a single apical seta; pedicel dark testaceous with metallic reflections of cupreous, gold, and violet, lacking any setae; flagellum dark testaceous, antennomeres 3–4 with metallic cupreous and violet reflections, with ring of apical setae and additional sparse setae throughout, antennomeres 5–11 dull textured without metallic reflections and possessing erect setae in apical rings only, covered with fine pubescence throughout.

Thorax. Pronotum 1.70–2.50 mm in width, slightly polished with metallic finish, brassy-cupreous with metallic blue or blue-green sulci, slightly wider than long, nearly trapezoidal in shape and widest near anterior margin, width to length ratio 1.2 to 1.3, setae sparse and present along lateral third of dorsal surface; disc finely rugose to vermiculate with thin but distinct median line and deeply impressed sulci; notopleural sutures clearly defined, not visible from dorsal view; proepisternum bright polished copper with gold and green reflections more ventrally, abruptly transitioning to blue-violet on ventral third and posterior third, in male setae present throughout surface of

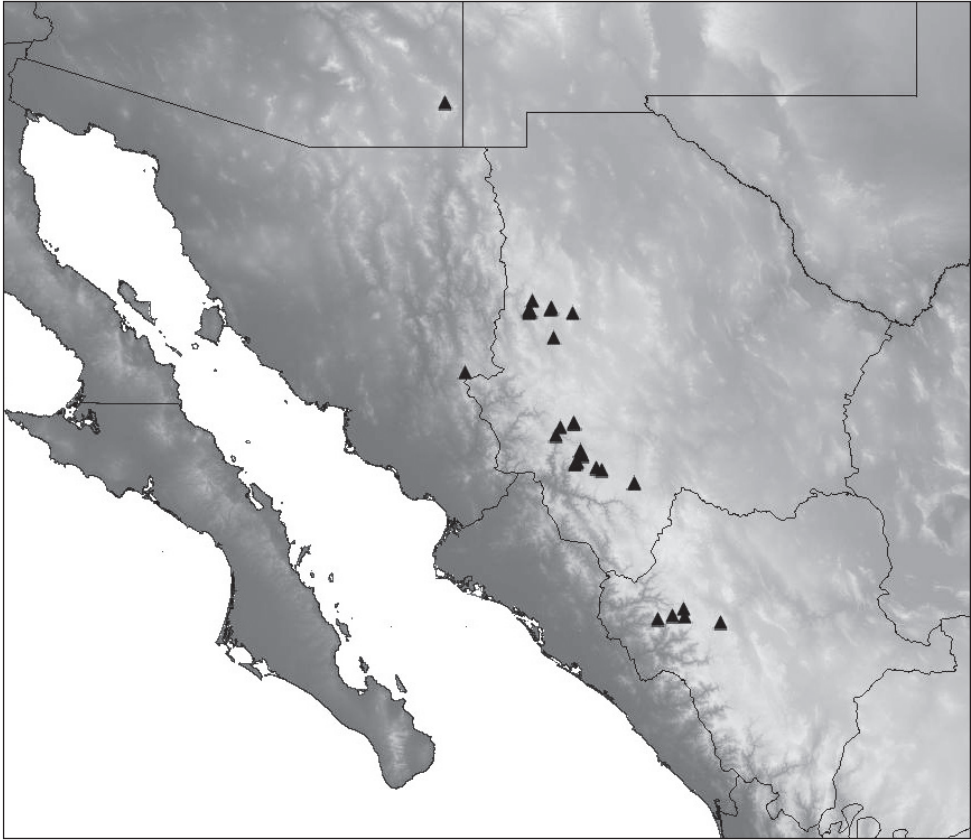


**Figure 11.** Distribution map of the known localities for *Cicindelidia melissa*. Lines indicate political boundaries of states in Mexico and the United States. Shading indicates topographical relief.

proepisternum, but in female setae are typically sparsely present only along ventral third and along anterior margin; all other ventral segments of thorax are glabrous, dark blue-violet to black with greenish reflections. Elytra elongate, 5.1–6.7 mm length, shape similar in both sexes, but slightly wider in female, especially toward apical third; sutural spine small to nearly absent, fine microserrations present on elytral apices (Fig. 8), extremely fine to nearly indistinct in some individuals; elytral dorsal surface relatively flat, not markedly convex, texture dull throughout with slight metallic sheen near pronotal base in a some individuals, elytral coloration mostly a dull cupreous brown color, under magnification this color is comprised of the pointillistic mixing of mostly cupreous ground color with many small patches of dark blue-violet bordered in green; subsutural foveae are present, but nearly indistinct in a small percentage of individuals; elytral maculations white, and consist of a small humeral and posthumeral spot, a moderately short middle band which does not touch the margin and with “knee” and “foot” regions connected with a thin but complete line, an isolated marginal spot between the middle

band and apical lunule, and an apical lunule comprised of a subapical spot that is broken from the thin apical line; epipleura dark blue-violet to black.

Legs. Procoxae and mesocoxae dark metallic green to black, covered in dense setae; metacoxae dark metallic green to blue-violet to black, with a single apical setae present; trochanters glabrous, dark green to violet-black; femora dark metallic green with blue-violet reflections near the insertion of the tibia, femoral surface with rows of erect white setae dorsally and ventrally; tibiae violet to dark cupreous with dark green reflections near the apices, clothed with white setae that are sparser and shorter than those of the femora; tarsi violet with blue reflections dorsally, first three dilated protarsomeres in male with dense greyish-white setal pad.

Abdomen. Ventrites 1–4 dark violet with strong metallic greenish reflections throughout most surfaces, dark orange to testaceous coloration along lateral edges in some individuals, setae present mostly along lateral third of each ventrite; ventrites 5–6 orange to dark orange-testaceous throughout, setae present along lateral margins, but often abraded.

Reproductive structures. Aedeagus (Fig. 9) elongate, widest in middle, length 3.40–3.60 mm, width 0.65–0.75 mm, slightly arcuate in ventral view, apical portion produced into a narrow tip with a slight hooklike projection; internal sac and sclerites prominent in cleared aedeagus and visible both ventrally and laterally. Ovipositor (Fig. 10) deeply notched and possessing two heavily sclerotized bifurcated hooks ventrally, setae present especially along lateral margins and near base of hooks.

**Etymology.** This new *Cicindelidia* is named after the first author's wife, Melissa, for her constant support, love, and friendship.

**Distribution and habitat.** *C. melissa* is currently known from northwestern Durango, western Chihuahua, eastern Sonora, and southeastern Arizona. All known occurrences are from forested hillsides and trails above 2000 m. Typical habitats contain rocky substrates derived from limestone and/or rhyolite, with forest cover generally dominated by Ponderosa pine. This species is mostly active following monsoon rains, but frequents upland areas and is not closely associated with muddy or riparian microhabitats.

## Discussion

Given the superficial similarity to *C. sedecimpunctata* in dorsal habitus, *C. melissa* may have been overlooked and assumed to be a form of that widely distributed species. However, despite the general resemblance, multiple diagnostic morphological characters exist, as discussed above. Previous authors acknowledged that additional cryptic species may be present in the *C. sedecimpunctata/rufiventris* group (Cazier 1954, Murray 1980), but the taxonomy of the group has not been revisited since. The relatively small number of available specimens of *C. melissa* in museums is likely due to its occurrence in less-accessible geographic areas and in a habitat that is less visited by most tiger beetle collectors.

It is interesting to note that the ecological differences between *C. melissa* and *C. sedecimpunctata* are stark, and habitat alone separates the two species in almost all cases. Tiger beetle taxonomy has relied nearly exclusively on fixed morphological characters to date, yet we believe that this present example underscores the importance of habitat

and ecological factors that may not be apparent when comparing dead specimens of tiger beetles. Given the ecological and morphological similarities and apparently allopatric ranges, we propose that *C. melissa* and *C. nebuligera* are most closely related. Increasingly, higher-level and species-level phylogenies are based on molecular data, in part or entirely, and recent authors have examined relationships of Nearctic tiger beetles (Vogler et al 2005), although Mexican species were not as well represented. The authors of this description are conducting a thorough revision of *Cicindelidia* using a combination of molecular, morphological, and ecological characters, and this species description is the first of a series of papers on the group.

## Acknowledgements

The authors thank David W. Brzoska, Ronald L. Huber, John Stamatov, and Eric Sangregorio for providing specimens for this study. We also thank Walter Johnson for providing specimens and for the habitat photograph used in Figure 1. The first author thanks Floyd Shockley (Smithsonian Institution) for his help with preparation of the aedeagus and for comments on the manuscript. We also thank Karie Darrow (Smithsonian Institution) for taking the images for Figures 2–10. Finally, we thank two anonymous reviewers for providing comments on the manuscript.

## References

- Bates HW (1890) Additions to the Cicindelidae fauna of Mexico, with remarks on some of the previously-recorded species. The Transactions of the Entomological Society of London for the year 1890: 493–510.
- Cazier MA (1954) A review of the Mexican tiger beetles of the genus *Cicindela* (Coleoptera, Cicindelidae). Bulletin of the American Museum of Natural History 103: 227–310.
- Duran DP, Moravek J (2013) A new species of the genus *Pentacomia* from Panama (Coleoptera: Cicindelidae). Acta Entomologica Musei Nationalis Pragae 53(1): 49–57.
- Klug JCF (1834) Uebersicht der Cicindelidae der sammlung des Berliner Museum. Jahrbücher der Insectenkunde, mit besonderer Rücksicht auf die Sammlung im Königl. Museum zu Berlin, 1, 296 pp.
- Murray RR (1980) Systematics of *Cicindela rufiventris* Dejean, *Cicindela sedecimpunctata* Klug, and *Cicindela flobri* Bates (Coleoptera: Cicindelidae). PhD dissertation, Texas A&M University, 301 pp.
- Rivalier E (1954) Démembrement du genre *Cicindela* Linné. II. Faune américaine. Revue Française d'Entomologie 21(4): 249–268.
- Vogler AP, Cardoso A, Barraclough TG (2005) Exploring Rate Variation Among and Within Sites in a Densely Sampled Tree: Species Level Phylogenetics of North American Tiger Beetles (Genus *Cicindela*). Systematic Biology 54(1): 4–20. doi: 10.1080/10635150590906028
- Wiesner J (1992) Verzeichis der Sandlaufkäfer der Welt. Verlag, Erna Bauer, Keltern-Weiler, Germany. 366 pp.



# Two new species of *Myrmedonota* Cameron (Staphylinidae, Aleocharinae) from Mexico

Quiyari J. Santiago-Jiménez<sup>1</sup>

<sup>1</sup> Museo de Zoología, Facultad de Biología-Xalapa, Universidad Veracruzana, Zona Universitaria, Circuito Gonzalo Aguirre Beltrán s/n, Xalapa, Veracruz, C.P. 91090, MÉXICO

Corresponding author: Quiyari J. Santiago-Jiménez ([qsantiago@uv.mx](mailto:qsantiago@uv.mx))

---

Academic editor: J. Klimaszewski | Received 3 September 2014 | Accepted 12 November 2014 | Published 16 December 2014

<http://zoobank.org/B809DD17-B7FA-4836-BDE2-A8E4CA3CDDC0>

---

**Citation:** Santiago-Jiménez QJ (2014) Two new species of *Myrmedonota* Cameron (Staphylinidae, Aleocharinae) from Mexico. ZooKeys 464: 49–62. doi: 10.3897/zookeys.464.8549

---

## Abstract

Two new species of *Myrmedonota* are described from Mexico. Illustrations and a distribution map are provided, as are keys to identify *Myrmedonota* known from the Nearctic and Neotropics. Specimens were collected by means of mercury vapor light traps or flight interception traps.

## Keywords

Lomechusini, false Lomechusini, Nearctic, Neotropical

## Introduction

Recently, Hlaváč et al. (2011) cataloged 207 genera and 2,205 species belonging to the Lomechusini tribe. Although the Lomechusini tribe is a polyphyletic group distributed around the world, a clade of false Lomechusini, distributed exclusively in the Neotropics, has been identified using molecular markers (Elven et al. 2010, 2012, pers. obs.).

The genus *Myrmedonota* was described originally by Cameron in 1920. It only included species distributed in Asia and was recently expanded, when Maruyama et al. (2008) redescribed the genus, to include two new species from North America. Later, Eldredge (2010) described another species from Kansas, U.S.A. The latter author included a key to the species distributed in the America, north of Mexico. Later, Mathis

and Eldredge (2014) described two other species of *Myrmedonota* from Mexico and included commentary on the taxonomy and behavior of this genus. Now, I am adding another two species to this genus, one each from the states of Veracruz and Jalisco in Mexico. The specimens match the generic characters outlined by Maruyama et al. (2008) in their redescription.

## Materials and methods

Between 2004 and 2006, on two field trips to Jalisco and Veracruz in Mexico specimens were collected using mercury vapor light traps or flight interception traps. The samples were preserved in 96% ethanol, and some of the specimens were identified as belonging to *Myrmedonota*.

The specimens were observed using a Stemi DV4 stereomicroscope. Photographs from slides were taken using an image processing system (VELAB microscope model VE-633, with Digital LCD model DMS-153). Whereas, habitus photographs were taken using an Stemi 2000-C, with digital camera Canon PowerShot G10. Images were merged using the image stacking software Combine ZP. Illustrations were made based on those photographs of the structures. Permanent microscope slides were prepared using the techniques described by Santiago-Jiménez (2010). The terminology used here follows Santiago-Jiménez (2010), and in some cases Ashe (1984). Holotypes and paratypes were deposited at the Museo de Zoología, Universidad Veracruzana, Xalapa, Veracruz, Mexico. Some paratypes will be deposited in IEXA.

## Taxonomy

### *Myrmedonota* Cameron, 1920

The genus was redescribed by Maruyama et al. (2008). More recently, Eldredge (2010) and Mathis and Eldredge (2014) proposed a diagnosis for the genus, based only partially on the characters used by Maruyama et al. (2008). For example, they didn't mention nothing about pronotum transverse or medial projection on apodeme that used Maruyama et al. (2008) on their diagnosis. Eldredge (2010) made a key to the species of North America, but it has some problems (e.g. body length in the key does not coincide with body length in the descriptions). To date, the species from Mexico have not been included in any key.

### Taxonomic comments

Mathis and Eldredge (2014) mentioned that pseudo-Lomechusini from the New World belong to Athetini based on a Bayesian analysis run by Elven et al. (2010).

However, there is a misunderstanding about the phylogenetic relationships, because the tree was not completely resolved to support the conclusion that *Myrmedonota* belongs to Athetini. However, there is evidence that false (i.e., misidentified) *Lomechusini* from the Neotropics are a completely different clade from those included in the true *Lomechusini* and *Athetini* based on molecular analysis with more taxa and more characters (Santiago-Jiménez and Gusarov, in prep.).

*Diagnosis.* Maruyama et al. (2008) characterized the genus as follows: 1) body surface finely punctate; 2) head with occipital suture; 3) pronotum transverse, >1.5 wider than long; 4) setation on abdomen sparse to moderate; 5) cardo of maxilla covers bases of stipes and lacinia; 6) lacinia extremely narrowed and parallel-sided; 7) mentum almost as long as wide; 8) apodeme of labium with medial projection; 9) 1<sup>st</sup> segment of labial palpus longer than 2<sup>nd</sup> segment; 10) each lobe of ligula with 2 setulae.

### Key to *Myrmedonota* species from the Nearctic and the Neotropics

- 1 Length of body 3.0 mm or less .....2
- Length of body more than 3.0 mm (maximum 4.2 mm) .....6
- 2 Pronotum yellowish; spermatheca with proximal end curved over itself (Fig. 20 in Eldredge 2010)..... ***M. heliantha* Eldredge**
- Pronotum reddish brown, dark brown or black; spermatheca with proximal end not curved over itself.....3
- 3 Abdominal segments unicolored, black; spermatheca V-shaped (Fig. 21 in Maruyama et al. 2008).....***M. lewisi* Maruyama & Klimaszewski**
- Abdominal segments bicolored, usually II–IV or only anterior half of IV paler than V–VIII; spermatheca S-shaped, or if V-shaped, then abdominal tergites bicolored, with II–III and base of IV dark brown, and posterior half of IV to VIII black.....4
- 4 Abdominal tergites II–IV dark brown, and V–VIII black; spermatheca V-shaped (Fig. 4 in Mathis and Eldredge 2014).....***M. shimmerale* Mathis & Eldredge**
- Abdominal tergites II–IV yellowish to reddish brown, with at most a dark brown spot on each one, and tergites V–VIII darker; spermatheca S-shaped.....5
- 5 Abdominal tergites II–IV yellowish with a dark spot on medial area of tergites III–IV (Fig. 2), tergites V–VIII black; apex of median lobe, short, slightly curved ventrally (Fig. 15); spermatheca with apex of the neck plain, as in Fig. 18.....***M. jaliscensis* sp. n.**
- Abdominal tergites II–IV reddish brown and V–VIII blackish brown (sometimes medial areas of tergite IV and V blackish brown); apex of median lobe, long, looking more sharply curved ventrally (Fig. 8 in Maruyama et al. 2008); spermatheca with apex of the neck concave (Fig. 12 in Maruyama et al. 2008) ..... ***M. aidani* Maruyama & Klimaszewski**
- 6 Pronotum yellowish to dark brown; elytra bicolored with humeral region yellow and rest of elytra dark brown; abdominal tergites II–IV yellowish and

- V–VIII dark brown to black (except basal region of tergite V is yellowish); apex of median lobe, slightly curved ventrally (Fig. 6 in Mathis and Eldredge 2014); spermatheca without accessory gland (Fig. 8 in Mathis and Eldredge 2014).....*M. xipe* Mathis & Eldredge
- Pronotum dark brown to black; elytra not bicolored, humeral region not yellow, elytra entirely brown; abdominal tergites III–V with apical region yellowish brown, appearing paler than the rest (Fig. 1); apex of median lobe, more sharply curved ventrally (Fig. 7); spermatheca with accessory gland close to the neck as in Fig. 10 .....*M. cordobensis* sp. n.

***Myrmedonota cordobensis* sp. n.**

<http://zoobank.org/0DC18D13-34C6-45A4-9978-7BE0C0095556>

Figures 1, 3–10, 19

**Type locality.** Mexico, Veracruz: Córdoba, Matlaquiahuitl, 1570m, 18°59'41"N, 96°53'35.1"W, cloud forest, light trap, 6.VII.2006, J. Asiain, J. Márquez, L. Delgado and Q. Santiago leg.

**Type material.** Holotype male, pinned. Original label: “MÉXICO: Veracruz, Córdoba, Matlaquiahuitl. 6.VII.2006. Bosque Mesófilo de Montaña perturbado, 1,570m, 18°59'41"N, 96°53'35.1"W, ex. trampa de luz. J. Asiain, J. Márquez, L. Delgado y Q. Santiago”/“MUZ-UV-COL-00000065”/“HOLOTYPE *Myrmedonota cordobensis* Santiago-Jiménez, 2014” [red label].

**Other material.** Paratypes, same data as holotype (42 males, 14 females MUZ-UV, IEXA).

**Description.** Body length: 3.5–4.1 mm. Most of body black to dark brown; elytra and legs brown; apical region of abdominal segments III–V, usually brown. Pubescence dense to sparse on head, pronotum and elytra, denser on elytra; dorsal surface of abdomen almost glabrous, dense pubescence on ventral surface of abdomen.

Head: Transverse, with or without impression on disc; without protuberance or carinae. Antennal articles 1–3 brown, 4–11 black, tip of 11 brown. Antennal articles 1–2 very elongate, 3–9 elongate, 10 slightly elongate, and 11 very elongate.

Mouthparts: Labrum: with 8 setae on each side of the midline; most of the setae on anterior half; with more than 30 sensory pores on each side of midline; sensillae on apical margin of epipharynx, arranged in a pattern of anterior or  $\alpha$ -sensilla, medial or  $\beta$ -sensilla, posterior or  $\gamma$ -sensilla, and lateral or  $\epsilon$ -sensilla, one on each side of the midline (see Ashe 1984, Santiago-Jiménez 2010); apico-medial margin of epipharynx not modified to setose or with spinose process; basal region of epipharynx with only four pores, more or less in one transverse row; medial region of epipharynx with more than 50 pores in an irregular array; mesal region of epipharynx without a multiporose sensory structure on each side of the midline; with 8 to 10 pores on mesolateral region. Mandibles: asymmetrical; right mandible with medial tooth on dorsal position; left mandible without tooth; without incisor tooth; with serration on apical half of both



**Figure 1.** Habitus of *Myrmedonota cordobensis* Santiago-Jiménez, sp. n., male.

mandibles; with large velvety patch wider than half of mandible base, composed of small denticles; prostheca with short setae along entire length, except base, which has a ctenidium; prosthecal setae not bifurcated in medial area. Maxilla: with a row of seven spines and two rows of large setae contiguous with the apical spines on apical third of the lacinia, between two rows of setae there is a glabrous area; the two rows of setae continue with numerous setae on middle third of the lacinia; practically glabrous on the basal third of the lacinia; with pseudopores on the cardo. Labium: with short ligula and divided near base; with a small pair of setulae on each lobe of the ligula (one very

short); without medial spines. Prementum with two medial setae, insertions widely separated; medial pseudopore field present; lateral pseudopore field composed of one setose pore, and two asetose pores, with setae on aboral margin of hypoglossa, adoral margin also with setae. Mentum without microsculpture on surface; with scarcely distributed pores on mentum (around 30 pores on each side of the midline), more densely distributed toward the apex.

Thorax: Pronotum transverse, wider on anterior third; surface finely punctured, moderately dense; without reticulate microsculpture; setae moderately dense on surface; with 4 macrosetae along lateral margins, 3 macrosetae on each side of the midline, 2 macrosetae between lateral and medial macrosetae, distributed on anterior half. Scutellum with surface smooth, moderately covered with short setae. Elytra slightly wider on apical area; surface finely punctured, moderately dense; without reticulate microsculpture; setae moderately dense, covering the surface; with 6 macrosetae: 3 on lateral margin, and 3 diagonally placed starting from the base of midline outward. Hind wings well developed, flabellum with 16–17 spines. Mesocoxal acetabula completely margined posteriorly. Mesocoxal cavities moderately separated (approx. 0.20 mm) by meso- and metaventral processes; mesoventral process short (approx. 0.18 mm) with apex truncated; metaventral process medium-sized (approx. 0.56 mm), marginate and with apex acuminate; isthmus distinctly present (approx. 0.09 mm). Legs short, tarsal formula 4–5–5, every leg with an empodium, one seta on empodium and a pair of tarsal claws, each claw with a subbasal tooth.

Abdomen: Subparallel-sided, narrower than elytra, wider around segments IV–V; surface smooth, tergites III–VII almost glabrous, but with a row of 3 macrosetae along posterior margins on each side of midline of every segment and one macroseta closer to the meso-lateral region; tergite VIII (Figs 3–4) with 5 macrosetae on each side of the midline; tergite IX with 4 macrosetae on each side of the midline; tergite X with 4 macrosetae on each side of the midline. Other conspicuous characters are: tergites III–VI with basal impression; sternite IV with a central and transverse reservoir, without glands on basal region, without striae or cuticle vesicles on anterocentral region, without spiracles on basal region, without transversal cuticular impressions on basal region, without pseudopores on basal region.

Secondary sexual structures: Sternite VII of male with external gland on basal region and pseudopores on posterior margin of gland. Tergite VIII of male (Fig. 3) with posterior margin truncate and crenate (around 6–7 denticles), and one lateral protrusion on each external margin. Tergite VII of female without external gland or pseudopores. Tergite VIII of female (Fig. 4) not crenate and without lateral protrusion. Sternite VIII of male and female as illustrated in Figures 5 and 6, respectively.

Aedeagus: Median lobe pear-shaped (Figs 7–8); internal sac of medial lobe with many spinules; median lobe with short, well defined compressor plate; apical lobe curved to the ventral side (visible in lateral view), and pointed; basal ridge convex. Paramere as in Fig. 9; anterodorsal margin of paramerite with prominent sensory pores present beneath the velar sac; hinge zone of paramerite faint, extended from dorsal surface to near articulation between condylite and paramerite; apical process of para-

merite clearly articulated anterior to edge of velum; condylite with a line of sensory pores; velum short (less than one half of the length of the paramere). Apical lobe with 4 macrosetae visible (see Eldredge 2010).

Spermatheca: Basal bulb simple, rounded at base; tube S-shaped; internal tube of neck with denticles; with accessory gland (Fig. 10).

**Remarks.** It is very similar in size to *M. xipe*, but *M. cordobensis* sp. n. is easy to distinguish because it is darker, the elytra are not bicolored, the apical region of tergites III–V is brown–yellowish, and the spermatheca is different in shape.

**Etymology.** The name makes reference to the municipality where the specimens were collected, Córdoba in the state of Veracruz.

**Habitat.** Unknown. The adult specimens were collected with mercury vapor light traps. The larval habitat is not known.

**Distribution.** *Myrmedonota cordobensis* sp. n. is only known from the type locality in the central region of the state of Veracruz, Mexico. This locality is 1,570 m above sea level, in a disturbed cloud forest. Matlaquiahuitl is the highest mountain in the municipality of Córdoba, Veracruz (Fig. 19).

***Myrmedonota jaliscensis* sp. n.**

<http://zoobank.org/BA2F7DF8-089F-4ED8-8CE6-DF555594BBA2>

Figures 2, 11–18, 19

**Type locality.** Mexico, Jalisco: Chapala, 4 Km. Ajijic–Chapala, 20°17'48.8"N, 103°12'55.5"W, dry deciduous forest (*Acacia* sp.), flight interception trap, 17.IX.2004, S. Gámez, A. López and Q. Santiago leg.

**Type material.** Holotype male, pinned. Original label: “MÉXICO: Jalisco, Chapala, 4 Km. Ajijic–Chapala. 15–17.IX.2004. Huizache, 1,620 m, 20°17'48.8"N, 103°12'55.5"W, ex. trampa de intercepción de vuelo. S. Gámez, A. López y Q. Santiago”/“MUZ-UV-COL-00000603”/“HOLOTYPE *Myrmedonota jaliscensis* Santiago-Jiménez, 2014” [red label].

**Other material.** Paratypes, same data as holotype (15 males, 5 females MUZ-UV, IEXA).

**Description.** Body length: 2.6–3.0 mm. Most of body black to dark brown; anterior edge of elytra, abdominal segments III–IV, and legs (except apical half of meso- and metafemur darker) yellowish brown. Densely pubescent on head, pronotum and elytra; dorsal surface of abdomen almost glabrous, densely pubescent on ventral surface of abdomen.

Head: Transverse, with or without impression on disc; without protuberance or carinae. Antennal articles 1–3 brown, 4–11 black, but tip of 11 is brown. Antennomeres 1–3 very elongate, 4–10 elongate, and 11 very elongate.

Mouthparts: Labrum: with 8 setae on each side of the midline; most of the setae on anterior half; with more than 30 (around 32–37) sensory pores on each side of the midline; sensillae on apical margin of epipharynx, arranged in a pattern of anterior or



**Figure 2.** Habitus of *Myrmedonota jaliscensis* Santiago-Jiménez, sp. n., male.

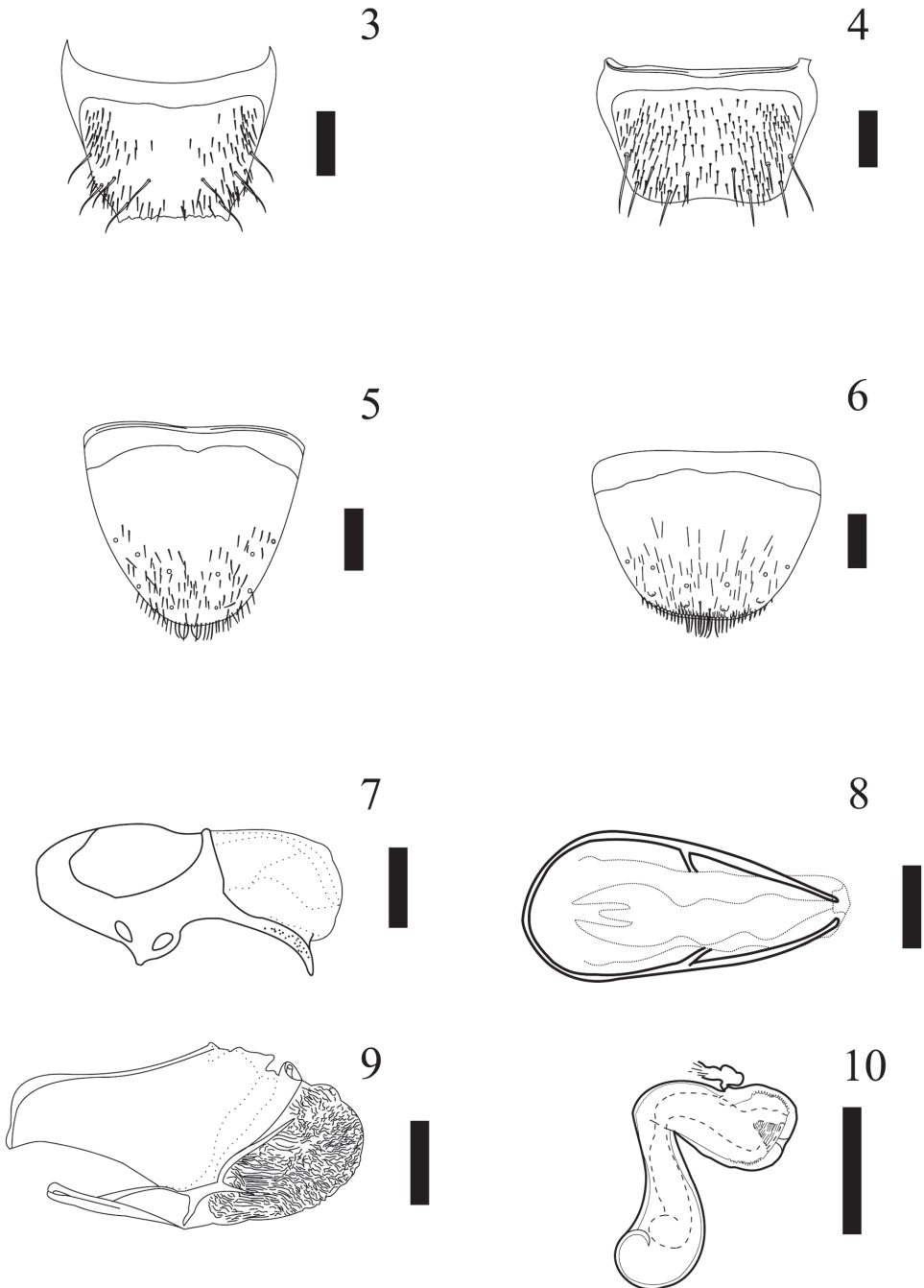
$\alpha$ -sensilla, medial or  $\beta$ -sensilla, posterior or  $\gamma$ -sensilla, and lateral or  $\epsilon$ -sensilla, one on each side of the midline (see Ashe 1984, Santiago-Jiménez 2010); apico-medial margin of epipharynx not modified to setose or spinose process; basal region of epipharynx with six pores more or less in one transverse row; medial region of epipharynx with around 30–32 pores in an irregular array; mesal region of epipharynx without a multiporose sensory structure on each side of midline; with several pores (around 8)

on mesolateral region. Mandibles: asymmetrical; right mandible with medial tooth on dorsal position; left mandible without tooth; without incisor tooth; with serration between apex and medial area of mandibles; with large velvety patch, wider than half of mandible base, composed of small denticles; prostheca with short hairs along entire length, except base, which has a ctenidium; prosthecal hairs not bifurcated on medial area. Maxilla: with a row of seven spines and two rows of large setae contiguous with the apical spines on apical third of the lacinia, between two rows of setae there is a glabrous area; the two rows of setae continue with numerous setae on middle third of the lacinia; scarcely distributed setae present on basal third of the lacinia; with pseudopores on cardo. Labium: with a short ligula and divided to near the base; with a small pair of setulae on each lobe of the ligula (one very short on the apex); without medial spines. Prementum with two medial setae, insertions widely separated; medial pseudopore field present; lateral pseudopore field composed of one setose pore, and two asetose pores; with setae on aboral margin of hypoglossa, adoral margin with setae too. Mentum without microsculpture on surface; with scarce pores on mentum (around 20–22 pores on each side of midline), more densely toward the apex.

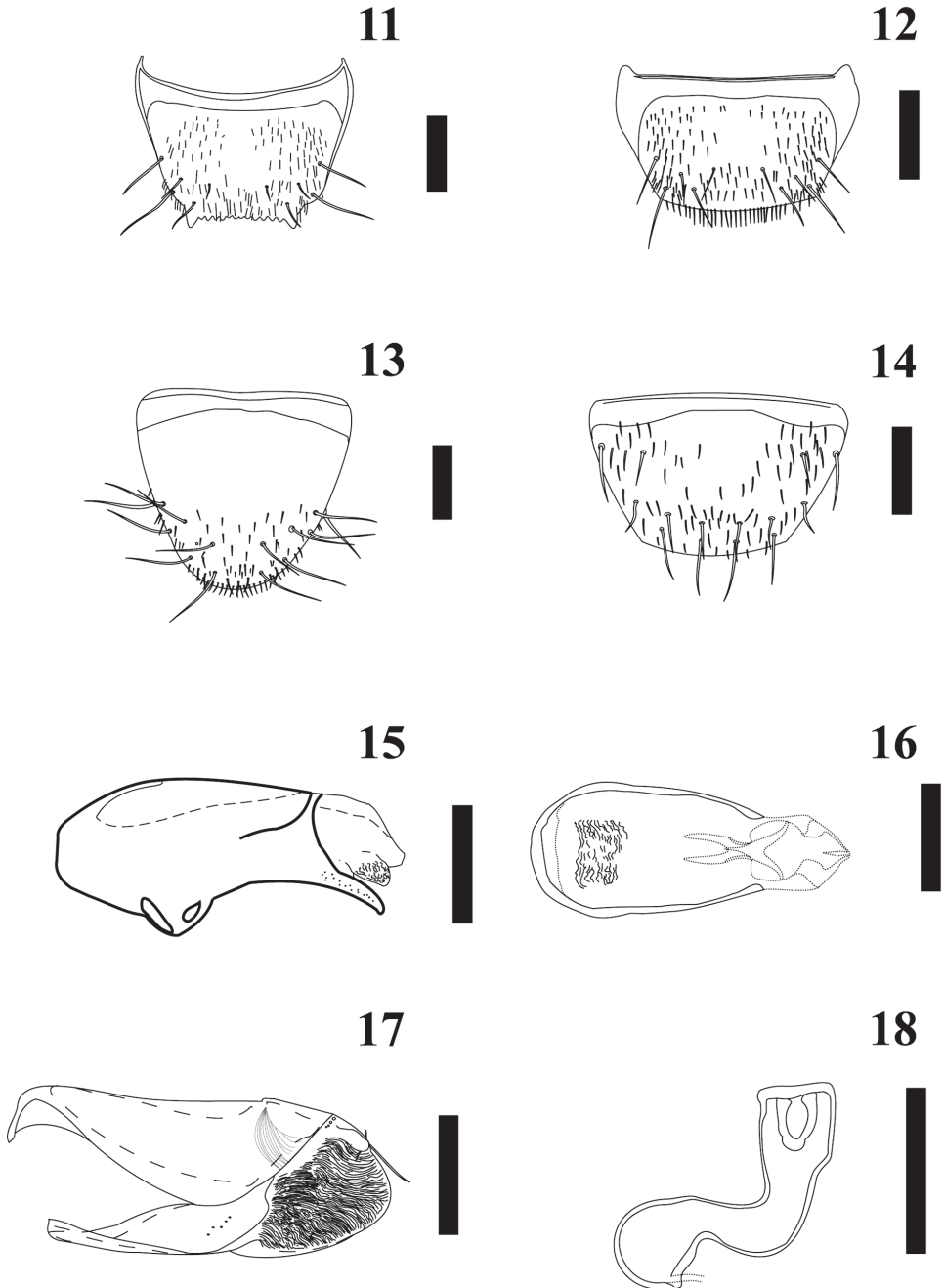
Thorax: Pronotum transverse, wider on anterior third; surface finely punctured, moderately dense; without reticulate microsculpture; setae moderately dense on surface; with 4 macrosetae along lateral margins, 3 macrosetae on each side of the midline, 2 macrosetae between lateral and medial macrosetae distributed on anterior half. Scutellum with reticulate microsculpture, moderately covered with short setae. Elytra slightly wider on apical area; surface finely punctured, moderately dense; without reticulate microsculpture; covered moderately with setae; with 8 macrosetae: 3 on lateral margin, 3 on mesal area, and 2 in diagonal closer to inner border. Hind wings well developed, flabellum with 15 spines (one female had only 10 spines). Mesocoxal acetabula completely margined posteriorly. Mesocoxal cavities moderately separated (approx. 0.16 mm) by meso- and metaventral processes; mesoventral process short (approx. 0.17 mm) with apex truncated; metaventral process medium-sized (approx. 0.56 mm), marginate and with apex acuminate; isthmus distinctly present (approx. 0.07 mm). Legs short, tarsal formula 4–5–5, every leg with an empodium, one seta on empodium and a pair of tarsal claws, each claw with a subbasal tooth.

Abdomen: Subparallel-sided, narrower than elytra, wider around segments IV–V; surface smooth, tergites III–VII almost glabrous, but with a row of 3 macrosetae along posterior margins on each side of the midline of every segment and one macroseta closer to the meso-lateral region; tergite VIII (Figs 11–12) with 5 macrosetae on each side of midline; tergite IX with 4 macrosetae on each side of midline; tergite X with 4 macrosetae on each side of midline. Other conspicuous characters are: tergites III–VI with basal impression; sternite IV with a central and transverse reservoir sac; without glands in basal region; without striae or cuticle vesicles on anterocentral region; without spiracles in basal region; without transversal cuticular impressions in basal region; without pseudopores in basal region.

Secondary sexual structures: sternite VII of male without external gland in basal region. Tergite VIII of male (Fig. 11) with posterior margin truncate and crenate



**Figures 3–10.** *Myrmedonota cordobensis* Santiago-Jiménez, sp. n. male (3, 5, 7–9) and female (4, 6, 10). 3 tergite VIII 4 tergite VIII 5 sternite VIII (note that macrosetae were lost, only pores were illustrated) 6 sternite VIII (note that macrosetae were lost, only pores were illustrated) 7 median lobe, lateral view 8 median lobe, dorsal view 9 paramere, outer lateral view 10 spermatheca. Scale bar = 0.2 mm, except scale bar of spermatheca = 0.1 mm.



**Figures 11–18.** *Myrmedonota jaliscensis* Santiago-Jiménez, sp. n. male (11, 13, 15–17) and female (12, 14, 18). 11 tergite VIII 12 tergite VIII 13 sternite VIII 14 sternite VIII 15 median lobe, lateral view 16 median lobe, dorsal view 17 paramere, outer lateral view 18 spermatheca. Scale bar = 0.2 mm, except scale bar of spermatheca = 0.1 mm.



**Figure 19.** Collection sites of *Myrmedonota cordobensis* Santiago-Jiménez, sp. n. (black square) and *M. jaliscensis* Santiago-Jiménez, sp. n. (black circle).

(around 6 denticles), and one lateral protrusion on each side of the midline. Tergite VIII of female (Fig. 12) is not crenate and it has a lateral protrusion. Sternite VIII of male and female as illustrated in Figures 13 and 14, respectively.

**Aedeagus:** Median lobe pear-shaped (Figs 15–16); with internal sac of median lobe with many spinules; medial lobe with short, well defined compressor plate; apical lobe curved to the ventral side (visible in lateral view), and pointed; basal ridge convex. Paramere as in Fig. 17; anterodorsal margin of paramerite with prominent sensory pores present beneath the velar sac; hinge zone of paramerite faint, extended from dorsal surface to near articulation between condylite and paramerite; apical process of paramerite clearly articulated anterior to edge of velum; condylite with a line of sensory pores; velum short (less than one half of the length of the paramere). Apical lobe with 3 macrosetae visible.

**Spermatheca:** Basal bulb simple, rounded at base; tube S-shaped; internal tube of neck with denticles; without accessory gland (Fig. 18).

**Remarks.** *Myrmedonota jaliscensis* is 3 mm or less in size and is easy to distinguish from other species: from *M. heliantha* because the proximal end of the spermatheca

is not curved over itself; from *M. lewisi* because the abdomen is bicolored; from *M. shimmerale* because the spermatheca is S-shaped; and finally, from *M. aidani* because tergites II–IV are yellowish with a dark spot on medial area of tergites III–IV, and the differently shaped spermatheca.

**Etymology.** The name makes reference to the state of Jalisco, Mexico, where the specimens were collected.

**Habitat.** Unknown. The adult specimens were collected with interception flight traps. The larval habitat is not known.

**Distribution.** *Myrmedonota jaliscensis* sp. n. is only known from the type locality around Lake Chapala in Jalisco state, Mexico (Fig. 19). This locality is 1,620 m above sea level, where it is common to find *Acacia* sp. trees, the common name of which is Huizache.

## Discussion

More species of *Myrmedonota* are being described from the Nearctic and Neotropical regions, and here I have described two new species, and it is possible that more species will be discovered in the future. Although Eldredge (2010) and Mathis and Eldredge (2014) presented a new diagnosis of *Myrmedonota*, it is not clear what specimens they used to select their diagnostic characters. Specimens reviewed here matched with diagnostic characters proposed by Eldredge (2010) and Mathis and Eldredge (2014); however, as mentioned above, they didn't mention anything about pronotum transverse or medial projection on apodeme that used Maruyama et al. (2008) on their diagnosis. Moreover, there is an inconsistency about labial palpomeres from diagnosis by Mathis and Eldredge (2014) compared to previous diagnosis by Eldredge (2010). I think it should be labial palpomeres I and III subequal in length, not II and III as mentioned by Mathis and Eldredge (2014). Therefore, I suggest we follow the redescription proposed by Maruyama et al. (2008) because they reviewed the type species of *Myrmedonota* and it has been useful to diagnose Nearctic and Neotropical species. Diagnostic characters should be proposed in a future analysis by mean of synapomorphies on a phylogenetic context.

Misunderstandings in Elven et al. (2010) about the limits of the Lomechusini-Athetini complex are causing confusion for people working with both tribes. That phylogeny was not completely resolved, and the main conclusion is that the species of false Lomechusini from the Neotropics belong to a different clade, but it was not possible to conclude whether they should be part of Athetini.

Finally, it is quite interesting that more species of *Myrmedonota* are being described from the Neotropics because new biogeographical questions are also emerging. Future efforts should aim to test whether *Myrmedonota* is a monophyletic clade that includes Oriental, Nearctic and Neotropical species, and to investigate the relationships between species.

## Acknowledgments

The author is very grateful to colleagues for their support at the Facultad de Biología, Universidad Veracruzana and Instituto de Ecología, A.C., particularly M. Morales, R. Ortega and R. Novelo for the use of the microscopes and to C. Álvarez-Castillo for preparing the illustrations. J. Asiain, J. Márquez, L. Delgado, S. Gámez, and A. López assisted on collection trips. I thank B. Delfosse and two anonymous reviewers for their comments, which helped improve the manuscript.

## References

- Ashe JS (1984) Generic revision of the subtribe Gyrophaenina (Coleoptera: Staphylinidae: Aleocharinae) with a review of described subgenera and major features of evolution. *Questiones Entomologicae* 20(3): 129–349.
- Cameron M (1920) New species of Staphylinidae from Singapore. Part III. *Transactions of the Entomological Society of London* 1920(1–2): 212–284.
- Eldredge KT (2010) A new species of *Myrmedonota* Cameron from eastern Kansas (Coleoptera, Staphylinidae, Aleocharinae). *ZooKeys* 53: 17–24. doi: 10.3897/zookeys.53.493
- Elven H, Bachmann L, Gusarov VI (2010) Phylogeny of the tribe Athetini (Coleoptera: Staphylinidae) inferred from mitochondrial and nuclear sequence data. *Molecular Phylogenetics and Evolution* 57: 84–100. doi: 10.1016/j.ympev.2010.05.023
- Elven H, Bachmann L, Gusarov VI (2012) Molecular phylogeny of the Athetini-Lomechusini-Ecitocharini clade of aleocharinae rove beetles (Insecta). *Zoologica Scripta* 41(6): 617–636. doi: 10.1111/j.1463-6409.2012.00553.x
- Hlaváč P, Newton AF, Maruyama M (2011) World catalogue of the species of the tribe Lomechusini (Staphylinidae: Aleocharinae). *Zootaxa* 3075: 1–151.
- Maruyama M, Patrick LB, Klimaszewski J (2008) First record of the genus *Myrmedonota* Cameron (Coleoptera, Staphylinidae) from North America, with descriptions of two new species. *Zootaxa* 1716: 35–43.
- Mathis KA, Eldredge T (2014) Descriptions of two new species of *Myrmedonota* Cameron (Staphylinidae: Aleocharinae) from Mexico with comments on the genus taxonomy and behavior. *Zootaxa* 3768(1): 95–100. doi: 10.11646/zootaxa.3768.1.7
- Motschulsky MV (1858) Énumération des nouvelles espèces de Coléoptères rapportés de ses voyages. 2-d. Article (continuation). *Bulletin de la Société Impériale des Naturalistes de Moscou* 31(3): 204–264.
- Santiago-Jiménez QJ (2010) Revision of the genus *Falagonia* (Coleoptera: Staphylinidae: Aleocharinae: Lomechusini), with description of related genera. *Sociobiology* 55(3): 1–82.

# A new species and synonymy of the Neotropical *Eucelatoria* Townsend and redescription of *Myiodoriops* Townsend

Diego J. Inclán<sup>1,2</sup>, John O. Stireman III<sup>2,3</sup>

**1** DAFNAE-Entomology, Università degli Studi di Padova, Viale dell'Università 16, 35020 Legnaro, Padova, Italy **2** Research Associate, Museo Ecuatoriano de Ciencias Naturales, Sección Invertebrados, Rumipamba 341 y Av. de los Shyris, Quito, Ecuador **3** Department of Biological Sciences, Wright State University, 3640 Colonel Glenn Highway, Dayton, OH 45435, USA

Corresponding author: *Diego J. Inclán* ([diegojavier.inclanluna@studenti.unipd.it](mailto:diegojavier.inclanluna@studenti.unipd.it))

---

Academic editor: *P. Cerretti* | Received 24 June 2014 | Accepted 7 November 2014 | Published 16 December 2014

---

<http://zoobank.org/85F4D36F-99DF-4E1D-8214-36D9F53C6784>

---

**Citation:** Inclán DJ, Stireman III JO (2014) A new species and synonymy of the Neotropical *Eucelatoria* Townsend and redescription of *Myiodoriops* Townsend. ZooKeys 464: 63–97. doi: 10.3897/zookeys.464.8155

---

The New World tropics represents the most diverse region for tachinid parasitoids (Diptera: Tachinidae), but it also contains the most narrowly defined, and possibly the most confusing, tachinid genera of any biogeographic region. This over-splitting of genera and taxonomic confusion has limited progress toward our understanding the family in this region and much work is needed to revise, redefine, and make sense of the profusion of finely split taxa. In a recent analysis of the Neotropical genus *Erythromelana* Townsend, two species previously assigned to this genus, *Euptilodegeeria obumbrata* (Wulp) and *Myiodoriops marginalis* Townsend were reinstated as monotypic genera. In the present study, we demonstrate that *Euptilodegeeria obumbrata* (Wulp), previously assigned to three different genera, represents in fact a species of the large New World genus *Eucelatoria* Townsend, in which females possess a sharp piercer for oviposition. We also show that the species *Eucelatoria carinata* (Townsend) belongs to the same species group as *Eucelatoria obumbrata*, which we here define and characterize as the *E. obumbrata* species group. Additionally, we describe *Eucelatoria flava* **sp. n.** as a new species within the *E. obumbrata* species group. Finally, we redescribe the genus *Myiodoriops* Townsend and the single species *M. marginalis* Townsend.

## Keywords

Exoristinae, Blondeliini, *Euptilodegeeria*, *Erythromelana*, *Machairomasicera*, *Hypostena*, Tachinidae, Diptera, Parasitoid

## Introduction

The New World tropics represents one of the most biodiverse regions of the world, but its flora and fauna remains poorly known. This is particularly true for flies in the family Tachinidae, where the Neotropical fauna represents more than 35% of the total described species (O'Hara 2013a, b). In this region, approximately 3000 species belonging to 817 genera are known (O'Hara 2012; O'Hara 2013a, b), making the Neotropics the region with the highest number and the most narrowly defined tachinid genera of any biogeographic region. The primary describer of these taxa, C.H.T. Townsend (1863–1944), assigned an average of slightly more than one species per genus in his description of over 1555 species in 1491 genera, the vast majority of which are Tachinidae (Arnaud 1958; O'Hara 2013a). This over-splitting, compounded by the great diversity of tachinids in the Neotropics, has limited progress toward our understanding of the family in this region (e.g., it is the only major biogeographic region without a generic key). There currently remain 544 valid tachinid genera described by Townsend (O'Hara 2012, 2013a), and much work is needed to revise, redefine, and make sense of this profusion of finely split taxa.

An example of the taxonomic instability of Neotropical tachinid genera is witnessed in the species *Euptilodegeeria obumbrata* (Wulp). This species was first classified in the former tachinid genus *Hypostena* by Wulp (1890; along with many other blondeliines), based on specimens collected in Guerrero, (southwest) Mexico. The main traits from the original description that were used to distinguish this genus were the narrow and bare parafacial and the wing vein  $R_{4+5}$  haired along its proximal three-fourths (Wulp 1890). The species was moved by Townsend (1931) to the new genus *Euptilodegeeria*, moved again to the genus *Erythromelana* Townsend by Wood (1985) and recently excluded from *Erythromelana* and resurrected to its previous genus (*Euptilodegeeria*) by Inclán and Stireman (2013). Although the taxonomy of Tachinidae, particularly of the Blondeliini, is challenging due to the scarcity of clear synapomorphies, the confusion in the generic assignment of *E. obumbrata* was also due to the limited number of specimens evaluated, the lack of examination of male terminalia and the use of only males for the descriptions. In the present study, we use additional information from male and female terminalia to demonstrate that these “*obumbrata*” specimens, previously assigned to *Hypostena*, *Euptilodegeeria* and *Erythromelana*, actually belong to the genus *Eucelatoria* Townsend (1909), in which females possess a sharp piercer for internal oviposition in the host. We also argue that the former species *Machairomasicera carinata* described from a single female by Townsend (1919) in the monotypic genus *Machairomasicera*, and later synonymized with *Eucelatoria* by Wood (1985), belongs to this same species group of *Eucelatoria*, which we here define and characterize. In the end, taxa that were assigned to four different genera in fact belong to one species group of *Eucelatoria*, providing an example of the taxonomic confusion that plagues many groups of Neotropical tachinids.

Similar to the situation described above, although somewhat less confusing, is the situation of the other species recently excluded from *Erythromelana* by Inclán and Stireman (2013), *Myiodoriops marginalis* Townsend. Townsend (1935) originally

described the monotypic genus *Myiodoriops* based on the type species *M. marginalis* Townsend, which was collected in the South American country of British Guiana (now Guyana). The genus was originally characterized by the shiny black coloration of the thorax and the black with yellow coloration of the abdomen on the lateral sides of first three tergites (Townsend 1935). It was subsequently synonymized (together with *Euptilodegeeria*) as *Erythromelana* by Wood (1985) in his comprehensive revision of the Blondeliini of North and Central America. This placement was based on the external morphological similarities that these genera share including large eyes, bare and extremely narrow parafacial, vibrissa arising at the anteroventral corner of the head, narrow postgena and gena, and postpronotum with two bristles.

In our recent revision of the Neotropical *Erythromelana* (Inclán and Stireman 2013), we removed the former species *Euptilodegeeria obumbrata* and *Myiodoriops marginalis* due to strong morphological differences between them and other *Erythromelana* taxa in the male terminalia and other traits. These differences were sufficient to question even a close phylogenetic relationship between these genera, suggesting that in the absence of clear knowledge concerning relationships, these taxa should be resurrected as distinct genera. In the present work, we confirm that the species *Euptilodegeeria obumbrata* and *Myiodoriops marginalis* do not belong in the genus *Erythromelana*, showing that the former is a species of the genus *Eucelatoria* and the latter should be placed in the resurrected genus *Myiodoriops*. Because the original descriptions of these taxa were cursory, with limited evaluation of morphological characters and their variation, no useful means of identifying the taxa and no figures, we redescribe and illustrate these taxa. Additionally, we define the *E. obumbrata* species group and we describe *E. flava* as a new species of *Eucelatoria*.

## Methods

### Specimens

This revision was based on 28 adult specimens from four collections. Additional Nearctic and Neotropical taxa in the genus *Eucelatoria* from the NMNH, CNC and JOS collections were examined for comparison. Additional specimens of *Blondelia* Robineau-Desvoidy, *Celatoria* Coquillett, *Myiopharus* Brauer & Bergenstamm, *Opsomeigenia* Townsend, *Euthelyconychia* Townsend, *Lixophaga* Townsend and *Vibrissina* Rondani in the JOS collection were also examined for comparison. Acronyms used in the text for the collections and museums from which specimens were borrowed appear below, with their names and respective curators.

**BMNH** Natural History Museum, Department of Entomology, London, UK; N.P. Wyatt.

**CNC** Canadian National Collection of Insects, Agriculture and Agri-Food Canada, Ottawa, Ontario, Canada; J.E. O'Hara.

- INBio** National Biodiversity Institute of Costa Rica, Department of Entomology, Santo Domingo de Heredia, Costa Rica; M. Zumbado.
- NMNH** National Museum of Natural History, Department of Entomology, Smithsonian Institution, Washington, USA; N.E. Woodley.
- JOS** Private collection of John O. Stireman III, housed at Wright State University, Dayton, Ohio, USA.

### **Examination and illustration**

Adult specimens were examined with a Nikon SMZ1000 stereoscopic microscope equipped with an ocular micrometer and a digital Nikon Coolpix 8800 camera (Nikon, Tokyo, Japan). To create images with a greater depth of field, 15–30 photos of each specimen/structure at different focal points were taken. Final photos were compiled into a single image using the image stacking software CombineZM (Hadley 2013). Male and female terminalia photos were taken using a depression slide with glycerin. Line drawings were made based on digital photos using Adobe Illustrator CS2 12.0.1 (Adobe Systems, Inc., San Jose, California, USA).

### **Terminology and species description format**

Descriptions and redescriptions of species follow terminology and abbreviations used in the *Manual of Central American Diptera* (Cumming and Wood 2009). In addition, the terms proposed by O'Hara (1989) for the male abdominal sternum 5 are used. Terms for the cerci follow the nomenclature used by Wood (1987). Three specific measures, the upper lobes, medial section, and apical cleft of the cerci, follow Inclán and Stireman (2013).

### **Dissection of male and female terminalia**

Male terminalia of tachinids provide some of the best characters for taxonomic studies at the species level. Dissections were performed according to the procedure described by O'Hara (1989, 2002). Briefly, this procedure involves the removal of the abdomen of an adult specimen, partial clearing of it in 10% NaOH, dissection of terminalia, re-attachment of the abdomen to the specimen, extra clearing of the terminalia in 100% lactic acid, and finally storage of the terminalia in a microvial with glycerin.

### **Morphological characterization and measurements**

Morphological traits of 17 *Eucelatoria* specimens (14 males and 3 females), and 11 *Myiodoriops* specimens (5 males and 6 females) were measured. Additionally, male ter-

minalia from 6 *Eucelatoria* and 2 *Myiodoriops* specimens were dissected. In species descriptions, the number of specimens for which particular characters were measured is given by “N”. When possible, means “ $\bar{x}$ ” are reported for continuous characters.

### Citation of specimen label data

Data from each type specimen and other specimens examined are cited exactly as they appear on the label, with each line separated by a diagonal slash (/) and information for each individual label enclosed within quotation marks. Additional information not appearing on the label is enclosed within brackets. Finally, the depository is cited in parentheses.

### Distribution maps

Maps were created using SimpleMappr (Shorthouse 2010), which uses coordinates in decimal degrees as latitude and longitude to create point distribution maps. For specimens with labels that did not include coordinates, Google Earth 6.2 (Google Inc., Silicon Valley, California, USA) was used to obtain the approximate latitude and longitude of given localities.

## Systematics

### *Eucelatoria* Townsend, 1909

*Eucelatoria* Townsend, 1909: 249. Type species: *Tachina* (*Masicera*) *armigera* Coquillett, 1889, by original designation.

*Euptilodegeeria* Townsend, 1931: 465. Type species: *Hypostena obumbrata* Wulp, 1890, by original designation. **Syn. n.**

See Guimarães 1971, Wood 1985 and O’Hara and Wood 2004 for a full list of synonymies and selected references.

**Remarks.** In the recognition of the genus *Eucelatoria* provided by Sabrosky (1981) and Wood (1985) the wing vein  $R_{4+5}$  is dorsally setose only at its base. The *E. obumbrata* species group described here differs from these generic definitions because specimens in this group have the wing vein  $R_{4+5}$  dorsally setose from its base nearly to crossvein r-m. Although Wood (1985) already considered *Machairomasicera carinata* as belonging to *Eucelatoria*, and this species has the vein  $R_{4+5}$  dorsally setose, Wood did not include this variation in the generic description of *Eucelatoria* because his revision was restricted to Central America, and *M. carinata* is known only from Ecuador. This trait appears to be a synapomorphy of the *E. obumbrata* species group, clearly distinguishing it from

other *Eucelatoria* species. The presence of sex patches on ventral abdominal tergites 4 and 5 of males also serves to unite this group, however similar sexual patches have been observed in other *Eucelatoria* species (Stireman and Z.K. Burington, pers. obs.).

### ***Eucelatoria obumbrata* species group**

*Eucelatoria obumbrata* (Wulp, 1890), **comb. n.**

*Eucelatoria carinata* (Townsend, 1919).

*Eucelatoria flava* Inclán & Stireman **sp. n.**

**Diagnosis.** The *Eucelatoria obumbrata* species group can be distinguished from other species of *Eucelatoria* and other blondeliines (see discussion section below) using a combination of character states: (1) presence of sexual patches on the ventral portions of abdominal tergites 4 and 5 of males, (2) wing vein  $R_{4+5}$  setose from its base nearly to crossvein r-m in both sexes, and (3) a piercing ovipositor formed by abdominal sternite 7 in the female. Additional distinguishing traits include: mid-dorsal depression reaching only half way to hind margin of syntergite 1+2 and short spine-like setae on the ventral edge of the tergite 4 in females. This group can be easily separated from *Erythromelana*, in which *E. obumbrata* was formerly included (Inclán and Stireman 2013), by the above characters along with presence of at least one additional bristle on the facial ridge ventral to the vibrissa. The male terminalia of species in the *E. obumbrata* group, are also clearly distinct from the formerly congeneric species of *Erythromelana* and *Myiodoriops*. Distinctions include: (1) basal section of sternite 5 equal to or longer than the apical lobes, considerably shorter in the latter two genera; (2) surstylus, though similar to that in *Erythromelana*, differs from the anteriorly curved, somewhat pointed surstylus of *Myiodoriops* that bears spine-like setae on the anterior edge of its apex; and (3) postgonite is strongly curved towards its apex, which is similar to that of other *Eucelatoria* and to the reduced postgonite of *Myiodoriops*, but distinct from the short paddle-like one of *Erythromelana*.

**Geographic distribution and seasonal occurrence.** Species in the *E. obumbrata* species group are widely distributed in the Neotropical Region, from southern Mexico to Ecuador (Fig. 1). Species occur in montane tropical forest at high elevations (e.g., Mexico and Ecuador, > 2000 m). In particular, the species with a yellow abdomen (*E. flava* sp. n.) appears to occur only in the Andes Mountains, similar to the pattern found for Andean species of *Erythromelana* (see Inclán and Stireman 2013). See the distribution of *E. obumbrata*, *E. flava* sp. n. and *E. carinata* below, except for three undescribed specimens (see discussion below) that were collected near the border of Costa Rica and Panama. These specimens from Costa Rica were collected from 1400 m to 1800 m.

**Discussion.** *Eucelatoria* is a diverse new world tachinid genus, with Central and South America harboring most of the species. The genus belongs to a core clade of Blondeliini, along with *Blondelia*, *Celatoria*, *Vibrissina* and several other genera, that

share the derived traits of females with a midventrally keeled abdomen, often with short stout bristles, and sternite seven modified into a hook-like piercer. Boundaries between genera within this group are less clear (Stireman 2002, Tachi and Shima 2010, Cerretti et al. 2014b), and Wood (1985) has suggested that there is little justification in maintaining them as separate genera, but *Eucelatoria* is generally distinguished from related genera by a well-developed genal dilation, frequent lack of apical scutellar bristles, mesonotum with four narrow black stripes, mid-tibia with a single median anterodorsal bristle, lack of hairs on the parafacial and the eyes usually bare or sparsely haired (Sabrosky 1981, Wood 1985). This list of characters, many of them probably plesiomorphic and most with exceptions, is not entirely satisfactory for defining a genus and careful morphological study, probably along with genetic data, is needed to establish relationships and delineate monophyletic groups within the *Blondelia*-group genera. An extensive treatment of this group however, is beyond the scope of the present study.

Each of the species treated here, *E. obumbrata*, *E. carinata* and *E. flava* sp. n., possesses at least some of the key traits of the *Blondelia*-group clade, including the keeled, spined abdomen with sternite 7 modified as a piercer in females, and well developed, anteriorly curved postgonites in males (Wood 1985). This argues strongly for their inclusion in the *Blondelia*-group clade, despite lacking certain other characteristic features including the depression on abdominal syntergite 1+2 extending to its hind margin, and the male surstylus with a notch on the posterodorsal margin (which appears to be absent in some other species of *Eucelatoria* as well; Z.K. Burington, unpub. data). Given the distinctive characters and incompletely understood phylogenetic position of the *E. obumbrata* species group, it might be argued that the genus *Machairomasicera* should be resurrected for these three taxa. Instead, we argue for their placement within *Eucelatoria* for the following reasons: (1.) These taxa share many of the traits that are used to distinguish *Eucelatoria* from related genera including: one median anterodorsal bristle on mid-tibia, lack of well-developed apical scutellar bristles (present in some *Eucelatoria* species), a small but distinct genal dilation, mesonotum with four narrow black stripes, tergite 4 ventrally keeled in females, and lack of hairs on the parafacial (Sabrosky 1981, Wood 1985). (2.) Wood (1985) previously placed one of the species in the group (*E. carinata*) in the genus *Eucelatoria* based at least in part on the characters mentioned above. (3.) Resurrecting yet another genus of *Blondelia*-group taxa is counterproductive given their clear morphological affinity with *Eucelatoria* and the taxonomic confusion resulting from the profusion of small, ill-defined Neotropical genera.

In the last revision of *Eucelatoria*, Wood (1985) synonymized a multitude of genera and species with this genus. In particular, the species *Lixinia carinata* Curran and *Machairomasicera carinata* were included, but as both share the same species name Wood stated that *L. carinata* is a “secondary homonym of *Machairomasicera carinata* Townsend 1919: 578, but is not renamed here pending revision of the genus”. Wood did not include *M. carinata* because it is from Ecuador. In the present revision, we treat *M. carinata* as a valid species name within our *E. obumbrata* species group, but we did not include *L. carinata* as it falls outside of this species group. The assignment

of a new species name for *L. carinata* will depend on a further revision of the genus *Eucelatoria*.

We found three additional specimens from Costa Rica that belong to this species group, but each one is sufficiently morphologically distinct that it appears to be an undescribed species close to *E. obumbrata*. Each of the three specimens exhibits slight but distinct differences in the external morphology and male terminalia, but it remains unclear if these differences represent extensive intra-species variation or distinct species. Therefore, we leave these specimens undescribed until additional material is available to describe them as new or determine whether they are allied with a described species.

### Key to species of the *Eucelatoria obumbrata* species group

- 1 Abdomen mostly or wholly black, with at most yellow laterally on tergites 1+2 to 4, males with median discal setae present on tergites 3 and/or 4 ..... **2**
- Abdomen wholly yellow, median discal setae absent on tergites 3 and 4 .....  
.....*E. flava* **sp. n.**
- 2 Eyes densely haired, abdomen mostly black, with yellow only laterally on tergites 1+2 to 4, males with median discal setae present on tergite3 and/or tergite4 ..... *E. obumbrata* (Wulp)
- Eyes sparsely haired, abdomen wholly black (only known from a single female) ..... *E. carinata* (Townsend)

### *Eucelatoria obumbrata* (Wulp), **comb. n.**

Figs 1–6

*Hypostena obumbrata* Wulp, 1890: 143.

*Euptilodegeeria obumbrata* (Wulp): Guimarães 1971: 134; Inclán and Stireman 2013.

*Erythromelana obumbrata* (Wulp): Wood 1985: 39–40.

**Type material.** Lectotype male, by designation of Wood (1985: 100), labeled: “LECTOTYPE”, “♂”, “Omiteme,/ Guerrero,/ 8000 ft. [feet]/ July H. H. Smith.”, “Central America/ Pres. By F.D. Godman,/ O. Salvin/ 1903-172.”, “B.C.A. Dipt. II./ Hypostena obumbrata v.d.W”, “Euptilodegeeria obumbrata/ Det. CHTT”, “LECTOTYPE ♂/ Of Hypostena obumbrata Wulp./ Designated 1979/ D.M. Wood”, “Eucelatoria obumbrata (Wulp)/ det. D.J. Inclán/ & J.O. Stireman” (BNHM).

**Other material examined.** 10 specimens examined. 2 males labeled: “Co-type”, “♂”, “Omiteme,/ Guerrero,/ 8000 ft. [feet]/ July H. H. Smith.”, “Central America/ Pres. By F.D. Godman,/ O. Salvin/ 1903-172.”, “B.C.A. Dipt. II./ Hypostena obumbrata v.d.W”, “PARALECTOTYPE/ Of Hypostena obumbrata Wulp./ Designated 1980/ D.M. Wood”, “Cotype/ 23967 U.S.N.M.”, “USNM 2049536”, “Eucelatoria obumbrata (Wulp)/ det. D.J. Inclán/ & J.O. Stireman”, “DI81NM”, “DI82NM”

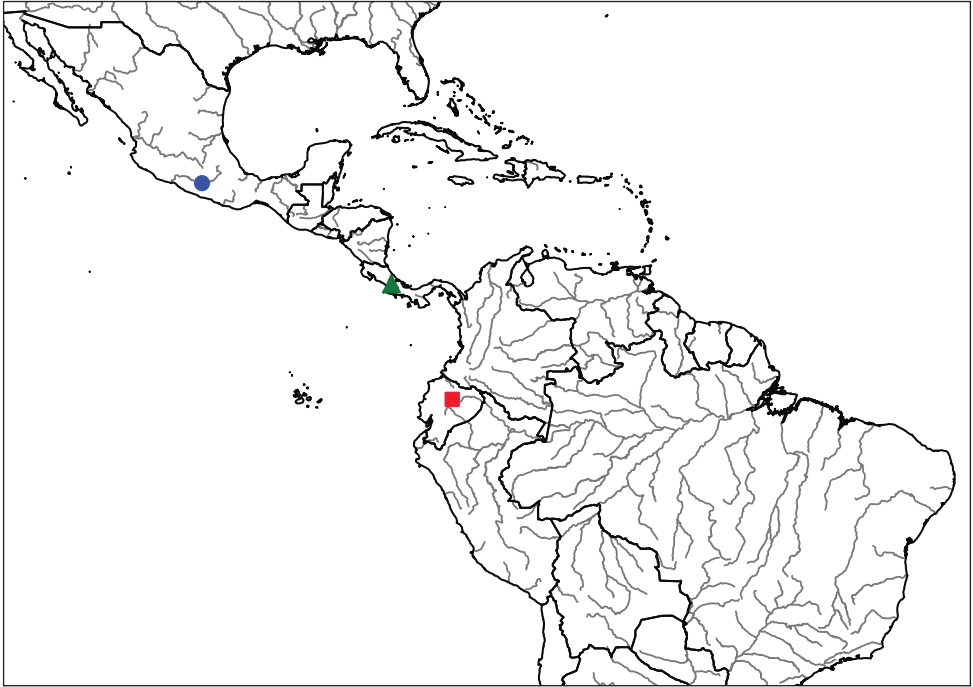


**Figure 1.** Known distributions of species in the *Eucelatoria obumbrata* species group. *E. obumbrata* (Wulp) is represented by a blue circle, *E. flava* sp. n. by a red square and *E. spp.* by a green triangle.

(NMNH); 2 males, as above except without the last label, “DI79NM”, “DI78NM” [1 specimen with terminalia dissected] (NMNH); 1 male, as above except without the “Cotype/...” labeled and having one extra label “Euptilodegeeria obumbrata/ Det. CHTT”, “DI80NM” (NMNH); 1 male, same as above except without the last two labels and the paralectotype label was attached in 1979, “DI105BM” (BNHM); 1 male, same as above except without the last two labels, the location label “Xucumanatlan [miss spelled Xocomanatlan]/ Guerrero/ 7000 ft./ July. H.H. Smith” and the paralectotype label was attached on 1979, “DI106BM” (BNHM); 1 male and 2 females, “Omiteme,/ Guerrero,/ 8000 ft. [feet]/ July H. H. Smith.”, “Central America/ Pres. By F.D. Godman,/ O. Salvin/ 1903-172.”, “Eucelatoria/ obumbrata (Wulp)/ det. D.J. Inclán/ & J.O. Stireman”, “DI109BM” [male with terminalia dissected], “DI108BM”, “DI107BM” (BNHM).

**Recognition.** This species can be distinguished from *E. flava* sp. n. by the primarily black coloration of the abdomen, with yellow coloration being restricted to the sides of tergites 1+2, 3, and 4. This contrasts with the entirely yellow abdomen of *E. flava*. *Eucelatoria obumbrata* usually bears median discals on tergite 3 and/or tergite 4, but these are absent in *E. flava*. The terminalia are similar between these species, but differ in several subtle respects including: the basal section of sternite 5 is distinctly shorter and broader basally in *E. obumbrata*; the surstylus, in lateral view, is equal to the cercus in length or slightly longer, whereas in *E. flava* it is markedly longer. In posterior view,

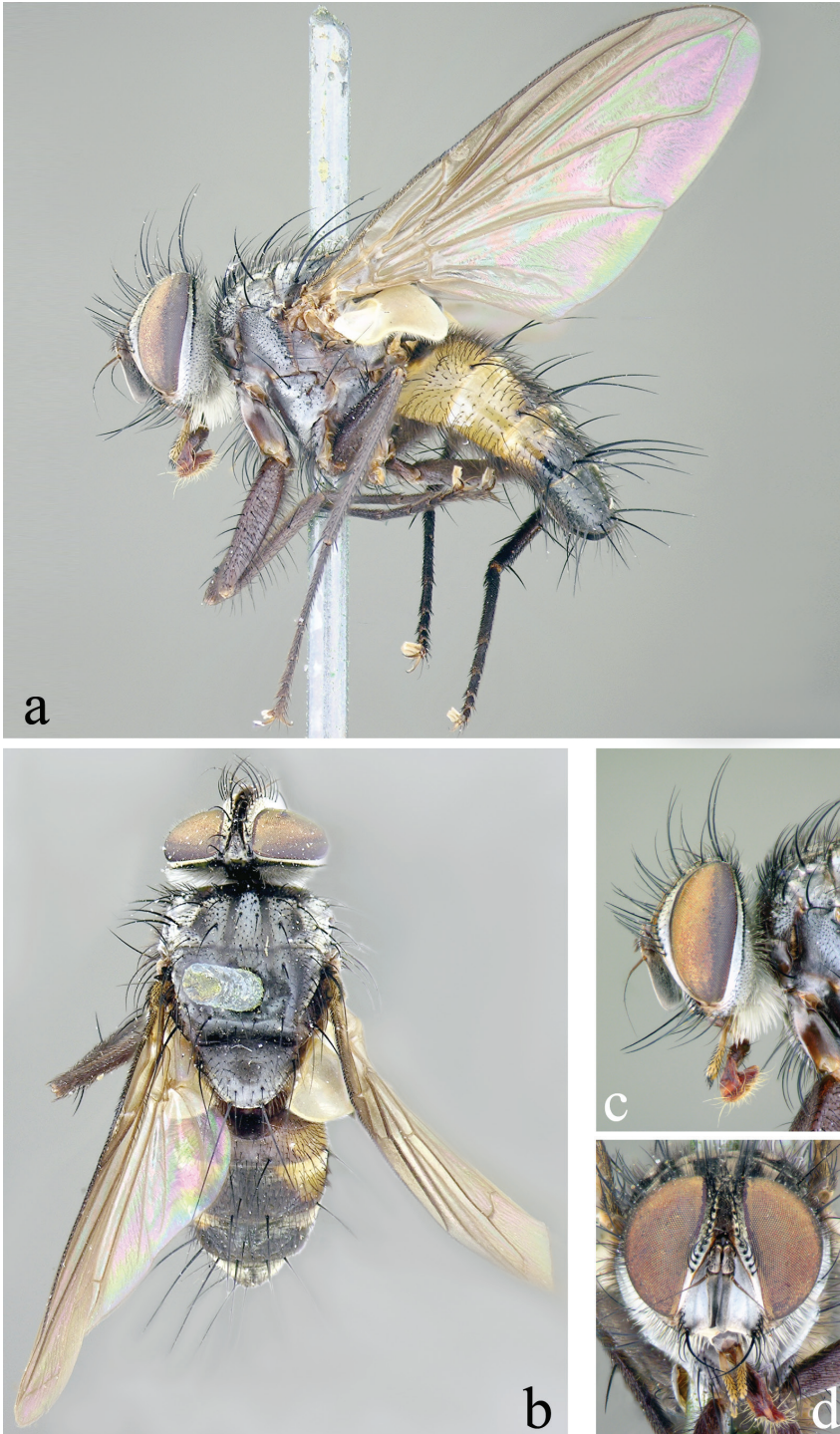


**Figure 2.** Male of *E. obumbrata* (Wulp). Full body from lateral (a) and dorsal (b) view and head from lateral (c) and frontal view (d).

the lateral margins of the cerci are narrowed linearly until the apical cleft, whereas in *E. flava* they are abruptly constricted below the upper lobes; the pregonite of *E. obumbrata* is relatively rectilinear, whereas that of *E. flava* triangular in shape, with a relatively broad at base, and strong narrowing toward apex. Females differ from *E. carinata* in having yellow coloration laterally on tergites 1+2, 3, and 4 (all black in *E. carinata*), densely haired eyes, more sparsely bristled palpi, and silvery parafrontals (bronzy in *E. carinata*).

**Redescription.** Redescribed from 11 males (including the lectotype and 4 paralectotypes), and 2 females, unless otherwise noted as “N”.

Length: males, 6.2–7.1 mm ( $\bar{x}$  = 6.8 mm); females, 6.1–7.0 mm ( $\bar{x}$  = 6.5 mm).

**Head** (Fig. 2): Parafacial covered with dull silver to slightly bronzy pruinescence in male, silvery in female. Fronto-orbital plate and vertex black in ground color, covered with silver pruinescence (appearing grayish or brownish from certain angles), usually with a faint golden or bronzy pruinescence. Frontal vitta usually entirely black, sometimes fading to dark-brown toward antenna. Pedicel black and first flagellomere black, covered with fine microtrichia, and appearing grayish. Arista long, with minute setae, black with brown on basal 1/3 or less, thickened only on basal 1/4 or less. Eye densely haired, with long ommatrichia. Eye 0.85–0.90 head height in male, 0.85 in female. Vertex width, at its narrowest point, 0.17–0.22 head width in male, 0.24–0.25 in female. Length of first flagellomere 0.38–0.58 head height in male, 0.40–0.42 in female. Width of first flagellomere 2.57–3.80 parafacial width at its narrowest point in male, 2.0–3.33 in female. Pedicel length 0.25–0.36 length of first flagellomere in male, 0.33–0.36 in female. Fronto-orbital plate with 8–11 mediocline frontal setae in male, 5–6 in female; 2 reclinate inner orbital setae in both sexes; female with 2 proclinate outer orbital setae, male without outer orbitals. The outer vertical seta varied from scarcely to moderate differentiated from the row of postocular setae in both sexes. Ocellar setae well-developed, proclinate. Parafacial bare and extremely narrow with the narrowest point equal to or narrower than the basal width of the palpus in both sexes. Facial ridge with hairs on basal 2/5 or less (occasionally higher, but if so, short and hairlike above lowest third), and lower margin of face descending to the level of vibrissa. Subvibrissal ridge short, usually with 1 or 2 setae; postgena narrow, with a distinct but small genal dilation. Posteroventral part of the head with the majority of setae fine and white-yellowish and posterodorsal part of the head without black setae behind the postocular row. Palpus yellowish; sparsely to moderately bristled; almost uniform in width, but sometimes slightly broadened at the apex.

**Thorax** (Fig. 2a, b): Shiny black in ground color; presutural scutum with thin white pruinescence, postsutural scutum with much sparser pruinescence revealing underlying black ground color. In dorsal view, only the presutural scutum appears grayish; whereas in lateral view the postsutural scutum appears grayish as well. Faint white pruinose stripes on presutural scutum leaving 4 black vittae; the inner 2 vittae longer and thinner, almost 1/2 the width of each of the outer 2 vittae. Prosternum with several hair-like setae. Postpronotum usually with 3 setae in a line. Proepisternum bare. Katepisternum with 3 setae. Scutum setae highly variable, with 2 or 3 presutural

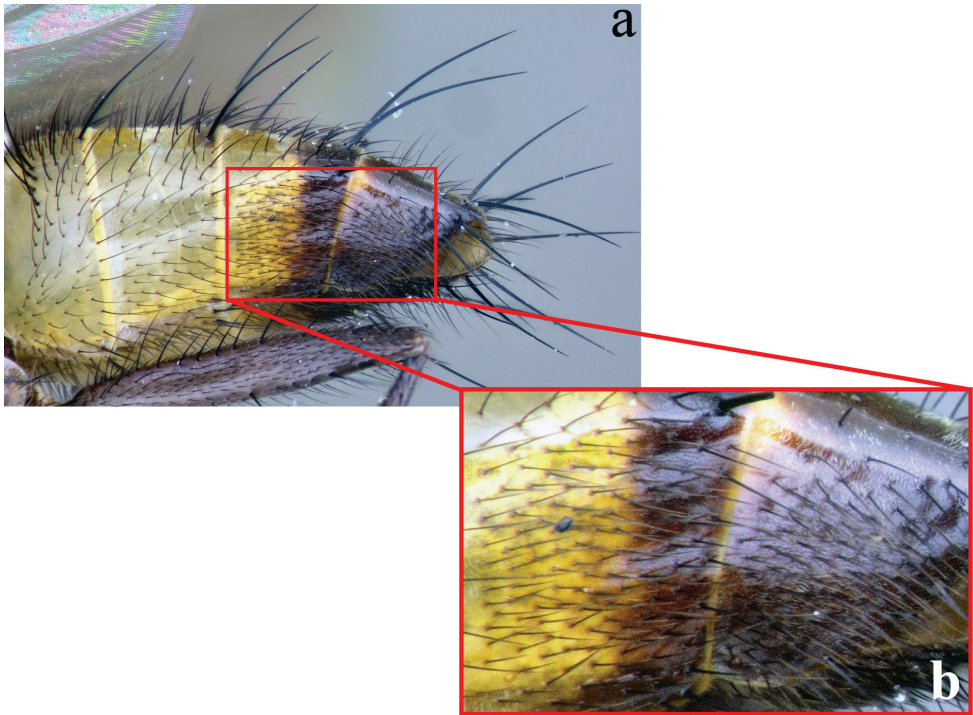


**Figure 3.** Lateral view of the male abdomen of *E. obumbrata* (Wulp) (a) showing the sexual patches on tergites 4 and 5 (b).

acrostichal setae; postsutural acrostichal setae varied from 1 to 3; 2 or 3 presutural dorsocentral setae; 2 or 3 postsutural dorsocentral setae; 1 presutural intra-alar seta, occasionally with 1 or 2 additional small seta; 2 to 4 postsutural intra-alar setae; 3 postsutural supra-alar setae, rarely 2. The first postsutural supra-alar seta is small or rarely absent. Scutellum with 3 pairs of setae: basal bristles of moderate length, short, usually divergent or parallel lateral bristles, long, divergent subapicals and without apical setae.

Legs entirely black. Tarsal claws longer than 5th tarsomere in male and shorter than 5th tarsomere in female. Mid tibia with 1 anterodorsal seta, 2 posterodorsal setae, and 1 ventral seta. Hind tibia with anterodorsal setae uneven in length and not closely spaced; 2 well-developed posterodorsal setae, rarely with 1 additional shorter seta; 2 well-developed anteroventral setae. Upper and lower calypteres brownish-yellowish. Wing varied from light to dark fumose on cells  $sc$ ,  $r_1$ ,  $r_{2+3}$ , and sometimes on  $r_{4+5}$ . Females with nearly hyaline wings. Wing vein  $R_{4+5}$  dorsally setose from its base nearly to crossvein  $r-m$ , and  $R_1$  bare, rarely only with 1 or 2 setae. Vein  $M$  smoothly curved at bend and ending at wing margin, separately from vein  $R_{4+5}$ .

**Abdomen** (Figs 2a, b; 3a, b): Mostly black with yellow laterally on  $tg1+2$  to  $tg4$ . Transverse bands of sparse white pruinosity on basal  $1/3$  to  $2/3$  of tergites 3 to 5, more noticeable medially on the black areas of the abdomen. Mid-dorsal depression of  $tg1+2$  only extending approximately half way to hind margin. One pair of median marginal

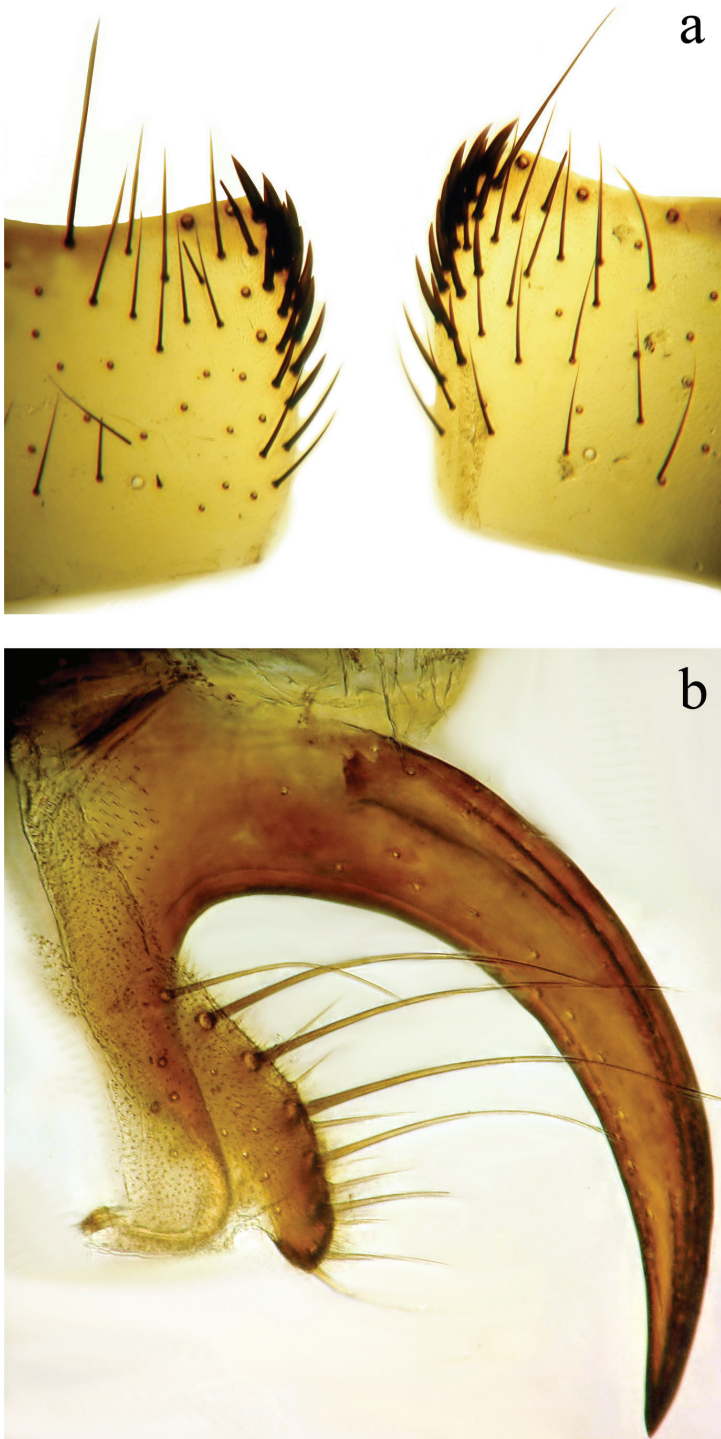


**Figure 4.** Female terminalia of *E. obumbrata* (Wulp). Spine-like setae on the ventral margins of tergite 4 (a) and tergite 7 and sternite 7 modified into a piercer, below the piercer is sternite 6 (b).

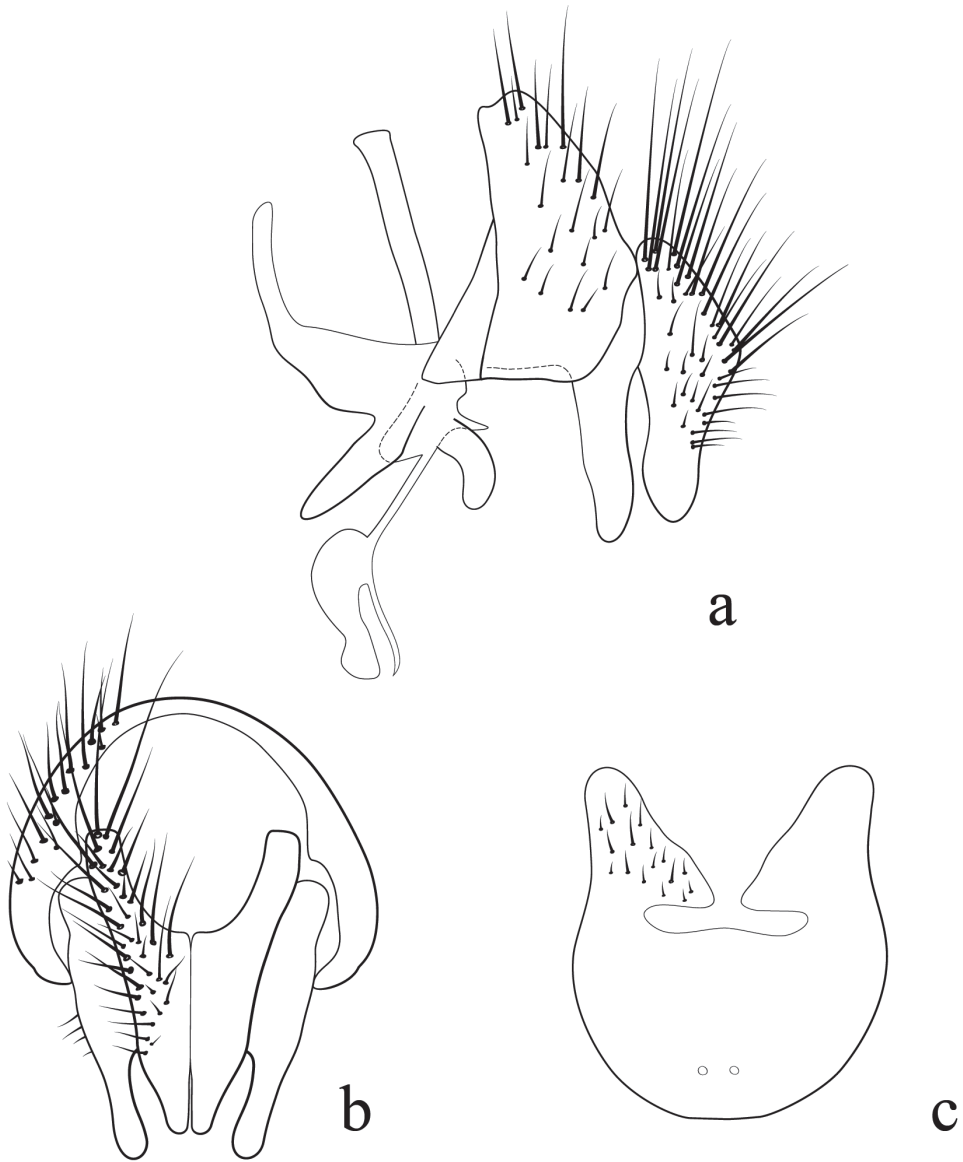


**Figure 5.** Lateral (a) and posterior view (b) of the male terminalia and sternite 5 (c) of *E. obumbrata* (Wulp).

setae on tg1+2 and tg3; a row of median marginals on tg4 and tg5; 1 pair of lateral marginal setae on tg1+2 and tg3; median discal setae present on tg3, usually also on tg4 in males, but absent in females. Males with dense patches of very short setae (sex patches; Cerretti et al. 2014a) present on the ventral surface of tg4 and tg5 (Fig. 3). Sternites completely overlapped by tergites. Females with spine-like setae on ventral margins of tg4 making two irregular rows of short, stout, curved and closely set of 7–10 spines per each row, which are concentrated in the distal 2/3 of the tergite (Figure 4a).



**Figure 6.** Lateral view of the hypandrial complex (a) and distiphallus (b) of *E. obumbrata* (Wulp).

**Male terminalia** (N = 2, Figs 5, 6): Sternite 5 with median cleft smoothly V-shaped; inner margin somewhat projecting, with minute setae; internal margins of the apical lobes slightly convex anteriorly; apical lobe slightly rounded apically with small scattered, setae (Fig. 5). The basal section of st5 distinctly longer than the length of the apical lobes. Hypandrial arms separated. Pregonite slightly curved anteriorly and tapered to a narrow rounded tip. Postgonite well developed, parallel sided and strongly curved anteriorly, with rounded apex. Epiphallus reduced. Surstylus with small hairs on the outer surface. Surstylus, in lateral view, slightly narrowed toward the apex, and ending in a broad rounded point. Surstylus and cercus subequal in length, or surstyli slightly longer. Cercus, in lateral view, slightly curved along its anterior and posterior margins, ending in a rounded apex (Fig. 5). In posterior view, cerci narrowed linearly from upper lobes to apical cleft and then constricted on apical 1/3; upper lobe and medial section subequal in length, upper lobe longer than the apical cleft; apical cleft weakly defined (Fig. 5). Distiphallus divided at base into long, thin sclerite posteriorly and broader winged and sclerotized portion anteriorly, the latter studded with small dentate structures.

**Female terminalia** (Fig. 4): Tergite 6 laterally reduced in size. Tergite 7 fused with the sternite 7 and modified into a strong piercing ovipositor that is curved downward and anteriorly. Sternite 6 small, with hairs on its posterior margin. Cerci strongly reduced.

**Geographic distribution and seasonal occurrence.** Specimens of *E. obumbrata* have been collected in southwestern Mexico (Fig. 1) at high altitudes of about 2000 m. All of the specimens were collected in July.

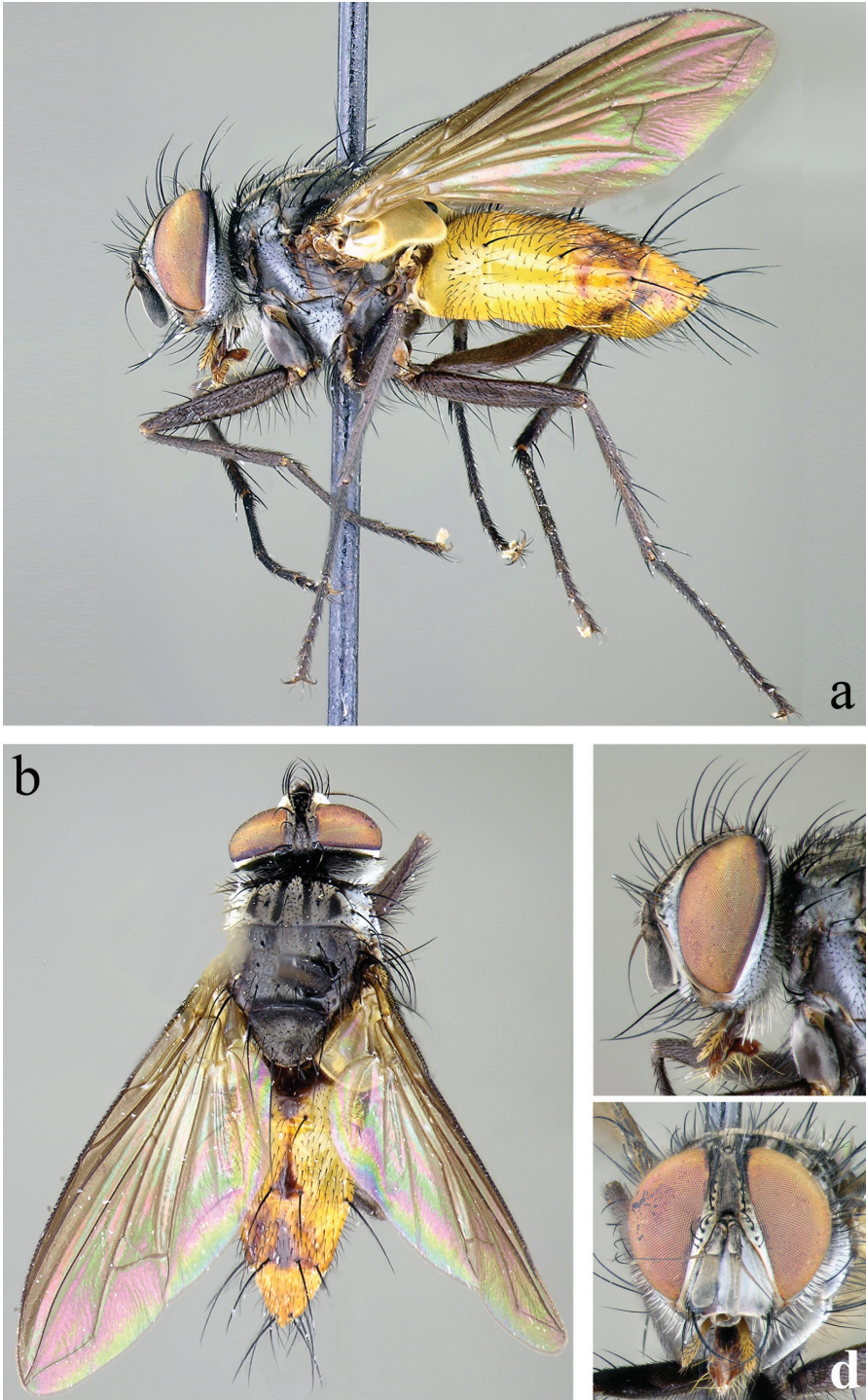


**Figure 7.** Male of *E. flava* sp. n. Full body from lateral (a) and dorsal (b) view and head from lateral (c) and frontal view (d).

***Eucelatoria flava* Inclán & Stireman, sp. n.**

<http://zoobank.org/7FF5BCF6-204C-4C91-ACF0-E18C28A3E0FC>

Figs 1, 7–10

**Type material.** Holotype male, labeled: “ECUADOR, Napo [Province]/ 7 km. s. [South] Baeza/ 20-25.II.79/ G. &M. Wood 2000m”, “HOLOTYPE/ *Eucelatoria flava*/ Inclán & Stireman [red label]”, “DI244CA [specimen ID]” (CNC).

Paratype, 1 male: “DI12CA” (CNC). As above, except the identification type label reads “PARATYPE/ *Eucelatoria flava*/ Inclán & Stireman [yellow label]”.

**Etymology.** From the Latin *flava*, meaning yellow, in reference to the yellow abdomen that distinguishes this species from its close related species, *E. obumbrata*.

**Recognition.** This species is morphologically very similar to *E. carinata* and *E. obumbrata*, but can be easily separated by the abdominal coloration. *Eucelatoria flava* sp. n. has a yellow abdomen, which contrasts with the abdomen of *E. carinata* that is entirely black and *E. obumbrata* that is primarily black, with yellow coloration confined to the sides of styntergite 1+2, and tergites 3 and 4. Additionally, median discal setae are lacking on tergites 3 and 4 in males of this species where they are present on tergites 3 and/or 4 in males of *E. obumbrata*. The eyes of this species are sparsely and short-haired, contrasting with the densely and long-haired eyes of *E. obumbrata* and from the sparsely, but long-haired eyes of *E. carinata*.

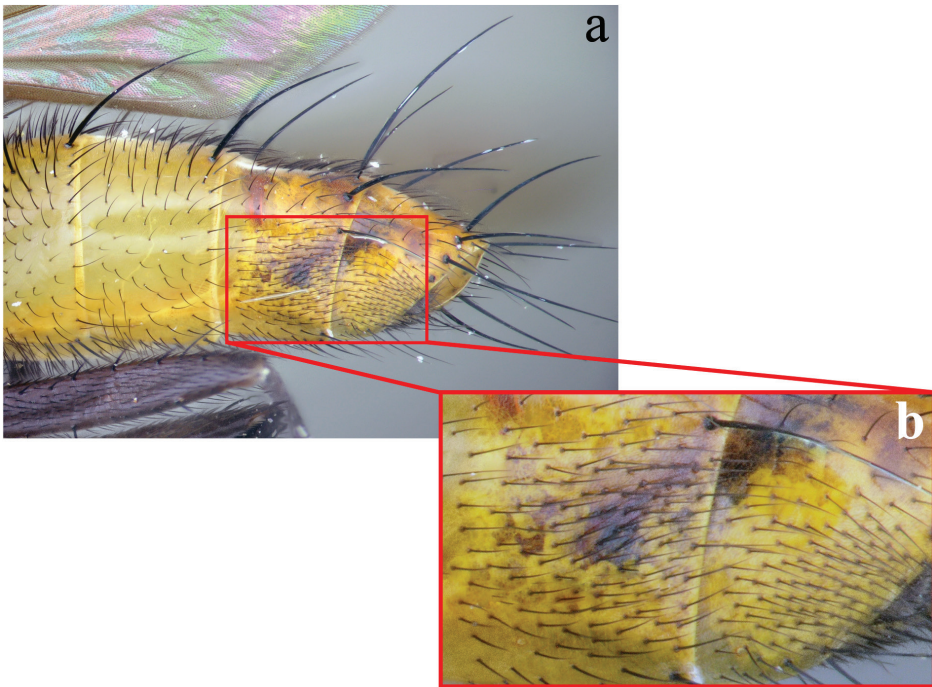


**Figure 8.** Lateral view of the male abdomen of *E. flava* sp. n. (a) showing the sexual patches on tergites 4 and 5 (b).

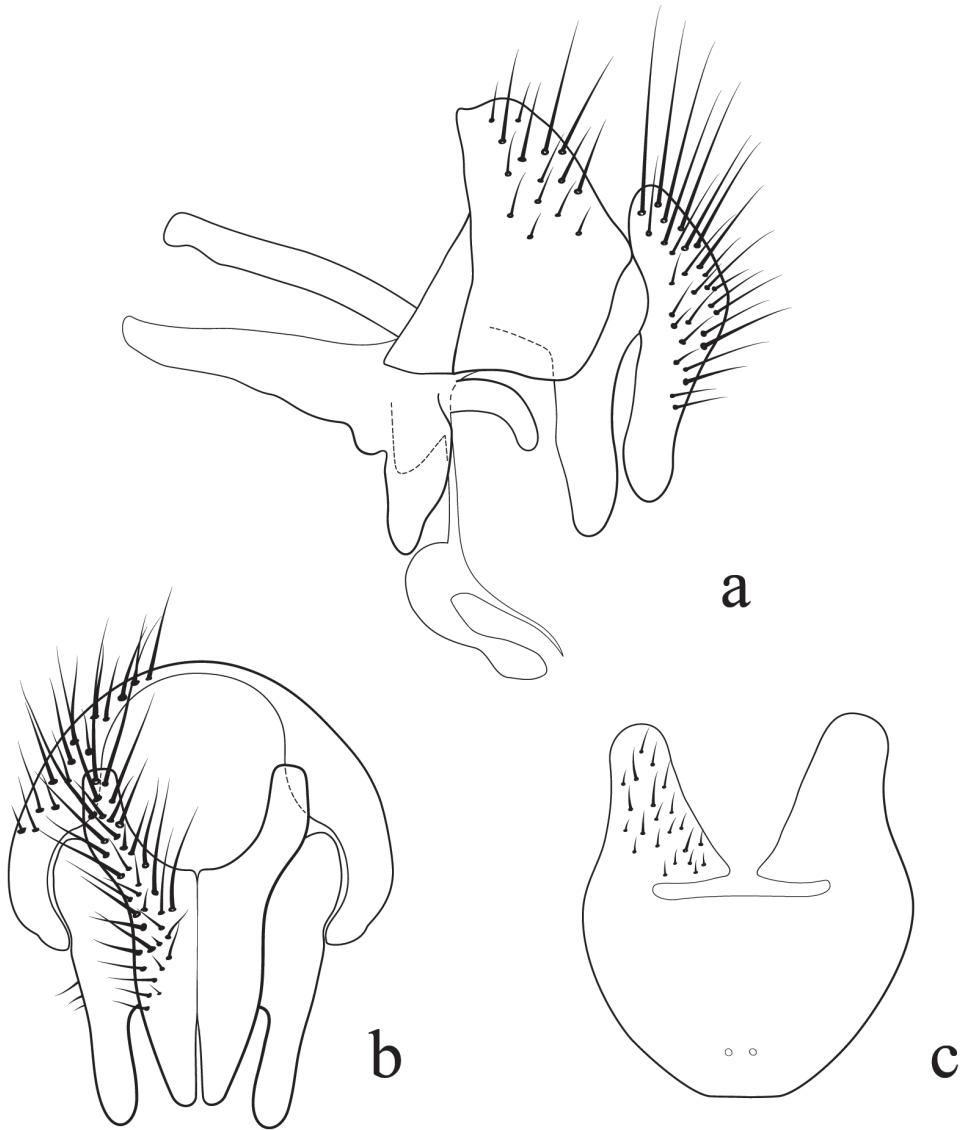


**Figure 9.** Lateral (a) and posterior view (b) of the male terminalia and sternite 5 (c) of *E. flava* sp. n.

**Description.** Described from 2 males, unless otherwise noted as “N”.

Length: 6.6–6.7 mm.

As described for *E. obumbrata* except for:

**Head** (Fig. 7): Eye sparsely haired. Eye 0.88 head height. Vertex width, at its narrowest point, 0.18–0.20 head width. Length of first flagellomere 0.41 head height. Width of first flagellomere 3.0–3.6 parafacial width at its narrowest point. Pedicel length 0.32–0.36 length of first flagellomere. Fronto-orbital plate with 7–9 medio-clinate frontal setae, 2 reclinate inner orbital setae in both sexes, male without outer



**Figure 10.** Lateral view of the hypandrial complex (a) and distiphallus (b) of *E. flava* sp. n.

orbitals. The outer vertical seta barely to undifferentiated from the row of postocular setae. Facial ridge with hairs on basal 1/3 or less. Posterodorsal part of the head only with a few black setae behind the postocular row.

**Thorax** (Fig. 7a, b): Scutum with 2 or 3 presutural acrostichal setae; postsutural acrostichal setae varied from 1 to 2; 2 presutural dorsocentral setae; 3 postsutural dorsocentral setae; 2 presutural intra-alar seta; 4 postsutural intra-alar setae; 1 presutural supra-alar seta, with 1 additional small seta; 3 postsutural supra-alar setae. The first postsutural supra-alar seta is small.

Wing varied from light to dark fumose on cells c, sc,  $r_1$ ,  $r_{2+3}$ , and  $r_{4+5}$ . Wing vein  $R_{4+5}$  dorsally setose from its base until nearly the crossvein r-m, and  $R_1$  bare.

**Abdomen** (Figs 7a, b; 8): Fully yellow, sometimes the tg5 appearing dark yellowish. Transverse bands of sparse white pruinosity scarcely visible to naked eye. Median discal setae absent on tg3 to tg5. Sexual patches of relatively dense hairs present on the ventral surface of tg4 and tg5, hardly noticeable to naked eye.

**Male terminalia** (N = 1, Figs 9, 10): The basal section of the st5 distinctly longer than the length of the apical lobes, and the internal sides of the apical lobes almost linear (Fig. 9c). Basal half of hypandrium not strongly bent, in line with more apical portion. Surstylus, in lateral view, slightly narrowed toward the apex ending in a broad rounded apex. Surstylus distinctly longer than cercus. Cercus, in lateral view, nearly straight

along anterior and posterior margins, ending in rounded apex (Fig. 9a). In posterior view, cerci abruptly constricted below upper lobes and narrowed on apical 1/3; upper lobe slightly shorter than medial section, but longer than the apical cleft; apical cleft weakly defined (Fig. 9b). Pregonite somewhat triangular in shape, relatively broad at base, narrowing toward apex. Postgonite slightly narrower than in *E. obumbrata*, and narrowed slightly towards apices, distinctly curved anteriorly, with rounded apex.

**Geographic distribution and seasonal occurrence.** The only two known specimens of *E. flava* sp. n. were collected in highland cloud forest at about 2000 m in altitude on the eastern slope of the Andes of Ecuador (Fig. 1). The two specimens were collected in February.

### *Eucelatoria carinata* (Townsend)

Figs 1, 11

*Machairomasicera carinata* Townsend, 1919: 578. Guimarães 1971: 139.

*Eucelatoria carinata* (Townsend): Wood 1985: 40–45.

**Type material.** Holotype female, labeled: “Manchi Ecuador/7000 ft/22-XI” [no year, but given as 1910 in description], “CHT Townsend/ Collector”, “Below/ Manchi Ec/ Nov 22”, “Type No. 22247/U.S.N.M.”, “*Machairomasicera carinata* ♀ Det CHTT 1”, “*Eucelatoria carinata* (Townsend)/ det. D.J. Inclán/ & J.O. Stireman” (NMNH).

**Recognition.** This species can be distinguished from *E. flava* sp. n. and *E. obumbrata* by the entirely black coloration of the abdomen, which contrasts with the entirely yellow abdomen of *E. flava*, and the yellow and black abdomen of *E. obumbrata*. It also differs from females of *E. obumbrata* in having sparsely haired eyes, more densely bristled palpi, strongly infuscated wing veins, and a bronze tinted parafacial (dull silver in known females of *E. obumbrata*).

**Redescription.** Length: 6.7 mm.

As described for *E. obumbrata* except for:

**Head** (Fig. 11): Eye sparsely, but long-haired. Eye 0.83 head height. Vertex width, at its narrowest point 0.26 head width. Length of first flagellomere 0.44 head height. Width of first flagellomere 4.6 parafacial width at its narrowest point. Pedicel length 0.28 length of first flagellomere. Fronto-orbital plate with 4–6 medioclinate frontal setae. Facial ridge with hairs on basal 1/2, but short and fine above basal 1/3. Postero-dorsal part of the head without black setae behind the postocular row.

**Thorax** (Fig. 11a, b): Scutum with 3 presutural acrostichal setae and 3 postsutural acrostichal setae; 2 presutural dorsocentral setae and 3 postsutural dorsocentral setae; 1 presutural intra-alar seta, with 1 additional small seta; 3 postsutural intra-alar setae. The first postsutural supra-alar seta present but reduced in size.

Wing moderately fumose on anterior half around veins C, Sc, R<sub>1</sub> and R<sub>4+5</sub>, light infuscation also present along veins M, CuA<sub>1</sub>, and dm-cu. Wing vein R<sub>4+5</sub> dorsally setose from its base until nearly the crossvein r-m, and R<sub>1</sub> bare.

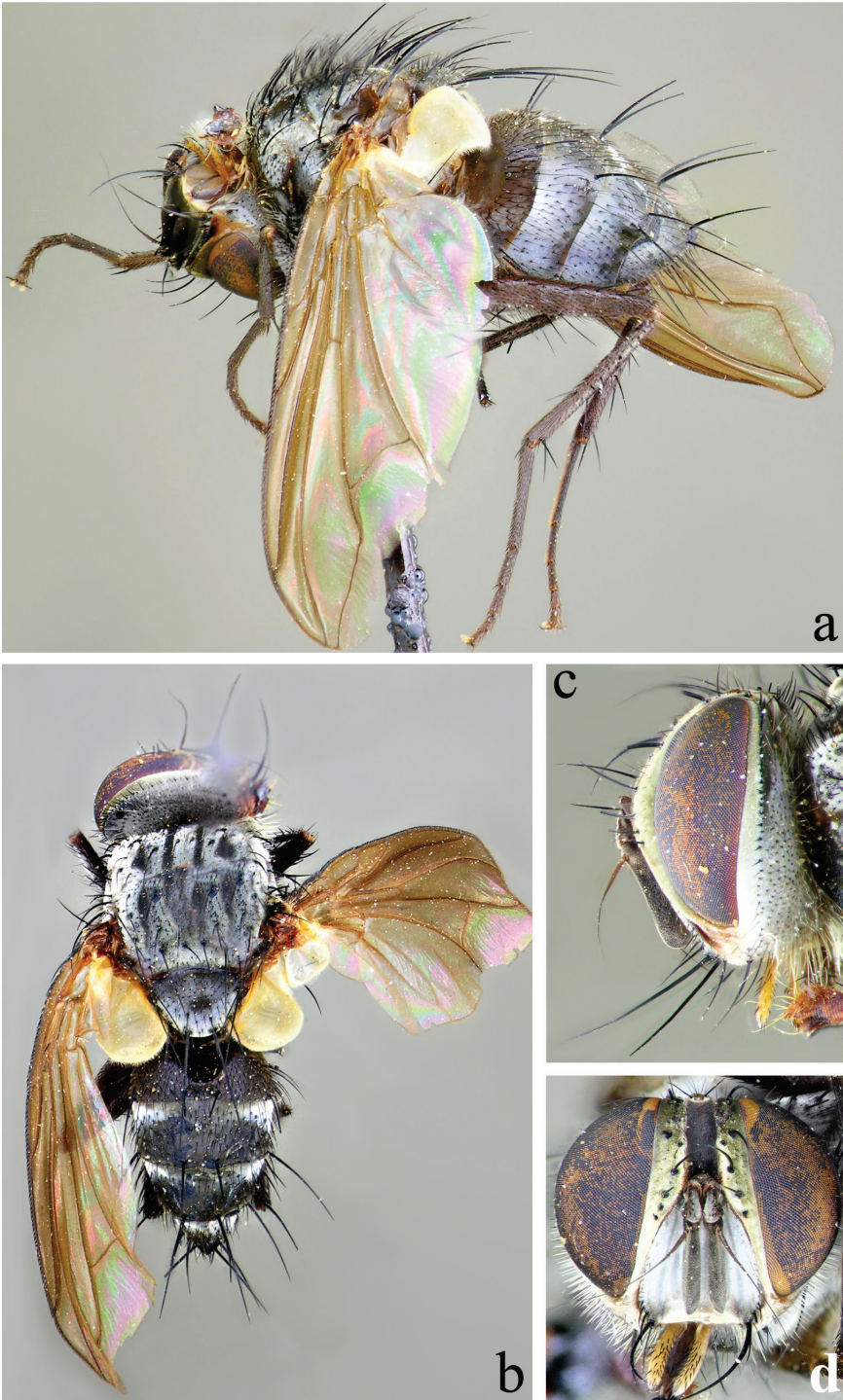


**Figure 11.** Female of *E. carinata* (Townsend). Full body from lateral (a) and dorsal (b) view and head from lateral (c) and frontal view (d).

**Abdomen** (Fig. 11a, b): Entirely black in ground color with transverse bands of sparse white pruinosity on basal 1/3 of tergites 3 and 4, and 1/2 of tergite 5. Median discal setae absent.

**Geographic distribution and seasonal occurrence.** The only known specimen of *E. carinata* was collected in Ecuador. The specimen was collected in the Andes Mountains at about 7000 ft (2100 m). The locality of the specimen reads “Below Manchi”, but it is unclear what this name refers to.

### *Myiodoriops* Townsend, 1935

*Myiodoriops* Townsend, 1935: 227. Type species: *Myiodoriops marginalis* Townsend, 1935: 227, by original designation. Guimarães 1971: 141 (catalog); Wood 1985: 39–40 (redescription, as junior synonym of *Erythromelana*); Wood and Zumbado 2011: 1403 (key to Central American genera, as junior synonym of *Erythromelana*); Inclán and Stireman 2013 (revision of *Erythromelana*, with *Myiodoriops marginalis* Townsend as revived status).

**Included species.** *Myiodoriops marginalis* Townsend, 1935.

**Diagnosis.** *Myiodoriops* can be separated from other blondeliine genera (see discussion section below) using a combination of external characters and traits of the male terminalia including: 2 katapisternal bristles, 2 postpronotal setae (or, if a small inner seta is present, all three arranged in a line or broad arc), sparsely haired eyes, facial ridge with hairs on lower 1/3 or less, vein M ending in  $R_{4+5}$  vein just before wing margin or in wing margin very close to  $R_{4+5}$ , lack of proclinate orbital setae in males, the mid-dorsal depression extending nearly to the hind margin of tg1+2, absence of a piercing structure in females, and short, spine-like setae on the anteriorly on the apex of the surstyli.

*Myiodoriops* is superficially similar to the *E. obumbrata* species group and to the genus *Erythromelana* in size, shape, and general appearance, which may explain the former grouping of these taxa into a single genus. However, it can be separated from these taxa using external morphological traits. It differs from the genus *Eucelatoria* generally in lacking the apomorphic piercing structure and associated short spines on ventral margins of abdominal tergites in females and absence of median discal setae on abdominal tergites 3 and 4, and it specifically lacks the apomorphic traits of the *E. obumbrata* group of  $R_{4+5}$  bristled nearly to crossvein r-m and sex patches in the male. *Myiodoriops* can be separated from *Erythromelana* by having the vibrissa inserted slightly above the lower facial margin (subtended by one or more setae), vein M ending in  $R_{4+5}$  vein or in wing margin very close to  $R_{4+5}$ , and the mid-dorsal depression extending nearly to the hind margin of tg1+2. Additionally, *Myiodoriops* has only 2 katapisternal setae, which differs from *Eucelatoria* and from most species of *Erythromelana* which have 3 (see Inclán and Stireman 2013). The male terminalia are also distinct from these other blondeliine taxa, particularly with respect to the surstylus, which is anteriorly curved and narrowed towards its tip with spine-like setae on the anterior side of its apex. Furthermore, males in this genus have the pregonite strongly curved anteriorly, which differs from the rectilinear one of *Erythromelana*.

The presence of short spines on the tip of the surstylus is reminiscent of *Myiopharus* (see Wood 1985; O'Hara 2007), which *Myiodoriops* resembles in a number of other respects. However, it appears distinct from the former genus in lacking proclinate orbital setae in the male, possessing bristles on the lower 1/3 of the facial ridge or less, an apparent lack of ommatrichia, three reclinate orbital setae in males, 2 postpronotal setae, or if 3, the innermost reduced in size and all 3 arranged in a broad arc, relatively short, stout surstylus and cercus, and a small and nearly pointed postgonite (see discussion section below).

**Redescription.** Redescribed from 5 males (including the type *M. marginalis*) and 6 females.

Length: males, 5.1–5.8 mm ( $\bar{x}$  = 5.42 mm); females, 3.9–5.1 mm ( $\bar{x}$  = 4.54 mm).

**Head:** Parafacial covered with dull silver pruinescence. Fronto-orbital plate and vertex black in ground color, covered with silver pruinescence appearing grayish from certain angles, usually with faint sparsely golden pruinescence dorsally. Frontal vitta usually entirely black, sometimes fading to dark-brown toward antenna. Pedicel black and first flagellomere black, covered with fine microtrichia and appearing grayish. Arista long, with minute setae, black with brown on basal 1/3 or less, thickened on basal 1/4 or less. Fronto-orbital plate with 5–7 mediocline frontal setae in male, 4–7 in female; 3 reclinate inner orbital setae in males, 2 in females; female with 2 proclinate outer orbital setae, male without outer orbitals. Vertex with one reclinate inner and usually one laterocline outer vertical seta, the latter often barely or undifferentiated from the row of postocular setae in both sexes. Inner orbital and vertical setae usually about twice the length of frontal setae. Ocellar setae well-developed, proclinate. Parafacial bare and narrow with the narrowest point about equal to the widest portion of the palpus in males; in females narrower, about the basal width of the palpus. Facial ridge with hairs on basal 1/3 or less, and lower margin of face descending slightly below the level of vibrissa. Subvibrissal ridge short, usually with 1 to 3 setae; postgena narrow, with a distinct but small genal dilation. Posteroventral part of the head with the majority of white-yellowish fine setae and posterodorsal part of the head with one row of black setae behind the postocular row. Palpus brownish to black in color, distinctly swollen apically, more markedly in females.

**Thorax:** Shiny black in ground color; presutural scutum with evident white pruinescence, postsutural scutum with much sparser pruinescence revealing underlying black ground color. In dorsal view, only the presutural scutum appears grayish; whereas in lateral view the postsutural scutum appears grayish as well. Faint white pruinose stripes on presutural scutum leaving 4 black vittae; the inner 2 vittae longer and thinner, almost 1/2 the width of each of the outer 2 vittae. Prosternum with several hair-like setae. Postpronotum with 2 or 3 setae, when 3, the inner most is reduced in size and together they form a broadly obtuse angle, ca. 130–150°. Proepisternum bare. Katepisternum with 2 setae. The first postsutural supra-alar seta smaller than the notopleural setae. Scutellum with 3 pairs of setae, without apical setae or with one small hair-like pair.

Legs entirely black. Tarsal claws longer than 5th tarsomere in male and shorter than 5th tarsomere in female. Mid tibia with 2 posterodorsal setae, and 1 ventral seta. Hind tibia with anterodorsal setae uneven in length and not closely spaced; 2 well-developed posterodorsal setae, rarely with 1 additional shorter seta; 2 anteroventral setae. Upper and

lower calypters translucent yellow-brownish. Wing length nearly equal to body length. Wing usually hyaline, rarely light fumose on the anterior edge. Wing vein  $R_{4+5}$  dorsally setose only at its base, and  $R_1$  bare. Vein M smoothly curved at bend and ending in vein  $R_{4+5}$  near the wing margin or separately in the margin closely approximated to vein  $R_{4+5}$ .

**Abdomen:** Mostly black with yellow laterally on  $tg1+2$  to  $tg4$  on males, fully black in females. Transverse bands of sparse white pruinosity usually on the anterior  $1/4$  of  $tg1+2$  to  $tg5$ . Mid-dorsal depression of  $tg1+2$  extending to marginal setae and nearly to hind margin. One pair of median marginal setae on  $tg1+2$  and  $tg3$ ; a row of median marginals on  $tg3$  to  $tg5$ ; 1 pair of lateral marginal setae on  $tg1+2$  and  $tg5$ ; discal setae absent in both sexes. Sternites completely overlapped by tergites.

**Male terminalia:** Sternite 5 with median cleft smoothly V-shaped; apical lobes narrowed to broad points at their apices. The anterior margin of  $st5$  clearly concave. The basal section of  $st5$  distinctly shorter than the length of the apical lobes. Hypandrial arms separated. Pregonite curved anteriorly and tapered to a narrow rounded tip. Postgonite distinctively curved anteriorly, with narrow, almost pointed apex. Epiphallus small, hidden between the pregonites. Surstylus, in lateral view, broad, anteriorly curved and narrowed toward the apex, considerably longer than cercus. Surstylus with several short spine-like setae on the anterior side of its apex. Cercus, in lateral view, broad, slightly concave along anterior margin and narrowed only on the posterior margin of the apex. In posterior view, the cerci with long rectilinear upper lobes, nearly as long as the medial section + apical cleft combined. Apices of cerci, in posterior view, with excavated inner margins. Lateral margins of cerci without a constriction towards the apical section; apical cleft well defined. Distiphallus divided at base into long and a broader sclerotized portion with a toothed margin anteriorly.

**Geographic distribution and seasonal occurrence.** See the distribution of *Myiodoriops marginalis* below, except for four undescribed specimens (see discussion below) that were collected in Brazil, Peru and Argentina (Fig. 12). All known specimens were collected at lower elevations (< 200 m) except one specimen collected in Peru at 1600 m. Specimens have been collected from January until October, but most of the material was collected in January.

**Discussion.** The phylogenetic affinities of *M. marginalis* are unclear. As indicated in the diagnosis, there is little reason to believe that the species belongs with its former congeners in the genus *Erythromelana* or *Eucelatoria*, nor does it appear to be closely related to these taxa (see also Inclán and Stireman 2013). *Myiodoriops marginalis* is morphologically similar to the large and difficult genus *Lixophaga*, but it lacks the enlarged pair of bristles on sternite 5 characteristic of males of this genus (although it does have a number of smaller bristles; Fig. 14c) and the postpronotal bristles of *M. marginalis*, if three, are arranged in a line. It even more closely resembles members of *Euthelyconychia* in general appearance and chaetotaxy, sharing with this genus some features of the male genitalia as well (e.g. surstylar and postgonite shape), but the cerci are differently shaped and *Euthelyconychia* appears to lack surstylar spines. The possession of the unusual, anteriorly directed surstylar spines, suggests a close relationship with *Myiopharus*, and it is possible that *M. marginalis* represents a highly autapomorphic

species of this genus, or of *Euthelyconychia*. Without detailed systematic study and analysis of these genera and the Blondeliini as a whole, which is beyond the scope of the present study, these possibilities cannot be confirmed or refuted. Therefore, we retain *M. marginalis* in its originally described genus.

The genus description is based primarily on the specimens available for the known species *M. marginalis*. However, we found four specimens from Peru, Brazil and Argentina that belong to this genus, but they appear represent one or more undescribed species near *M. marginalis*. We have included these specimens in the genus description to cover all the generic variability, but we did not describe these specimens given the limited material and their poor condition. Additionally, of these four specimens, three are females and each is from a different locality. These four specimens exhibit slight differences in external morphology (e.g., parafacial width and abdominal coloration), but it is unclear if these differences represent intraspecific variation, male-female dimorphism, or actual differences between species. Therefore, we leave these specimens undescribed until additional material is available that can be used to help establish their identity.

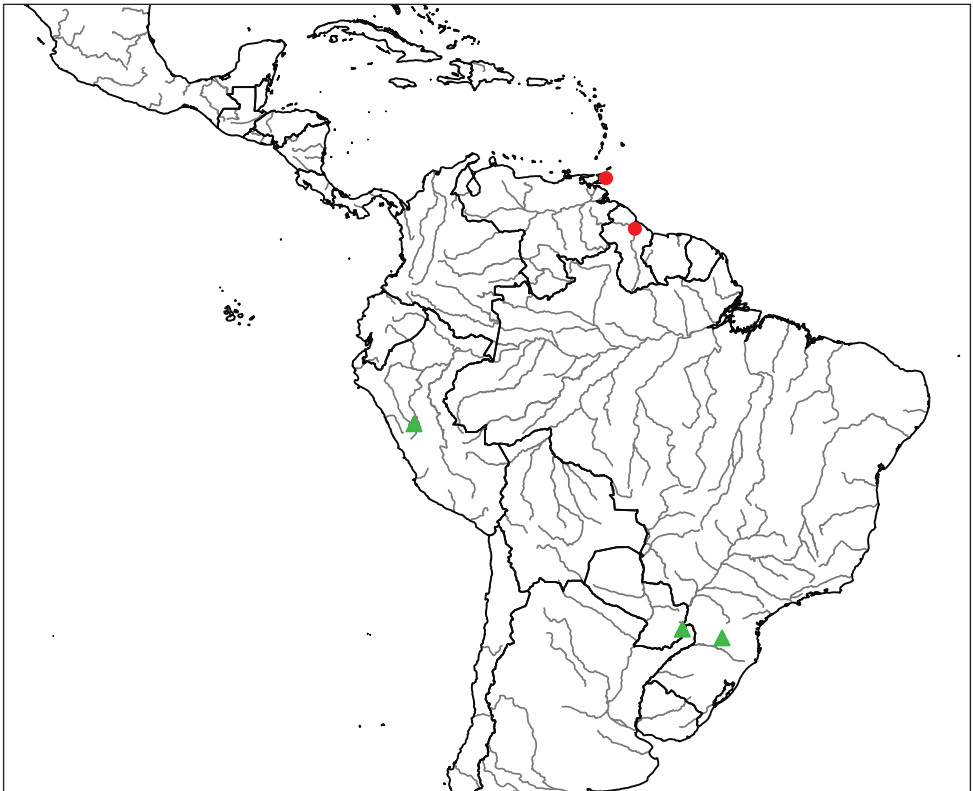


**Figure 12.** Known distributions of *Myiodoriops* species. *M. marginalis* Townsend is represented by red circles and *M. spp.* by green triangles.

***Myiodoriops marginalis* Townsend**

Figs 12–15

*Myiodoriops marginalis* Townsend, 1935: 227; Guimarães 1971: 141.*Erythromelana marginalis* (Townsend): Wood 1985: 39–40; Inclán and Stireman 2013.

**Type material.** Holotype male labeled: “HOLO-/TYPE”, “Type [red label]”, “Pariká/ Ruhunú/ B. Guiana/ Jan. 1934 [hand written]”, “Mycos/ 4401 [hand written]”, “Press. By/ J.G. Myers/ B.M. 1940-24” “*Myiodoriops/ marginalis* TT [hand written]/ DetCHTT ♂”, “*Myiodoriops/ marginalis* Townsend/ det. D.J. Inclán/ & J.O. Stireman” (BNHM).

**Other material examined.** Seven specimens examined. 1 male labeled: “St. Augustine,/ Trinidad, BWI./ 1. 24. 60”, “*Myiodoriops/ marginalis* [hand written]”, “DI240CA” (CNC). 1 male labeled: “St. Augustine,/ Trinidad, BWI./ JAN 8 1960”, “F. D. Bennett/ Collector”, “X P. (77)/ near/ *Myiodoriops* [hand written]”, “*Myiodoriops/ marginalis* Townsend/ det. D.J. Inclán/ & J.O. Stireman”, “DI-241CA” (CNC). 1 male labeled: “PIARCO/ Trinidad, BWI./ OCT. 29. 1953.”, “Collector/ F. J. Simmonds”, “77 [hand written]”, “*Myiodoriops/ n. sp.* ♂ [hand written]”, “*Myiodoriops/ marginalis* Townsend/ det. D.J. Inclán/ & J.O. Stireman”, “DI243CA” (CNC). 1 female labeled, same as previous except by “OCT. 29. 1953”, without sp. ID, “DI74CA” CNC. 1 male labeled: “W. ARIMA/ TRINIDAD/ 26-8-1964”, “*Myiodoriops/ marginalis* Townsend/ det. D.J. Inclán/ & J.O. Stireman”, “DI73CA” (CNC). 1 female labeled: “St. Augustine,/ Trinidad, BWI./ II. 17. 60”, “*Myiodoriops/ marginalis* Townsend/ det. D.J. Inclán/ & J.O. Stireman”, “DI39CA” (CNC). 1 female labeled: same as previous except by “II. 28. 60”, “DI236CA” (CNC).

**Recognition.** See diagnostic section for the genus *Myiodoriops*.

**Redescription.** Redescribed from 5 males (including the type *M. marginalis*) and 3 females.

Length: males, 5.1–5.8 mm ( $\bar{x}$  = 5.42 mm); females, 3.9–4.53 mm ( $\bar{x}$  = 4.21 mm).

As described for the genus except:

**Head** (Fig. 13): Eye sparsely haired, ommatrichia short, about as long as 2–3 eye facets. Eye 0.85–0.87 head height in male, 0.83–0.88 in female. Vertex width 0.20–0.22 head width in male, 0.24–0.27 in female. Width of frontal vitta 0.25–0.30 vertex width in male, 0.28–0.43 in female. Length of first flagellomere 0.38–0.46 head height in male, 0.39–0.45 in female. Pedicel length 0.31–0.37 length of first flagellomere in male, 0.28–0.36 in female.

**Geographic distribution and seasonal occurrence.** Specimens of *M. marginalis* have been collected only from Guyana in northern South America, and from the southern Caribbean islands of Trinidad and Tobago (Fig. 12). All collections are from lowland tropical forest. Adults have been collected mainly in January, but also in February, August and October.

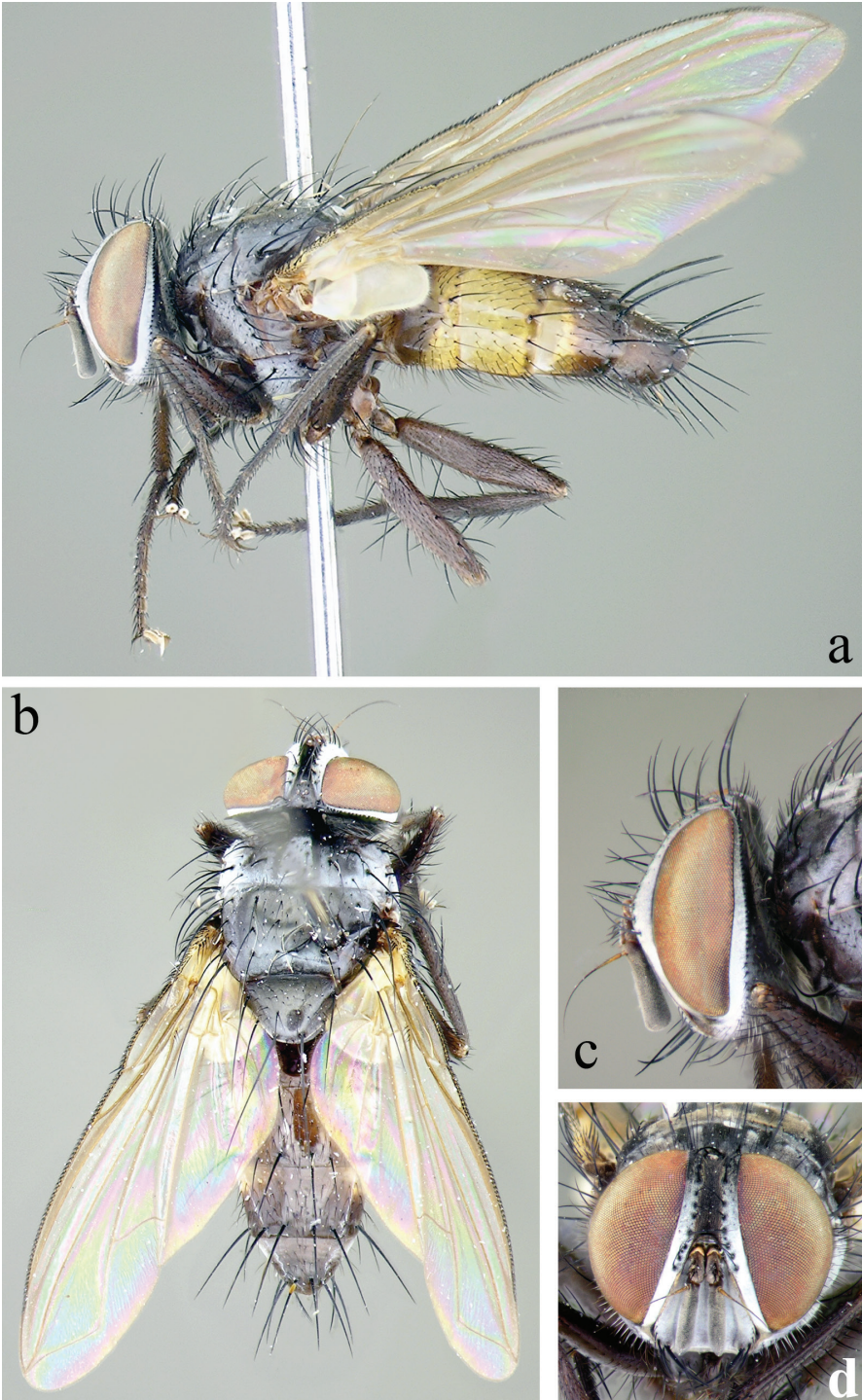


**Figure 13.** Male of *M. marginalis* Townsend. Full body from lateral (a) and dorsal (b) view and head from lateral (c) and frontal view (d).

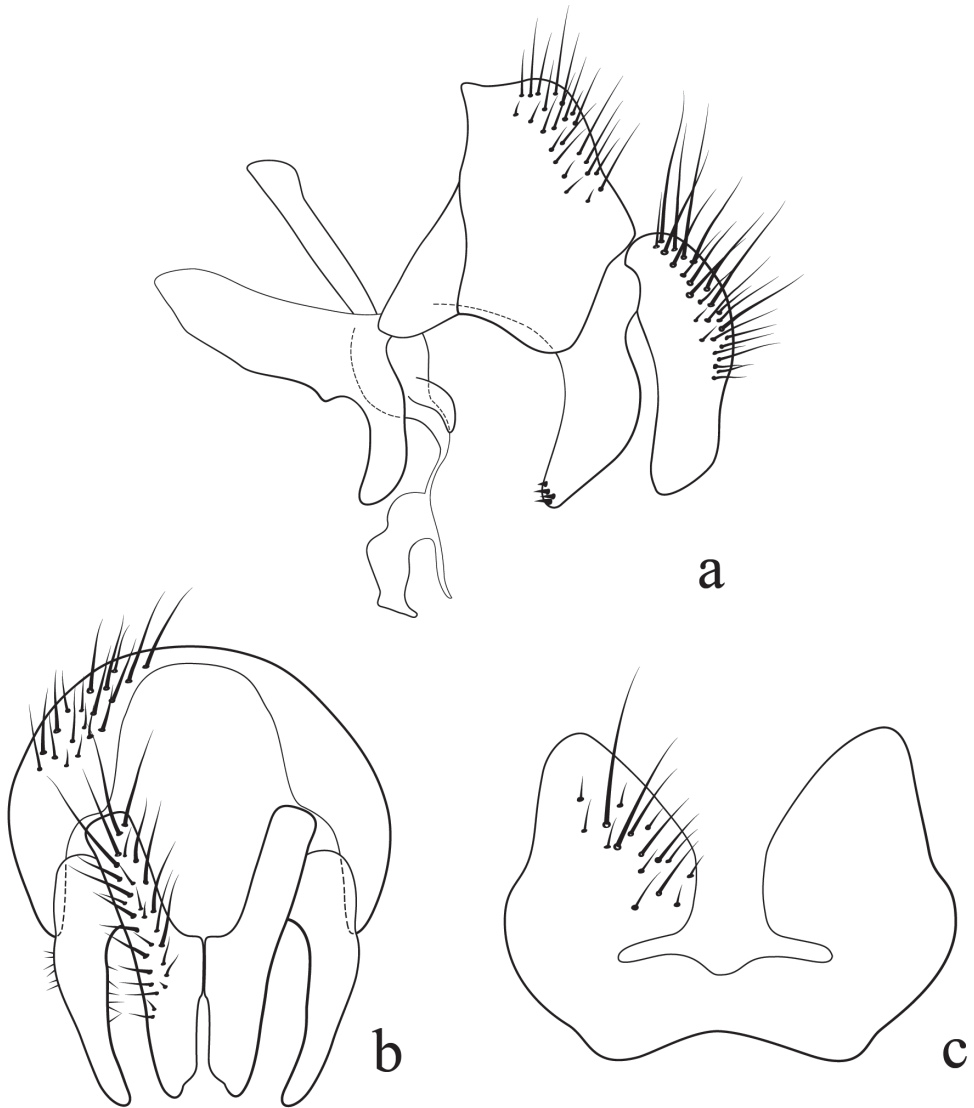


**Figure 14.** Lateral (a) and posterior view (b) of the male terminalia and sternite 5 (c) of *M. marginalis* Townsend.

### Key to genera

Identification of the *Eucelatoria obumbrata* species group, *Myiodoriops* and *Erythromelana* using Wood and Zumbado (2011).

All three genera should readily key to couplet 114 (along with nearly all blondeliines) in Wood and Zumbado's (2010) key to Tachinidae of Central America. From there, specimens should key using the following couplets (modified couplets are indicated with bold numbers):

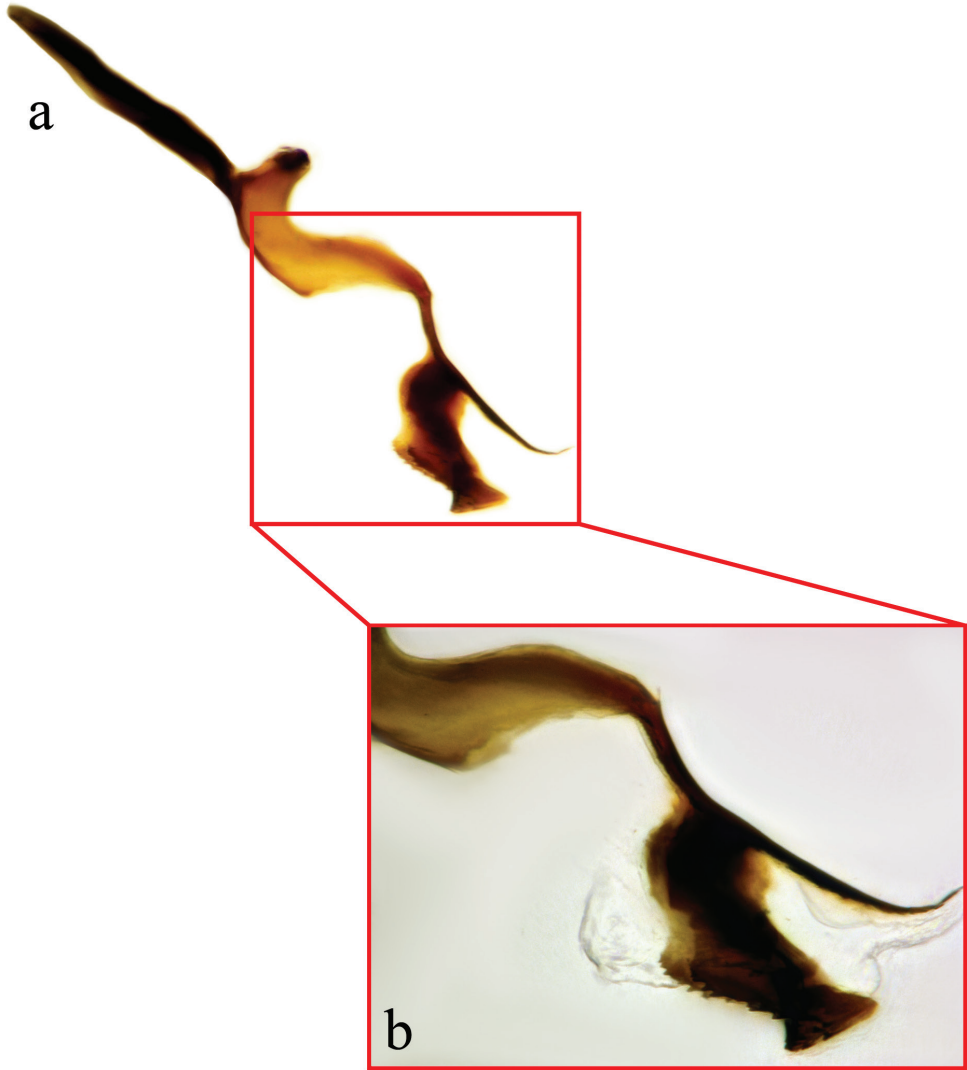


**Figure 15.** Lateral view of the hypandrial complex (a) and distiphallus (b) of *M. marginalis* Townsend.

- 114 Vein  $R_{4+5}$  setose on dorsal surface halfway or more from its base at junction of  $R_{2+3}$  and  $R_{4+5}$  to crossvein r-m (Figs 158, 160, 161) .....**115**
- Vein  $R_{4+5}$  dorsally with few setae at base only, not extending halfway to crossvein r-m.....**129**
- 115 Eye with conspicuous ommatrichia, each longer than combined diameter of four or more eye facets (as in Fig. 20) .....**116**
- Eye apparently bare.....**120**
- 116** Facial ridge bristled on lower half or more, with row of erect bristles along most of length (Figs 21–24) .....**117**

- Facial ridge bare except for few small recumbent bristles above vibrissa [specimens of some species of the *E. obumbrata* species group have fine setae nearly to one-half the height of the facial ridge, but these are short and hair-like above the lower third]..... **118**
- ...
- 118** Lateral scutellar bristles parallel to one another and shorter than subapical bristles (as in Fig. 130); ventral surfaces of abdominal tergites 4 and 5 of male each with patch of appressed black hair (sex patch, Fig. 165)..... **118a**
- Lateral scutellar bristles divergent and about as long as subapical bristles (Fig. 127); ventral surfaces of abdominal tergites 4 and 5 of male with or without patches of appressed hair..... **119**
- 118a** Male with a pair of proclinate orbital bristles; female abdomen and ovipositor unmodified; Two katepisternal bristles ..... ***Leptostylum* Macquart**
- Male without pair of proclinate orbital bristles; female with short stout bristles on the ventral margins of tergites, sternite 7 modified into sharp, hook-like piercer, usually concealed between ventral edges of tergites; usually three katepisternal bristles..... ***Eucelatoria* Townsend**, in part
- ...
- 120 Ventral katepisternal bristle as large as, or larger than, anterodorsal katepisternal bristle (rarely only slightly thinner) and situated close to upper margin of midcoxa, within no more than twice its diameter from coxal margin (Fig. 118); vein  $A_1$  ending at wing margin (Fig. 160), although apex of vein may be thin and easily overlooked without transmitted light or light reflected from upper surface..... **121**
- Ventral katepisternal bristle absent or distinctly smaller than anterodorsal katepisternal bristle and usually situated closer to anterodorsal bristle than to midcoxa (intermediate or closer to coxa in a few *Actia* and *Ceromya*), but not as close to coxa as twice its diameter (Fig. 117); vein  $A_1$  ending in membrane before reaching margin of wing (Fig. 161) ..... **122**
- ...
- 122 Vein  $R_{4+5}$  setulose dorsally from base to well beyond crossvein r-m (Fig. 161)..... **123**
- Vein  $R_{4+5}$  without setulae beyond crossvein r-m ..... **124**
- ...
- 124 Scutellum lacking both lateral and discal bristles (as in Fig. 132); basal portion of proboscis when extended longer than prementum (Fig. 82), and membrane between lower genal margin and clypeus thickened, forming convex paraclypeal sclerite (as in Fig. 80) (not visible if proboscis is retracted into base of head); labella extending forward..... ***Ginglymia* Townsend**
- Scutellum with lateral and discal bristles; basal portion of proboscis shorter than prementum, and membrane between lower genal margin and clypeus without sclerite; labella either padlike or extending posteriorly ..... **125**
- 125** Facial ridge with row of erect bristles on basal half or more ..... **126**

- Facial ridge bare except for few small setae above vibrissa [specimens of some species of the *E. obumbrata* species group have fine setae nearly to one-half the height of the facial ridge, but these are short and hair-like above the lower third]..... **127**  
...
- 127 Veins R<sub>4+5</sub> and M ending separately on either side of wing apex relatively far apart (Fig. 158)..... ***Chaetostigmoptera* Townsend**, in part
- Veins R<sub>4+5</sub> and M both ending before wing apex (as in Fig. 148) ..... **128**
- 128** Both lateral and subapical scutellar bristles long, stout, divergent (as in Fig. 131); vibrissa subtended by one or more subvibrissal bristles below it (as in Figs 20–22); three postsutural supra-alar bristles present, middle one largest ..  
..... ***Italispidea* Townsend**
- Lateral scutellar bristles either lacking or short and thin; subapical bristles divergent or convergent; vibrissa with or without one or more subvibrissal bristles below it; two or three postsutural supra-alar bristles present..... **128a**
- 128a** Lateral scutellar bristles either lacking or short, thin, convergent; subapical bristles also convergent, crossed medially; vibrissa arising from anteroventral corner of head without subvibrissal bristles below it (as in Fig. 25); postsutural supra-alar bristles reduced to two: the true first bristle absent; the apparent first, therefore, the larger of the two (Fig. 99). Males without obvious sex patches on abdominal tergites 4 and 5; female without short stout bristles on the ventral margins of tergites and without sternite 7 modified into a piercer.....  
..... ***Ischyrophaga* Townsend**
- Lateral scutellar bristles present, short, and parallel or divergent; subapical bristles divergent; vibrissa subtended by one or more subvibrissal bristles below it; usually 3 postsutural supra-alar bristles; males with sex patches on the ventral surfaces of abdominal tergites 4 and 5; female with short stout bristles on the ventral margins of tergites, sternite 7 modified into sharp, hook-like piercer, usually concealed between ventral edges of tergites.....  
..... ***Eucelatoria* Townsend**, in part
- 129 Eye with conspicuous ommatrichia, each longer than combined diameter of four or more eye facets (as in Fig. 20) ..... **130**
- Eye apparently bare..... **134**
- 130 Parafacial with row of stout erect bristles along entire length (Fig. 37); base of vein R<sub>4+5</sub> with single large bristle (as in Figs 156, 159)... ***Eulasiona* Townsend**
- Parafacial lacking row of erect bristles; base of vein R<sub>4+5</sub> with more than one small bristle..... **131**
- 131** Vibrissa arising at level of lower margin of head (as in Fig. 25); usually with two postpronotal bristles (as in Fig. 93), rarely with three; middorsal depression on abdominal syntergite 1+2 not extending back to hind margin of syntergite ..... ***Erythromelana* Townsend**, in part
- Vibrissa arising above level of lower margin of head, with at least one subvibrissal bristle (Fig. 20); three or more postpronotal bristles present; middorsal

- depression on abdominal syntergite 1+2 extending back to hind margin of syntergite (as in Figs 186, 188) ..... **132**  
 ...  
 134 Facial ridge setose on lower half or more, with row of erect bristles or hairs or both along most of length..... **135**  
 – Facial ridge bare except for few small recumbent bristles above vibrissa ... **150**  
 ...  
 150 Median discal bristles present on tergites 3 and 4..... **151**  
 – Median discal bristles absent from tergites 3 and 4 ..... **160**  
 ...  
 160 Eye exceptionally large, covering almost all of side of head; distance between eye and lower margin of head less than twice width of palpus (as in Fig. 14); ocellar triangle not raised to form tubercle; ocellar bristles arising beside or in front of anterior ocellus, their bases about as far apart as posterior ocelli .....  
 ..... ***Sphaerina* Wulp**  
 – Eye smaller, distance between eye and lower margin of head greater than twice width of palpus; ocellar triangle raised; ocellar bristles arising behind anterior ocellus, their bases closer together than posterior ocelli ..... **161**  
 161 Vibrissa arising from anteroventral corner of head (Fig. 25), with at most one subvibrissal bristle below it; parafacial very narrow; lateral scutellar bristle short or lacking (Fig. 132); postsutural supra-alar bristles usually reduced to two, true first bristle absent (as in Fig. 99) ..... **162**  
 – Vibrissa arising above anteroventral corner of head (Fig. 20), subtended by one or more subvibrissal bristles; parafacial narrow or broad; lateral scutellar bristle well developed (as in Figs 130, 131); postsutural supra-alar bristles three or more, middle one largest (as in Figs 100–104) ..... **163**  
 162 Arista plumose (Fig. 25); genal dilation extending forward to about vibrissal angle, anterior genal seta thus arising close to base of vibrissa; midtibia at most with small anterodorsal seta scarcely longer than width of tibia; lateral scutellar bristles lacking..... ***Phyllophilopsis* Townsend**, in part  
 – Arista bare; genal dilation distinctly separated from vibrissal angle by gap of membrane, so that single subvibrissal seta distinctly separated from genal setae; midtibia with well-developed anterodorsal seta; lateral scutellar bristles present..... ***Erythromelana* Townsend**, in part  
 163 Lateral scutellar bristles at least four-fifths as long and as straight as subapical scutellar bristles, strongly divergent (as in Fig. 131); parafacial extremely narrow; with two reclinate orbital bristles, markedly different from each other in size (as in Fig. 19) ..... ***Italisipidea* Townsend**, in part  
 – Lateral scutellar bristles about two-thirds (or less) as long as subapical scutellar bristle (as in Fig. 130); parafacial broader; reclinate orbital bristles more numerous or more uniform in size..... **164**  
 164 Ocellar setae minute, shorter than length of ocellar triangle; frontal and reclinate orbital bristles forming single even row, increasing in size toward vertex

- usually regularly (as in Figs 65, 66), or with abrupt increase in some species; body pale ochreous brown ..... **Ophirion Townsend**
- Ocellar setae present, longer than ocellar triangle; frontal and reclinate orbital bristles, if arising in single row, usually varying in size, with largest frontal bristles in middle of row (as in Figs 63, 64); body color usually brown or black, except on sides of abdomen ..... **165**
- 165 Veins M and R<sub>4+5</sub> each ending separately on either side of wing apex (Fig. 158) ...  
..... **Chaetostigmoptera Townsend**, in part
- M and R<sub>4+5</sub> both ending anterior to wing apex (as in Fig. 156)..... **165a**
- 165a** Male with two pairs of proclinate orbital setae (as in females); usually 2 reclinate orbital setae; three postpronotal bristles arranged in a triangle or strong arc; 2 or 3 katepisternal bristles .....  
..... **Myiopharus Brauer & Bergenstamm**, in part
- Male without proclinate orbital setae; usually 3 reclinate orbital setae; 2 apparent postpronotal bristles, innermost bristle reduced or absent, when present, the three are arranged in a broad arc forming an angle of > 120°; 2 katepisternal bristles.....**Myiodoriops Townsend**

## Acknowledgments

We would like to thank to Jim O'Hara, Monty Wood (Invertebrate Biodiversity, Agriculture and Agri-Food Canada, CNC), Norm Woodley (Systematic Entomology Laboratory, NMNH), Nigel Wyatt (Natural History Museum, Department of Entomology, BMNH) and Manuel Zumbado (National Biodiversity Institute of Costa Rica, INBio) who provided specimen loans. We also thank Matt Duncan for helping with some of the images and Z. "Kai" Burington for useful discussions concerning *Eucelatoria*. Thanks to Pierfilippo Cerretti, Jim O'Hara and one anonymous reviewer for carefully reviewing and editing this manuscript. This work was supported by a PhD Fellowship from the CARIPARO Foundation to DJ Inclán and a U.S. NSF grant (DEB 1020571) to JO Stireman.

## References

- Arnaud PH Jr (1958) The entomological publications of Charles Henry Tyler Townsend [1863–1944]; with lists of his new generic and specific names. *Microentomology* 23: 1–63.
- Cerretti P, Di Giulio A, Romani R, Inclán DJ, Whitmore D, Di Giovanni F, Scalici M, Minelli A (2014a) First report of exocrine epithelial glands in oestroid flies: the tachinid sexual patches (Diptera: Oestroidea: Tachinidae). *Acta Zoologica*. doi: 10.1111/azo.12085
- Cerretti P, O'Hara J, Wood DM, Shima H, Inclán DJ, Stireman JO III (2014b) Signal through the noise? Phylogeny of the Tachinidae (Diptera) as inferred from morphological evidence. *Systematic Entomology* 39: 335–353. doi: 10.1111/syen.12062

- Cumming JM, Wood DM (2009) Adult morphology and terminology. In: Brown BV, Borkent A, Cumming JM, Wood DM, Woodley NE, Zumbado M (Eds) Manual of Central American Diptera. Volume 1. NRC Research Press, Ottawa, 9–50.
- Guimarães JH (1971) Family Tachinidae (Larvaevoridae). A catalogue of the Diptera of the Americas south of the United States 104: 1–333.
- Hadley A (2013) CombineZM public domain image processing software. <http://www.hadleyweb.pwp.blueyonder.co.uk> [accessed 9 September 2013]
- Inclán DJ, Stireman III JO (2013) Revision of the genus *Erythromelana* Townsend (Diptera: Tachinidae) and analysis of its phylogeny and diversification. *Zootaxa* 3621: 1–82. doi: 10.11646/zootaxa.3621.1.1
- O'Hara JE (1989) Systematics of the genus group taxa of the Siphonini (Diptera: Tachinidae). *Questiones Entomologicae* 25: 1–229.
- O'Hara JE (2002) Revision of the Polideini (Tachinidae) of America north of Mexico. *Studia dipterologica* 10: 1–170.
- O'Hara JE (2007) A new species of *Myiopharus* Brauer & Bergenstamm (Diptera: Tachinidae) parasitic on adults of the sunflower beetle, *Zygogramma exclamationis* (Fabricius). *Zootaxa* 1521: 31–41.
- O'Hara JE (2012) World genera of the Tachinidae (Diptera) and their regional occurrence. Version 7.0. PDF document, 75 pp. [http://www.nadsdiptera.org/Tach/Genera/Gentach\\_ver7.pdf](http://www.nadsdiptera.org/Tach/Genera/Gentach_ver7.pdf) [accessed 9 February 2014]
- O'Hara JE (2013a) History of tachinid classification (Diptera, Tachinidae). *ZooKeys* 316: 1–34. doi: 10.3897/zookeys.316.5132
- O'Hara JE (2013b) Where in the world are all the tachinid genera? *The Tachinid Times* 26: 10–16.
- Sabrosky CW (1981) A partial revision of the genus *Eucelatoria* (Diptera, Tachinidae), including important parasites of *Heliothis*. United States Department of Agriculture, Science and Education Administration, Technical Bulletin 1635: 1–18.
- Shorthouse DP (2010) SimpleMappr, an online tool to produce publication-quality point maps. <http://www.simplemappr.net> [accessed 9 July 2013]
- Stireman JO III (2002) Phylogenetic relationships of tachinid flies in subfamily Exoristinae (Tachinidae: Diptera) based on 28S rDNA and elongation factor-1 $\alpha$ . *Systematic Entomology* 27: 409–435. doi: 10.1046/j.1365-3113.2002.00187.x
- Tachi T, Shima H (2010) Molecular phylogeny of the subfamily Exoristinae (Diptera, Tachinidae), with discussions on the evolutionary history of female oviposition strategy. *Systematic Entomology* 35: 148–163. doi: 10.1111/j.1365-3113.2009.00497.x
- Townsend CHT (1909) Descriptions of some new Tachinidae. *Annals of the Entomological Society of America* 2: 243–250.
- Townsend CHT (1919) New genera and species of muscoid flies. *Proceedings of The United States National Museum* 56: 541–592. doi: 10.5479/si.00963801.2301.541
- Townsend CHT (1931) New genera and species of American oestromuscoid flies. *Revista de Entomologia* 1: 313–465.
- Townsend CHT (1935) New South American Ostroidea (Dipt.). *Revista de Entomologia* 5: 216–233.

- Wood DM (1985) A taxonomic conspectus of the Blondeliini of North and Central America and the West Indies (Diptera: Tachinidae). *Memoirs of the Entomological Society of Canada* 132: 1–130. doi: 10.4039/entm117132fv
- Wood DM (1987) Tachinidae. In: McAlpine JF, Peterson BV, Shewell GE, Teskey HJ, Vockeroth JR, Wood DM (Eds) *Manual of Nearctic Diptera*. Volume 2. Agriculture Canada Monograph 28: 1193–1269.
- Wood DM, Zumbado MA (2010) Tachinidae (tachinid flies, parasitic flies). In: Brown BV, Borkent A, Cumming JM, Wood DM, Woodley NE, Zumbado MA (Eds) *Manual of Central American Diptera*. Volume 2. NRC Research Press, Ottawa, 1343–1417.
- Wulp FM van der (1890) Family Muscidae. In: Godman ED, Salvin O (Eds) *Biologia Centrali-Americana, Insecta, Diptera*. Volume 2. Taylor & Francis, London, 489 pp.



# Taxonomic study of the genus *Halolaguna* Gozmány (Lepidoptera, Lecithoceridae) from China, with descriptions of two new species

Kaijian Teng<sup>1</sup>, Shurong Liu<sup>1</sup>, Shuxia Wang<sup>1</sup>

<sup>1</sup> College of Life Sciences, Nankai University, Tianjin 300071, P. R. China

Corresponding author: Shuxia Wang ([shxwang@nankai.edu.cn](mailto:shxwang@nankai.edu.cn))

---

Academic editor: E. van Nieuwerkerken | Received 11 September 2014 | Accepted 14 November 2014 | Published 16 December 2014

---

<http://zoobank.org/BAC1FD7A-A575-49CC-A215-0F85A110F2B6>

---

**Citation:** Teng K, Liu S, Wang S (2014) Taxonomic study of the genus *Halolaguna* Gozmány (Lepidoptera, Lecithoceridae) from China, with descriptions of two new species. ZooKeys 464: 99–110. doi: 10.3897/zookeys.464.8571

---

## Abstract

The genus *Halolaguna* Gozmány, 1978 is studied in China. Two new species, *H. flabellata* sp. n. from Guangxi and *H. discoidea* sp. n. from Chongqing, Guangxi and Sichuan are described. The female of *H. guizhouensis* Wu, 2012 is reported for the first time. Photographs of adults and genitalia are provided. A checklist of all known *Halolaguna* species is included, along with a key to the Chinese species.

## Keywords

Lepidoptera, Lecithoceridae, *Halolaguna*, new species

## Introduction

The family Lecithoceridae occurs particularly in the Oriental and Australian Regions, with around 1,200 described species (van Nieuwerkerken et al. 2011). Wu (1997) recorded 206 species of Lecithoceridae from China and Park et al. (2013) listed 74 species of Lecithoceridae from Chinese Taiwan. To date, approximately 290 species of this family have been reported from China.

*Halolaguna* Gozmány, 1978 is a small genus of the subfamily Torodorinae in Lecithoceridae, which was established by Gozmány in 1978 based on the type species *H. subluxata* Gozmány, 1978 from China. Subsequently, Wu (2000) transferred *Lecithocera biferrinella* Walker, 1864 to *Halolaguna*, and described *H. orthogonia* Wu,

2000 from Malaysia; Park (2000) transferred *Cynicostola oncopteryx* Wu, 1994 to *Halolaguna*, and described *H. palinensis* Park, 2000 from Taiwan; Park (2011) further described *H. sanmaru* Park, 2011 from Thailand; and Wu (2012) described *H. guizhouensis* Wu, 2012 from Guizhou. To date, *Halolaguna* includes seven species confined to the Oriental and Palaearctic regions, but little is known about the biology of this genus so far.

*Halolaguna* is characterized by having an elongate and relatively narrow forewing with  $M_2$  and  $M_3$  coincident, and the valva tapering to the apex in the male genitalia. *Halolaguna* is similar to *Antiochtha* Meyrick, 1905 in both appearance and male genitalia, but can be distinguished by the presence of  $M_2$  in the hindwing, which is absent in *Antiochtha*. It is also similar to *Athymoris* Meyrick, 1935 in the venation, but differs in the valva in the male genitalia that is tapering to a pointed apex, whereas the valva is foot-shaped and widened terminally in *Athymoris*.

We report five *Halolaguna* species from mainland China in this paper, based on the specimens collected mostly from mountainous regions and natural reserves. Two species are described as new, and the female of *Halolaguna guizhouensis* Wu, 2012 is described for the first time.

## Material and methods

The specimens examined in this study were collected from mountains, botanical gardens and nature reserves in China by light traps. All specimens studied, including the types, are deposited in the Insect Collection, College of Life Sciences, Nankai University, Tianjin, China.

Genitalia dissections were carried out following Li (2002). Photographs of the adults were taken with a Leica stereo microscope M205A plus Leica Application Suite 4.2 software, and genitalia were photographed using a Leica DM750 microscope plus the same software as for adults.

## Taxonomic accounts

### *Halolaguna* Gozmány, 1978

*Halolaguna* Gozmány, 1978: 238. Type species: *Halolaguna subluxata* Gozmány, 1978. Type locality: China (Jiangsu).

## Checklist of *Halolaguna* species

*Halolaguna biferrinella* (Walker, 1864)

*Lecithocera biferrinella* Walker, 1864: 642.

*Halolaguna biferrinella*: Wu, 2000: 428.

Distribution. Malaysia, Indonesia.

*Halolaguna discoidea* sp. n.

Distribution. China (Chongqing, Guangxi, Sichuan).

*Halolaguna flabellata* sp. n.

Distribution. China (Guangxi).

*Halolaguna guizhouensis* Wu, 2012

*Halolaguna guizhouensis* Wu, 2012: 394.

Distribution. China (Chongqing, Guangdong, Guangxi, Guizhou).

*Halolaguna oncopteryx* (Wu, 1994)

*Cynicostola oncopteryx* Wu, 1994: 125.

*Halolaguna oncopteryx*: Park 2000: 240.

Distribution. China (Chongqing, Fujian, Guangxi, Sichuan, Taiwan, Yunnan, Zhejiang).

*Halolaguna orthogonia* Wu, 2000

*Halolaguna orthogonia* Wu, 2000: 427.

Distribution. Malaysia.

*Halolaguna palinensis* Park, 2000

*Halolaguna palinensis* Park, 2000: 241.

Distribution. China (Taiwan).

*Halolaguna sanmaru* Park, 2011

*Halolaguna sanmaru* Park, 2011: 201.

Distribution. Thailand.

*Halolaguna sublaxata* Gozmány, 1978

*Halolaguna sublaxata* Gozmány, 1978: 238.

Distribution. China (Hubei, Jiangsu, Liaoning, Shanxi, Taiwan, Zhejiang), Korea, Japan.

### Key to the Chinese *Halolaguna* species based on male genitalia

- 1 Juxta with postero-lateral lobe about 1/2 length of juxta ..... 2
- Juxta with postero-lateral lobe as long as juxta or slightly longer than juxta ... 4
- 2 Aedeagus without cornutus ..... *H. guizhouensis*
- Aedeagus with cornutus ..... 3
- 3 Juxta nearly rounded; aedeagus with a rounded apex ..... *H. flabellata* sp. n.
- Juxta nearly square; aedeagus with a pointed apex ..... *H. oncopteryx*
- 4 Gnathos slender, longer than uncus ..... *H. sublaxata*
- Gnathos obviously shorter than uncus ..... 5
- 5 Aedeagus extending to a discal process distally ..... *H. discoidea* sp. n.
- Aedeagus not extending to a discal process distally ..... *H. palinensis*

***Halolaguna discoidea* sp. n.**

<http://zoobank.org/E3FAFA75-8449-4793-AC0A-E7D624379185>

Figs 1a, 2a, 3a, 4a

**Type material.** Holotype ♂, **China:** Tudiyan, Mt. Simian (28°60'N, 106°40'E), Chongqing, 1200 m, 15.vii.2012, leg. Yinghui Sun and Aihui Yin, genitalia slide No. TKJ13023. Paratypes: 1 ♂, Mt. Simian, Chongqing, 1000 m, 21.vii.2010, leg. Xicui Du and Shengwen Shi; 1 ♂, same locality, 22.vii.2010, leg. Xicui Du and Lifang Song, genitalia slide No. WYQ13157, venation slide No. TKJ14008W; 1 ♂, 2 ♀, Labahe (30°17'N, 102°29'E), Tianquan County, Sichuan Province, 1300 m, 28.vii.2004, 29.vii.2004, leg. Yingdang Ren; 1 ♀, Mt. Daming (23°24'N, 108°30'E), Nanning, Guangxi Zhuang Autonomous Region, 1200 m, 5.viii.2011, leg. Shulian Hao and Yinghui Sun, genitalia slide No. TKJ14004.

**Diagnosis.** This species is similar to *H. oncopteryx* (Wu, 1994) and *H. flabellata* sp. n. in the forewing shape and the male genitalia, but can be separated from these by the juxta with thin claviform postero-lateral lobes slightly longer than the juxta, and the aedeagus with a discal process apically. In *H. oncopteryx* (Wu, 1994) and *H. flabellata* sp. n., the postero-lateral lobes of the juxta are short finger-shaped, about 1/2 length of the juxta, and the aedeagus is absent of discal process apically.

**Description.** Adult (Figs 1a, 2a) with wing expanse 16.5–18.0 mm. Head yellowish white, with scattered brown scales. Antenna yellowish white, scape brown on ventral surface, flagellum with pale brown annulations. Labial palpus yellowish white, with scattered brown scales; second segment with appressed scales; third segment slender, about same length as second. Thorax brown, tegula purple brown. Forewing with costal margin almost straight from basal 1/4 to 3/4; apex protruding triangularly; termen oblique, concave below apex; ground color deep grayish brown; subapical spot yellowish white, nearly triangular; discal and discocellular spots blackish brown, nearly rounded; a yellowish white line extending from costal 2/5 to above fold, edged with blackish brown scales along inner margin, curved triangularly inward to outer margin of discal spot; cilia blackish brown, yellowish white basally; venation:  $R_3$  stalked with  $R_{4+5}$  for basal half of its length,  $R_4$  and  $R_5$  stalked for 2/3 length,  $R_5$  to termen,  $M_1$  and  $R_{3+4+5}$  from upper angle of cell,  $M_2$  absent,  $M_3$  from above lower angle of cell,  $CuA_1$  and  $CuA_2$  shortly stalked at base, from lower angle of cell, cell closed. Hindwing and cilia grayish brown, yellowish white basally; venation:  $R_s$  and  $M_1$  stalked for 2/5 length,  $M_3$  and  $CuA_1$  stalked for about 1/3 length, remote from  $M_2$ , cell close partly. Fore leg with ventral surface brown, dorsal surface yellowish white, mottled brown scales, tarsus yellowish white on distal 1/3; mid leg yellowish white, mottled brown scales on ventral surface; hind leg blackish brown, yellowish white on dorsal surface of tibia and on distal half of tarsus.

Male genitalia (Fig. 3a): Uncus broad at base, narrowed to middle, distal half nearly parallel sided, bearing setae laterally, broadly rounded apically. Gnathos short, nearly triangular, curved distally, pointed apically. Valva broad at base, distinctly narrowed to middle, then slightly narrowed to narrowly rounded apex; costa gen-

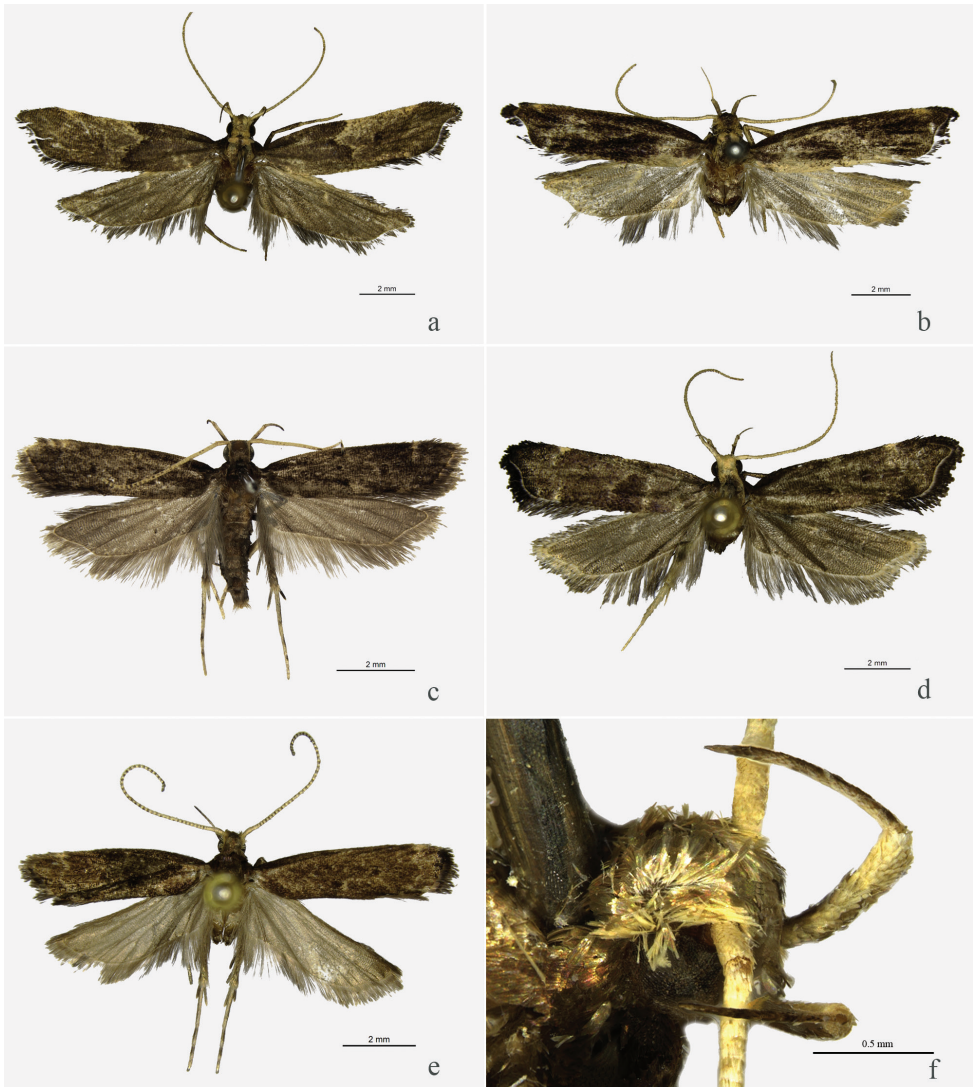


**Figure 1.** Male adults of *Halolaguna* species. **a** *H. discoidea* sp. n., paratype, Chongqing **b** *H. flabellata* sp. n., holotype, Guangxi **c** *H. guizhouensis*, Chongqing **d** *H. oncopteryx*, Chongqing **e** *H. sublaxata*, Zhejiang **f** *H. sublaxata*, Hubei, head from dorsolateral view.

tly concave beyond middle; ventral margin nearly straight. Sacculus narrow, reaching 1/3 length of dorsum. Juxta nearly quadrate, slightly convex antero-medially, almost straight posteriorly; postero-lateral lobe thin claviform, bearing setae laterally, bluntly rounded apically, longer than juxta. Vinculum narrow. Aedeagus stout, slightly longer than valva, broad basally, narrowed to apex; basal half with dense spinules, distal 2/5 with dense granules, apically produced to a discal process.

Female genitalia (Fig. 4a): Eighth sternite with caudal margin deeply concave in U shape at middle, bearing dense setae laterally. Posterior apophyses about twice length

of anterior apophyses. Antrum inconspicuous. Ductus bursae long and heliciform, about four times length of corpus bursae, slightly narrow basally, with numerous thumbtack-shaped spinules ranging from basal 1/4 to 1/2; ductus seminalis slender and long, arising from basal 1/4 of ductus bursae. Corpus bursae oval; signum nearly oval, placed at middle of corpus bursae, margined with teeth anteriorly and posteriorly, medially concave, forming a broad and flat central groove.

**Distribution.** China (Chongqing, Guangxi, Sichuan).

**Etymology.** The name of this species is derived from the Latin adjective *discoideus* (discal), in reference to the discal process of the aedeagus at apex.

***Halolaguna flabellata* sp. n.**

<http://zoobank.org/D3B12A57-853E-4B81-B865-F1A19028BAD1>

Figs 1b, 2b, 3b

**Type material.** Holotype ♂, **China:** Jinxiu County (24°07'N, 110°11'E), Guangxi Zhuang Autonomous Region, 650 m, 28.iv.2008, leg. Hui Zhen and Li Zhang, genitalia slide No. TKJ13034. Paratype: 1 ♂, Hongqilinchang (21°54'N, 107°54'E), Shanshi County, Guangxi Zhuang Autonomous Region, 260 m, 2.iv.2002, leg. Shulian Hao and Huaijun Xue, venation slide No. ZYM06260W.

**Diagnosis.** This species is similar to *H. oncopteryx* (Wu, 1994) superficially and in the male genitalia, but can be separated from the latter by the valva with a blunt apex lacking an apical spine, the juxta nearly rounded, and the apex-rounded aedeagus with two sclerotized plates. In *H. oncopteryx*, the apex of the valva has a strong apical spine, the juxta is nearly square, and the apex-pointed aedeagus has one sclerotized plate.

**Description.** Adult (Figs 1b, 2b): Wingspans 16.0–16.5 mm. Head brown, pale yellow on frons and around eye. Antenna yellowish white, with scattered pale brown scales. Labial palpus yellowish white, with scattered pale brown scales; second segment dark brown on outer surface, with appressed scales; third segment slender, slightly longer than second, pointed terminally. Thorax yellowish white, with brown scales medially; tegula purple brown. Forewing with costal margin almost straight from basal 1/5 to 4/5; apex protruding triangularly; termen oblique, slightly concave below apex; ground color dark brown; subapical spot pale yellow, nearly triangular; discal and discocellular spots blackish brown, small, nearly rounded (somewhat worn); cilia blackish brown, yellowish white basally; venation:  $R_3$  and  $R_{4+5}$  stalked for basal 1/3 length,  $R_4$  and  $R_5$  stalked for 3/5 length,  $R_5$  reaching termen,  $M_1$  and  $R_{3+4+5}$  shortly stalked at base,  $M_2$  absent,  $M_3$  and  $CuA_{1+2}$  from lower angle of cell,  $CuA_1$  and  $CuA_2$  shortly stalked, cell closed. Hindwing and cilia gray, yellowish white basally; venation:  $R_s$  and  $M_1$  stalked for basal 2/5 length,  $M_3$  and  $CuA_1$  shortly stalked, remote from  $M_2$  basally, cell close. Legs yellowish white; fore leg with femur having grayish brown scales on ventral surface, tibia purple brown, tarsus mottled dark brown scales; mid leg with scattered dark brown scales; hind leg dark brown on distal half of femur, at base of tibia and on basal half of tarsus.

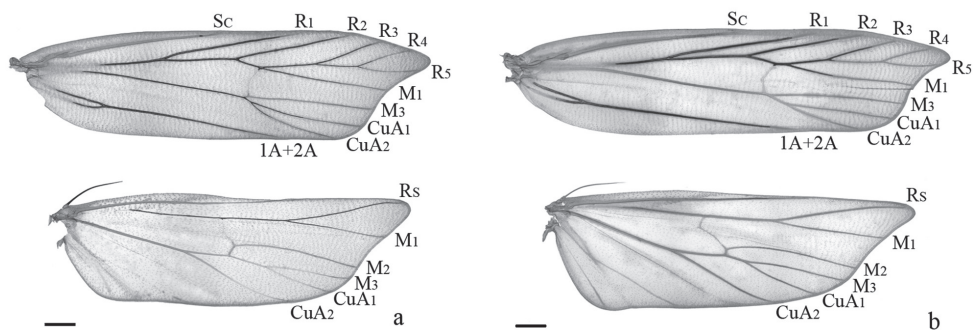


**Figure 2.** Wing venation of *Halolaguna* species. **a** *H. discoidea* sp. n., slide No. TKJ14008W **b** *H. flabellata* sp. n., slide No. ZYM06260W (Scales = 0.5 mm).

Male genitalia (Fig. 3b): Uncus broadened in fan shape basally, clubbed distally, bearing short setae laterally, rounded apically. Gnathos narrow, basal 1/3 nearly aequilate, median portion gradually narrowed, distal 1/3 sharply narrowed to pointed apex. Valva broad at base, slightly narrowed to middle, distal half obviously narrowed, slightly curved dorsad distally, narrowly rounded apically; costa concave medially. Sacculus broad at base, narrowed distally, reaching 1/4 length of dorsum. Juxta nearly rounded, convex antero-medially, slightly arched posteriorly; postero-lateral lobe short thumb-shaped, bearing setae apically. Vinculum narrow. Aedeagus straight, shorter than valva, broad at base, slightly narrowed to rounded apex, with numerous unequal-sized toothlike thorns at base, with dense spinules and granular teeth ranging from about middle to distal 1/4, distal half with two sclerotized irregular plates, one of them with teeth.

Female: Unknown.

**Distribution.** China (Guangxi).

**Etymology.** The specific name of this species is derived from the Latin adjective *flabellatus* (flabellate), in reference to the basally fan-shaped uncus.

### *Halolaguna guizhouensis* Wu, 2012

Figs 1c, 3c, 4b

*Halolaguna guizhouensis* Wu, 2012: 394. Type locality: China (Guizhou).

**Material examined. China:** Guizhou Province: 1 ♂, Linjiang (28°05'N, 105°32'E), Xishui County, 550 m, 26.ix.2000, leg. Haili Yu; Chongqing: 5 ♂, 1 ♀, Beipo (29°02'N, 107°11'E), Mt. Jinpo, 1100 m, 5.v.2013, 12.v.2013, leg. Xiaofei Yang; 1 ♂, same locality, 4.viii.2012, leg. Xiaofei Yang and Tengting Liu; Guangxi Zhuang Autonomous Region: 2 ♂, 1 ♀, Shaopinglinchang (22°03'N, 106°55'E), Pingxiang, 280 m, 28.iii.2013, 2.iv.2013, 10.iv.2013, leg. Xiaofei Yang, genitalia slide No. TKJ14087♀;

1 ♂, Qinmu Village (24°59'N, 109°59'E), Yongfu County, 160 m, 1.v.2008, leg. Hui Zhen and Li Zhang; 1 ♂, Hekoubaohuzhan, Jinxiu County (24°07'N, 110°11'E), 650 m, 28.iv.2008, leg. Hui Zhen and Li Zhang, genitalia slide No. TKJ13055; 1 ♂, Xijiao (24°15'N, 108°01'E), Nandan County, Hechi, 868 m, 10.viii.2011, leg. Shulian Hao and Yinghui Sun; Guangdong Province: 1 ♂, Heshan (22°25'N, 112°32'E), 26.viii.2002, leg. Guilin Liu; 1 ♂, Hebao Island (21°52'N, 113°10'E), Zhuhai, 30 m, 18.v.2010, leg. Bingbing Hu and Jing Zhang.

**Diagnosis.** Adult (Fig. 1c) with wing expanse 14.0–15.0 mm. This species is similar to *H. sublaxata* Gozmány, 1978 superficially by sharing small and rounded discal spot and relatively large fold and discocellular spots. It can be separated from the latter by the valva broadly rounded apically, the relatively short gnathos slightly shorter than the uncus, and the juxta with postero-lateral lobes shorter than the juxta in the male genitalia (Fig. 3c). In *H. sublaxata*, the valva is narrow and thin apically, the slender gnathos is distinctly longer than the uncus, and the postero-lateral lobes of the juxta are longer than the juxta.

Female genitalia (Fig. 4b): Eighth sternite bearing dense setae, with caudal margin slightly emarginated at middle. Anterior apophyses about 3/4 length of posterior apophyses. Ductus bursae about four times length of corpus bursae, long and heliciform; ductus seminalis slender, arising from basal 1/8 of ductus bursae. Corpus bursae nearly rounded; two small papillate signa placed posteriorly, with dense granules; one big rhombic signum placed at middle of corpus bursae, with a nearly triangular horizontal plate arising medially.

**Distribution.** China (Chongqing, Guangdong, Guangxi, Guizhou).

**Remarks.** *Halolaguna guizhouensis* was described by Wu (2012) based on two male specimens from Guizhou. The valva of this species is not distinctly narrowed distally, whereas the valva of its congeners is obviously narrowed to pointed apex. However, the venation of this species is consistent with that of the type species. The female is described here for the first time.

### *Halolaguna oncopteryx* (Wu, 1994)

Figs 1d, 3d, 4c

*Cynicostola oncopteryx* Wu, 1994: 125. Type locality: China (Sichuan).

*Halolaguna oncopteryx* (Wu): Park 2000: 240.

**Material examined. China:** Fujian Province: 1 ♂, 1 ♀, Mt. Meihua (25°20'N, 116°50'E), 19.vii.1988, 22.vii.1988, leg. Chinese Academy of Science; Chongqing: 1 ♂, 1 ♀, Mt. Simian (28°60'N, 106°40'E), 1000 m, 20.vii.2010, leg. Xicui Du and Lifang Song; Guangxi Zhuang Autonomous Region: 1 ♂, 1 ♀, Hongqilinchang (21°54'N, 107°54'E), Shangsi County, 260 m, 2.iv.2002, leg. Shulian Hao and Huaijun Xue; 2 ♂, 1 ♀, Shaoping linchang (22°03'N, 106°55'E), Pingxiang, 280 m, 19.iv.2012, 28.iii.2013, 13.iv.2013, leg. Xiaofei Yang; 2 ♀, Mt. Daming (23°24'N,

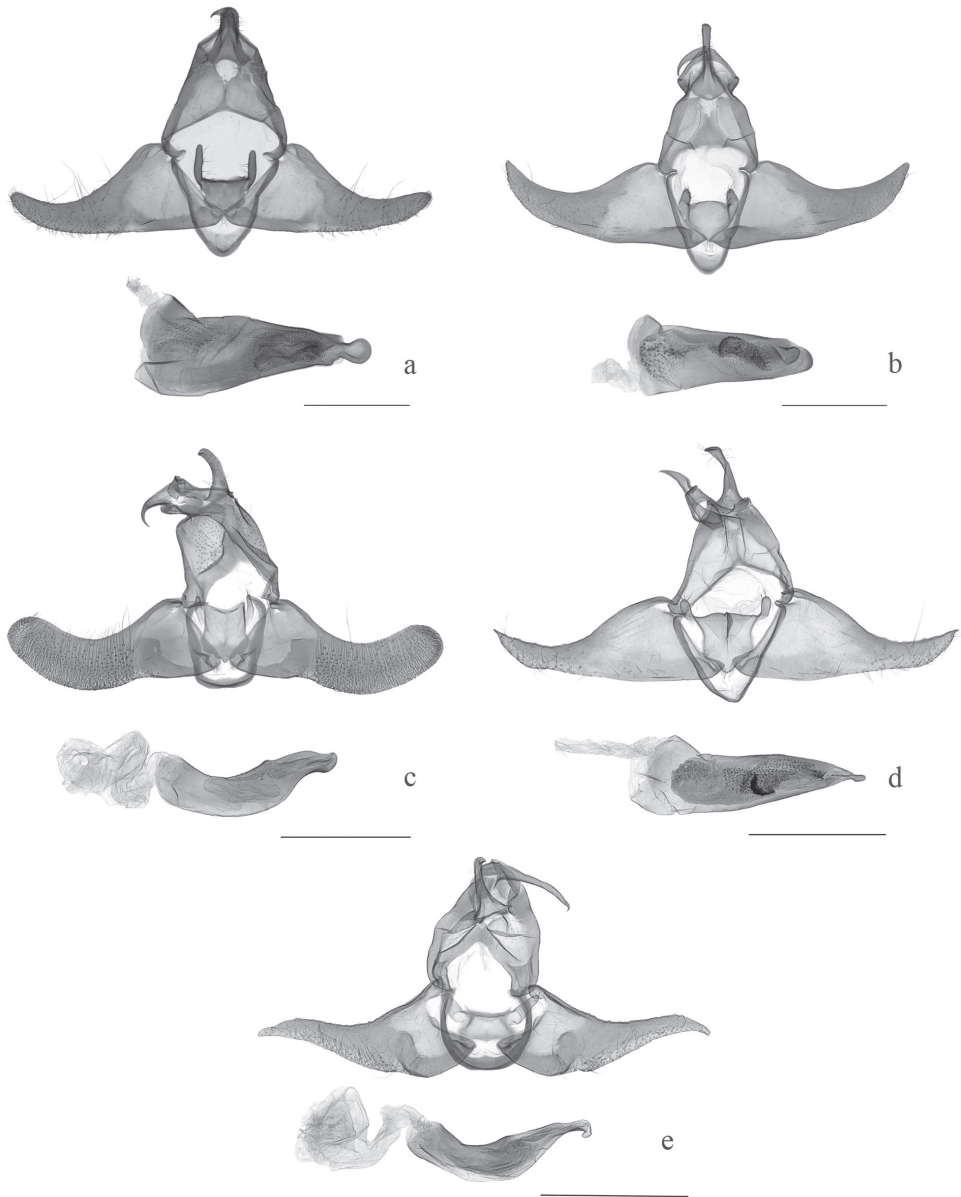


**Figure 3.** Male genitalia of *Halolaguna* species. **a** *H. discoidea* sp. n., slide No. WYQ13157 **b** *H. flabellata* sp. n., slide No. TKJ13034 **c** *H. guizhouensis*, slide No. TKJ13055 **d** *H. oncopteryx*, slide No. TKJ13039 **e** *H. subluxata*, slide No. TKJ13051 (Scales = 0.5 mm).

108°30'E), Nanning, 1200 m, 7.viii.2011, 8.viii.2011, leg. Shulian Hao and Yinghui Sun; Yunnan Province: 1 ♂, Tropical Botanical Garden (21°55'N, 101°17'E), Menglun County, 570 m, 13.viii.2005, leg. Yingdang Ren; Zhejiang Province: 1 ♀, Zhangkengkou (28°32'N, 118°99'E), Mt. Jiulong, 623 m, 5.vii.2013, leg. Aihui Yin

and Xiuchun Wang; 2 ♂, 1 ♀, Neijiujiang (28°40'N, 118°84'E), Mt. Jiulong, 430 m, 7.vii.2013, leg. Aihui Yin and Xiuchun Wang, genitalia slide No. TKJ13035♀; 1 ♂, 2 ♀, Yanping (28°38'N, 118°89'E), Mt. Jiulong, 530 m, 4.vii.2013, leg. Aihui Yin and Xiuchun Wang, genitalia slide No. TKJ13039♂; 2 ♂, 2 ♀, Huangtanyu (28°39'N, 118°84'E), Mt. Jiulong, 467 m, 8.vii.2013, leg. Aihui Yin and Xiuchun Wang; 1 ♂, Wuyanling (27°42'N, 119°39'E), Taishun County, 680 m, 28.vii.2005, leg. Yunli Xiao.

**Diagnosis.** Adult (Fig. 1d) with wing expanse 15.0–16.0 mm. This species is similar to *H. sanmaru* Park, 2011 in the male genitalia, but can be separated from it by the valva with a strong apical spine, the juxta with postero-lateral lobes about 1/2 length of the juxta, and the aedeagus with a pointed apex (Fig. 3d). In *H. sanmaru*, the valva does not bear an apical spine, the postero-lateral lobes of the juxta are slightly longer than the juxta, and the aedeagus is rounded apically. This species is also similar to *H. discoidea* sp. n. in the female genitalia, but can be separated from it by the eighth sternite with caudal margin slightly concave at middle, and the ductus seminalis as broad as the ductus bursae (Fig. 4c). In *H. discoidea* sp. n., the caudal margin of the eighth sternite is deeply concave in U shape medially, and the ductus seminalis is slenderer than the ductus bursae.

**Distribution.** China (Chongqing, Fujian, Guangxi, Sichuan, Taiwan, Yunnan, Zhejiang).

### *Halolaguna sublaxata* Gozmány, 1978

Figs 1e, 1f, 3e, 4d

*Halolaguna sublaxata* Gozmány, 1978: 238. Type locality: China (Jiangsu).

**Material examined.** **China:** Zhejiang Province: 1 ♂, Mt. Jiulong (28°29'N, 119°54'E), 400 m, 5.viii.2011, leg. Linlin Yang and Na Chen; 1 ♂, Houshanmen, Mt. Tianmu (30°15'N, 119°20'E), 500 m, 16.viii.1999, leg. Houhun Li et al.; Shanxi Province: 1 ♂, Mt. Li (35°26'N, 111°58'E), Jincheng, 1520 m, 16.viii.2006, leg. Xu Zhang and Haiyan Bai; Liaoning Province: 1 ♂, Shilizi (40°42'N, 124°42'E), Kuandian County, 10.viii.2009, leg. Weichun Li and Jiayu Liu; Hubei Province: 2 ♂, Mt. Wujia (31°05'N, 115°48'E), Yingshan County, 8.vii.2008, leg. Yunli Xiao, genitalia slide No. TKJ13051; 1 ♂, 2 ♀, Mt. Dahong (31°27'N, 113°00'E), Suizhou, 30.ix.2008, 1.x.2008, leg. Yunli Xiao, genitalia slide No. TKJ14088♀.

**Diagnosis.** Adult (Fig. 1e, f) with wing expanse 14.0–15.0 mm. *Halolaguna sublaxata* Gozmány, 1978 can be separated from its congeners by the slender gnathos longer than uncus, and the valva slightly curved ventrad before apex in the male genitalia (Fig. 3e). *Halolaguna sublaxata* is similar to *H. guizhouensis* in the female genitalia by the corpus bursae sharing three signa, but can be separated from it by the position of the signa: in *H. sublaxata*, one large sub-triangular signum placed posteriorly, one small triangular signum below it, and the shuttle-shaped signum placed anteriorly

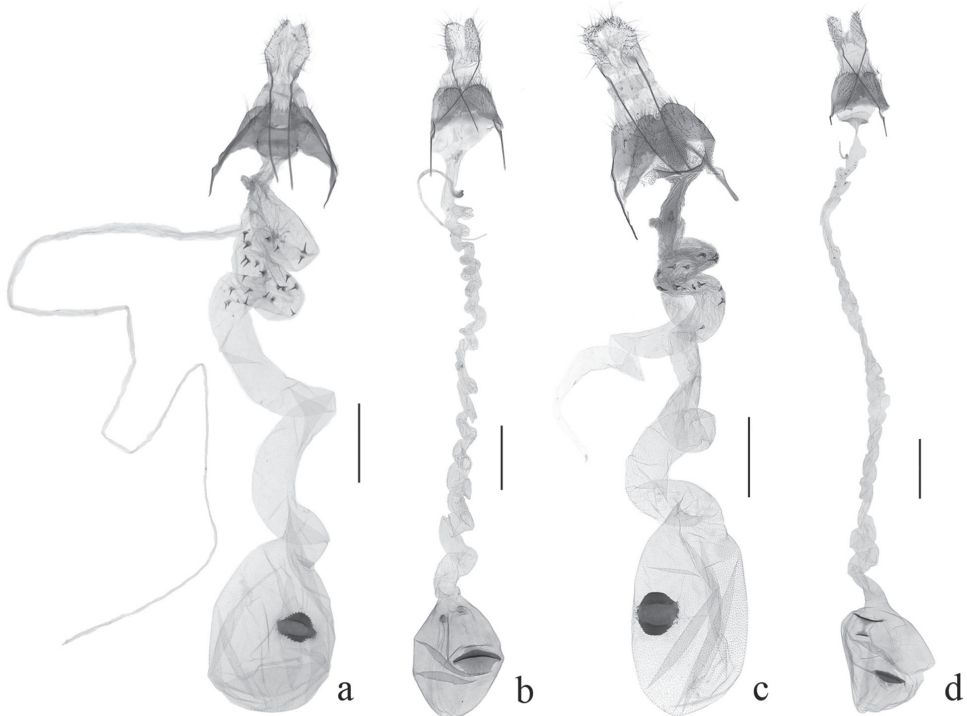


**Figure 4.** Female genitalia of *Halolaguna* species. **a** *H. discoidea* sp. n., slide No. TKJ14004 **b** *H. guizhouensis*, slide No. TKJ14087 **c** *H. oncopteryx*, slide No. TKJ13035 **d** *H. sublaxata*, slide No. TKJ14088 (Scales = 0.5 mm).

(Fig. 4d); in *H. guizhouensis*, two small papillate signa placed posteriorly, and the third large rhombic signum is placed at middle of the corpus bursae.

**Distribution.** China (Hubei, Jiangsu, Liaoning, Shanxi, Taiwan, Zhejiang).

## Acknowledgements

We express our cordial thanks to Dr. K. T. Park (Korea) for providing useful literature. This study is supported by the National Natural Science Foundation of China (No. 31372241 and No. J1210005).

## References

- Gozmány L (1978) Lecithoceridae. In: Amsel HG, Gregor F, Reisser H (Eds) *Microlepidoptera Palaearctica*. Georg Fromme & Co., Wien, Volume 5, 238–239.
- Li HH (2002) *The Gelechiidae of China (I) (Lepidoptera: Gelechioidea)*. Nankai University Press, Tianjin, 504 pp.

- van Nieuwerkerken EJ, Kaila L, Kitching IJ, Kristensen NP, Lees DJ, Minet J, Mitter J, Mutanen M, Regier JC, Simonsen TJ, Wahlberg N, Yen S-H, Zahiri R, Adamski D, Baixeras J, Bartsch D, Bengtsson BÅ, Brown JW, Bucheli RS, Davis DR, De Prins J, De Prins W, Epstein ME, Gentili-Poole P, Gielis C, Hättenschwiler P, Hausmann A, Holloway JP, Kallies A, Karsholt O, Kawahara A, Koster SJ, CKozlov MV, Lafontaine JD, Lamas G, Landry J-F, Lee S, Nuss M, Park K-T, Penz C, Rota J, Schmidt BC, Schintlmeister A, Sohn JC, Solis MA, Tarmann G, Warren AD, Weller S, Yakovlev Y, Zolotuhin VV, Zwick A (2011) Order Lepidoptera Linnaeus, 1758. In: Zhang Z-Q (Ed.) Animal biodiversity: An outline of higher-level classification and survey of taxonomic richness. Zootaxa 3148: 212–221.
- Park KT (2000) Lecithoceridae (Lepidoptera) of Taiwan (V): Subfamily Torodorinae: *Thubana* Walker, *Athymoris* Meyrick, *Halolaguna* Gozmány, and *Philharmonia* Meyrick. Insecta Koreana 17(4): 229–244.
- Park KT (2011) A new species of *Halolaguna* Gozmány from Thailand (Lepidoptera: Lecithoceridae). Journal of Asia-Pacific Entomology 14: 201–203. doi: 10.1016/j.aspen.2010.12.006
- Park KT, Heppner JB, Bae YS (2013) Two new species of Lecithoceridae (Lepidoptera, Gelechioidea), with a revised check list of the family in Taiwan. ZooKeys 263: 47–57. doi: 10.3897/zookeys.263.3781
- Walker F (1864) List of the specimens of the lepidopterous insects in the collection of British Museum. Part XXIX & XXX, Tineites. British Museum, London, 533–835, 837–1096.
- Wu CS (1994) The Lecithoceridae (Lepidoptera) of China with descriptions of new taxa. Sinozoologia 11: 123–154.
- Wu CS (1997) Fauna Sinica. Insecta, Lepidoptera: Lecithoceridae 7. Science Press, Beijing, 306 pp.
- Wu CS (2000) A taxonomic study of the subfamily Torodorinae from Malaysia, with description of three new species (Lepidoptera: Lecithoceridae). Acta Zootaxonomica Sinica 25(4): 427–430.
- Wu CS (2012) Lecithoceridae. In: Dai RH, Li ZZ, Jin DC (Eds) Insects from Kuankuoshui Landscape. Guizhou Science and Technology Publishing House, Guiyang, 392–396.